

Supporting information

The efficient conversion of H₂S into mercaptan alcohols mediated in protic ionic liquids under mild condition

Wenjie Xiong ^a, Mingzhen Shi ^a, Xiaomin Zhang ^{a,b,*}, Zhuoheng Tu ^a, Xingbang Hu ^{a,b}, Youting Wu

^{a,b,*}

^a Key Laboratory of Mesoscopic Chemistry of MOE, School of Chemistry and Chemical Engineering, Nanjing University, Nanjing 210023, P.R. China.

^b Yuxiu Postdoctoral Institute, Nanjing University, Nanjing 210023, P.R. China

* Corresponding author: xmzhang@nju.edu.cn; ytwu@nju.edu.cn

Experimental

Materials and instruments

The specifications and sources of the chemicals used in this work are summarized in **Table S1**.

All reagents were used without further purification. NMR spectra was obtained on a Bruker DPX 400 MHz spectrometer with CDCl₃ as internal standard solvent at ambient temperature. FT-IR spectra was carried out on Nicolet iS50 infrared spectrometer, with the spectral resolution and the number of scans of 4 cm⁻¹ and 32, respectively. Conversion and selectivity of epoxides were determined by HPLC analysis. ESI-MS was used to characterize the molecular weight of the product at m/z.

Preparation and Characterization of PILs

These PILs were synthesized by neutralization reaction. Taking a typical run, 50 mL of the ethanol solution of MeOAc (20 mmol) was added dropwisely to the ethanol solution of BDMAEE (25 mmol). The reaction was stirred in an ice bath until it was raised to room temperature and stirred

for 12 hours. Then, ethanol was removed by vacuum distillation and the remaining crude product was washed three times by diethyl ether to remove the excess reactant. The product was dried in a vacuum at 60 °C for 24 hours to remove trace solvents, and finally, a clear liquid [BDMAEH][MeOAc] was obtained.

The typical experiment of epoxides with H₂S

In a typical run, styrene oxide (1.0 g, 8.3 mmol) in a reaction vessel. The amount of catalyst is 0.1 Equiv. of the reactant and the condition of cycloaddition are 30 °C and 2 hours. Pure mercaptan alcohol was obtained by thin-layer chromatography (TLC) with petroleum ether (PE) and ethyl acetate (EA) as eluent (3:1). The structures of mercaptan alcohol were verified by ¹H and ¹³C NMR spectra with CDCl₃ as solvent.

Determination of H₂S Absorption

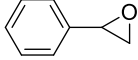
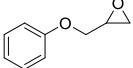
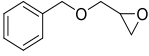
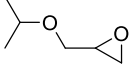
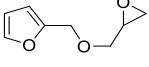
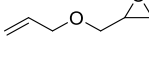
The whole absorption equipment consists of a water bath, a pressure recording system and two 316L stainless steel chambers whose volumes 119.871 cm³ (V₁) and 48.854 cm³ (V₂), respectively. The big chamber, named as gas reservoir, are used to isolate H₂S before it contacts with the IL sample in the small chamber, which is equipped with a magnetic stirrer and used as equilibrium cell. The temperature (*T*) of both chambers is controlled by the water bath with an accuracy of ±0.1K. The pressures in the two chambers are monitored online using two pressure transducers (Wideplus Precision Instruments) which are linked to a Numeric Instrument (WP-D821-200-1212—N-2P). The uncertainty of the pressure recording system is ±0.2% in relation to the full scale. In a typical run, a known mass (*w*) of IL sample was placed into the equilibrium cell. Then the air in the two chambers was evacuated (<10 Pa). While the two chambers were separated using a needle valve, H₂S was fed into the gas reservoir from gas cylinder to a pressure of *P*₁ and the equilibrium cell was recorded to be *P*₀. The needle valve between the two chambers was turned on to let H₂S be introduced to

equilibrium cell. Absorption equilibrium was thought to be obtained when the pressures of the two chambers remained constant for at least 2 h. The equilibrium pressures were denoted as P_2 for the equilibrium cell and P_1' for the gas reservoir. The H₂S partial pressure in the equilibrium cell was $P_S = P_2 - P_0$. The H₂S uptake, n (P_S), can thus be calculated using the following equation

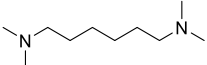
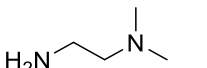
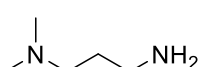
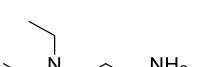
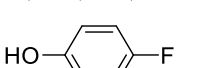
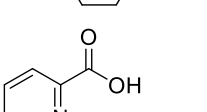
$$n(P_S) = \rho_g(P_1, T)V_1 - \rho_g(P_1', T)V_1 - \rho_g(P_S, T)(V_2 - \omega / \rho_{IL}) \quad (S1)$$

Where $\rho_g(P_i, T)$ represents the density of H₂S in mol/cm³ at P_i (i=1, S) and ρ_{IL} is the density of the ionic liquid sample in g/cm³ at T . V_1 and V_2 represent the volumes in cm³ of the two chambers. Subsequent determination of solubility data at elevated pressures were performed by introducing more H₂S into the equilibrium cell to reach new equilibrium.

Table S1. Specifications and sources of chemicals used in this work.

Molecular structure	Chemical name	CAS registry number	MW. (g/mol)	Mass fraction	Source
				purity	
	Styrene Oxide	96-09-3	120.15	0.98	Adamas
	Ethylene Oxide	75-56-9	58.08	0.99	Adamas
	Glycidyl phenyl ether	122-60-1	150.17	0.98	Macklin
	Benzyl Glycidyl Ether	89616-40-0	164.20	0.97	Macklin
	Glycidyl Isopropyl Ether	4016-14-2	116.16	0.96	Aladdin
	Furfuryl glycidyl ether	5380-87-0	154.16	0.96	Aladdin
	Cyclohexene oxide	286-20-4	98.14	0.98	Aladdin
	Allyl glycidyl ether	106-92-3	114.14	0.99	Adamas
	2-hexyl-oxirane	2984-50-1	128.21	0.97	Adamas

	1,4-Butanediol diglycidyl ether	2425-79-8	202.25	0.95	Aladdin
	o-Cresyl glycidyl ether	2210-79-9	164.20	0.90	Aladdin
	trans-Stilbene oxide	1439-07-2	196.24	0.98	Aladdin
	Tert-butyl glycidyl ether	7665-72-7	130.19	0.96	Aladdin
	4,4-dimethyl-3,5,8-trioxabicyclo[5.1.0]octane	57280-22-5	144.17	0.99	Adamas
	Trityl glycidyl ether	129940-50-7	316.39	0.98	Adamas
	1,2-Epoxy-5-hexene	10353-53-4	98.14	0.96	Aladdin
	ethyl oxirane-2-carboxylate	4660-80-4	116.12	0.98	Adamas
	3,4-Epoxytetrahydrofuran	285-69-8	86.09	0.97	Adamas
	2-phenylpropylene oxide	2085-88-3	134.18	0.95	Macklin
	Cyclopentene oxide	285-67-6	84.12	0.98	Adamas
	3,4-Epoxy-1-butene	930-22-3	70.09	0.98	Aladdin
	Ethyl 3-phenylglycidate	121-39-1	192.21	0.90	Macklin
	Methoxyacetic Acid	625-45-6	90.08	0.98	Macklin
	Bis(2-dimethylaminoethyl) ether	3033-62-3	160.26	0.98	Adamas
	1-ethyl-3-methylimidazolium acetate	143314-17-4	170.21	0.98	Adamas
	N,N,N',N'-tetramethylethylenediamine	110-18-9	116.21	0.99	Adamas
	N,N,N',N'-Tetramethyl-1,3-propanediamine	110-95-2	130.23	0.98	Adamas

	1,6-bis(dimethylamino)Hexane	111-18-2	172.31	0.98	Adamas
	2-Dimethylaminoethylamine	108-00-9	88.15	0.99	Aladdin
	3-Dimethylaminopropylamine	109-55-7	102.18	0.99	Aladdin
	3-Diethylaminopropylamine	104-78-9	130.23	0.99	Adamas
	4-Fluorophenol	371-41-5	112.10	0.98	Adamas
	picolinic acid	98-98-6	123.11	0.97	Adamas
HBr	Hydrogen bromide	10035-10-6	80.91	0.40	in Nanjing water reagent
HI	Hydroiodic acid	10034-85-2	127.91	0.45	in Nanjing water reagent
CH ₃ I	Iodomethane	74-88-4	141.94	0.98	Adamas

H₂S was purchased from Nanjing Tianze Gas Co., Ltd.

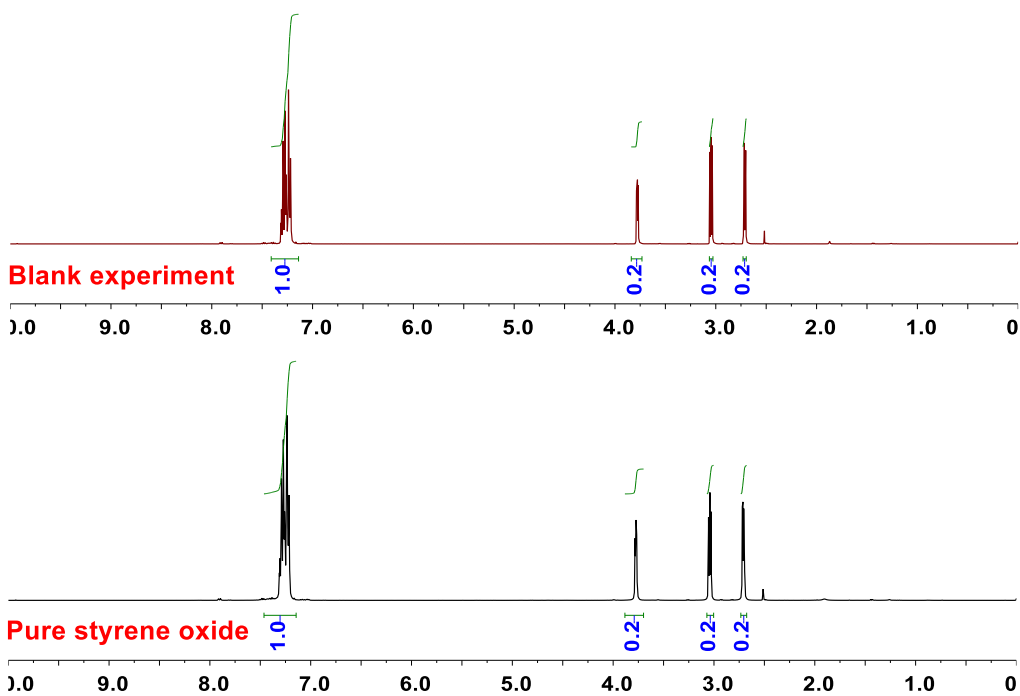


Figure S1. ¹H NMR of styrene oxide (**1a**) after and before reaction with H₂S in the absence of catalyst.

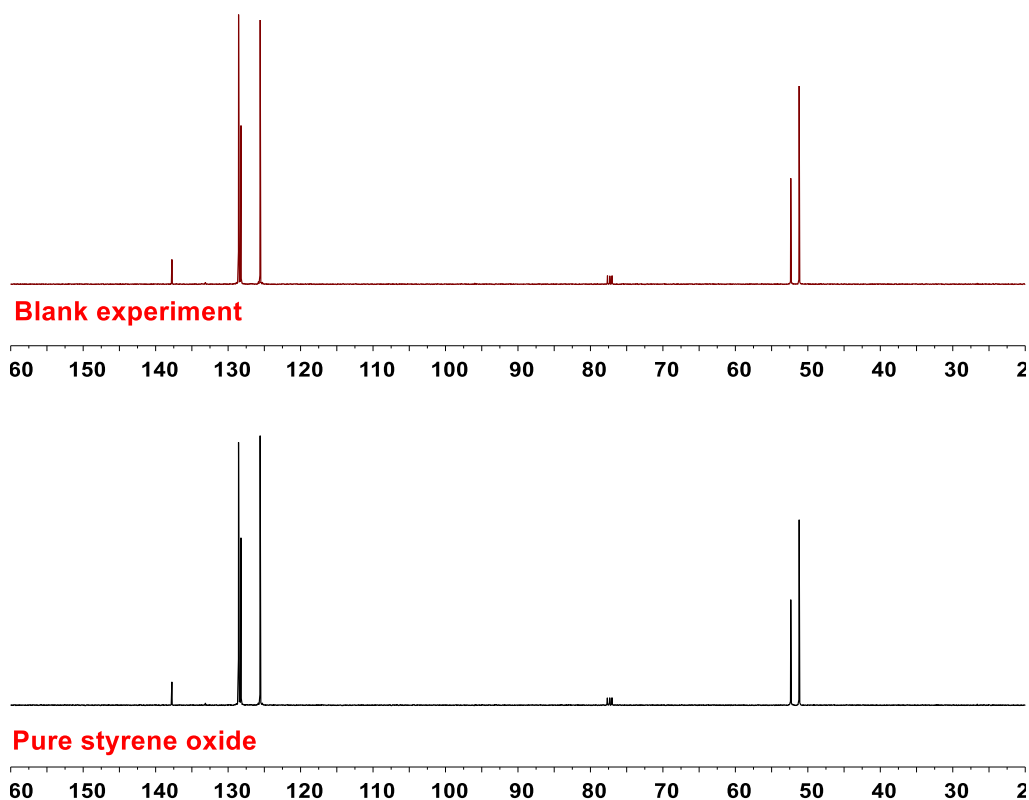


Figure S2. ¹³C NMR of styrene oxide (**1a**) after and before reaction with H₂S in the absence of the catalyst.

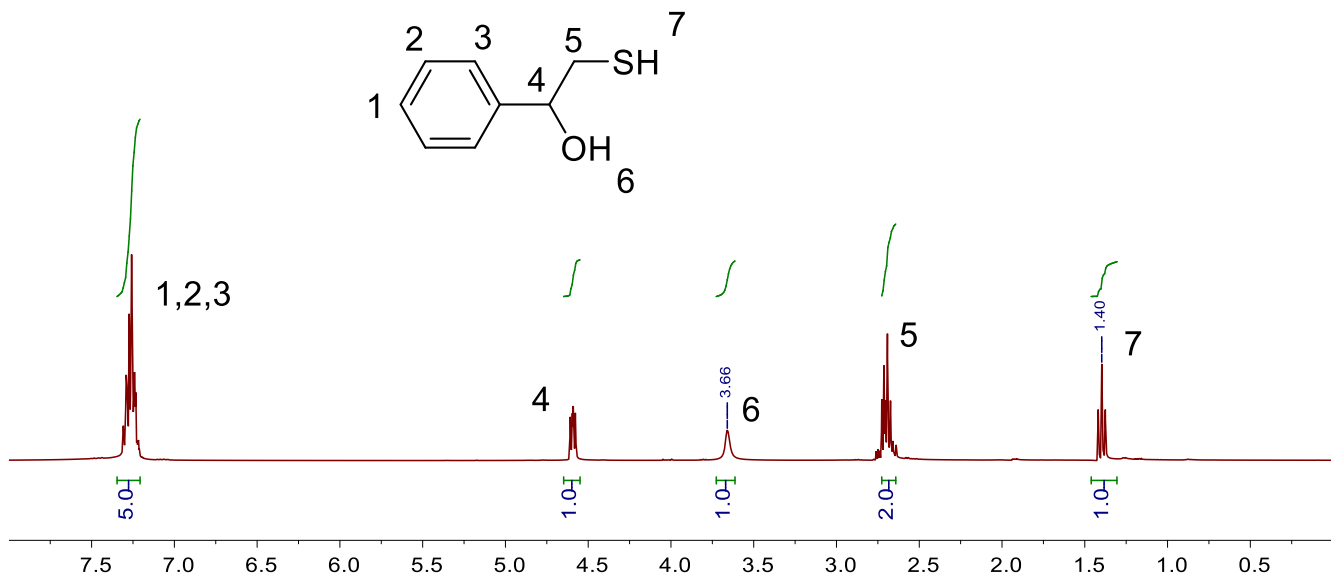


Figure S3. ¹H NMR of 2-mercaptopro-1-phenylethan-1-ol (**1b**).

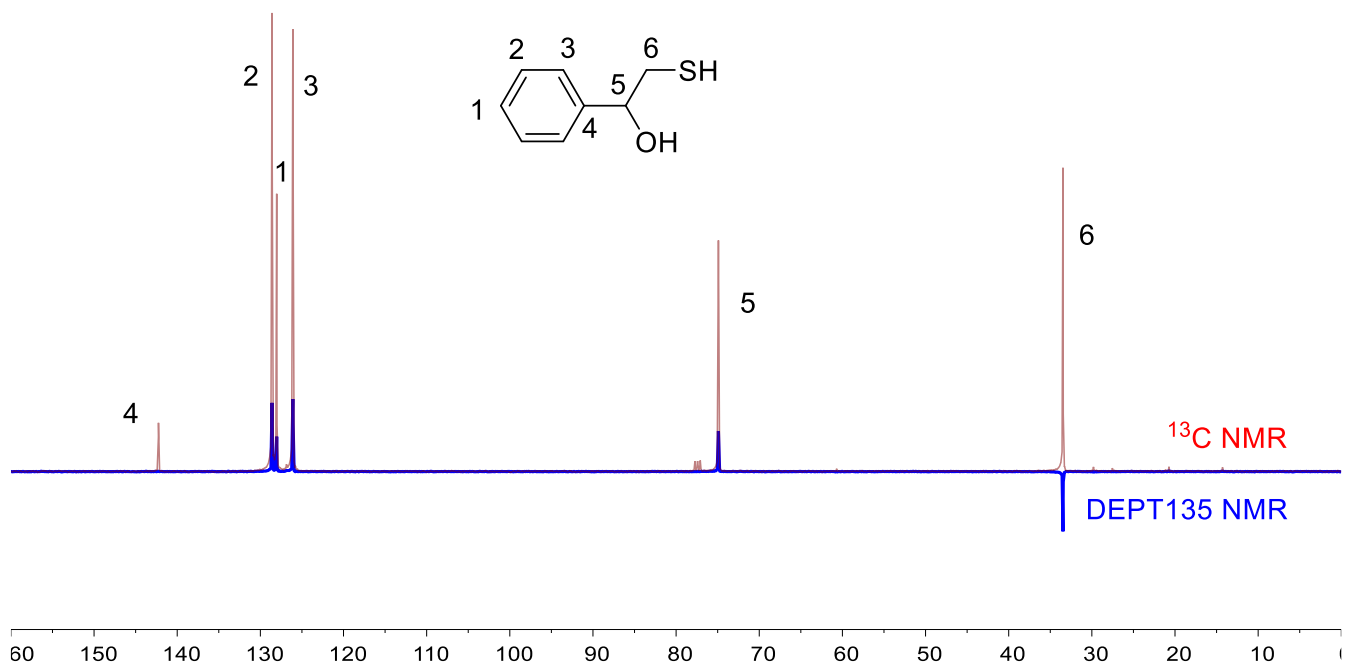


Figure S4. ¹³C NMR of 2-mercaptopro-1-phenylethan-1-ol (**1b**).

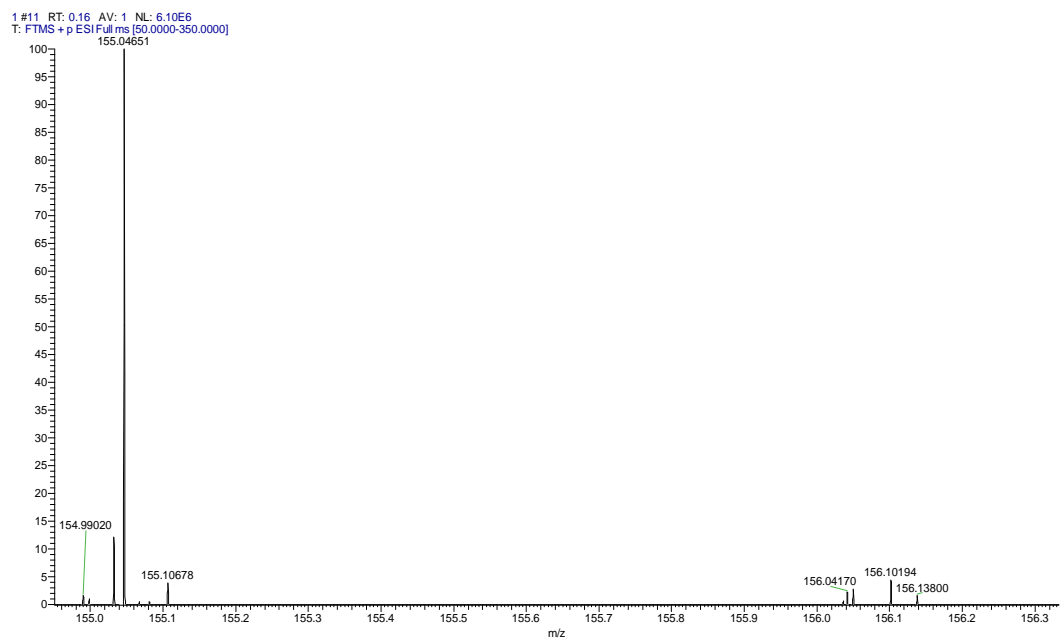


Figure S5. ESI-MS of 2-mercaptophenylethan-1-ol (**1b**) at m/z $[M^++1]$.

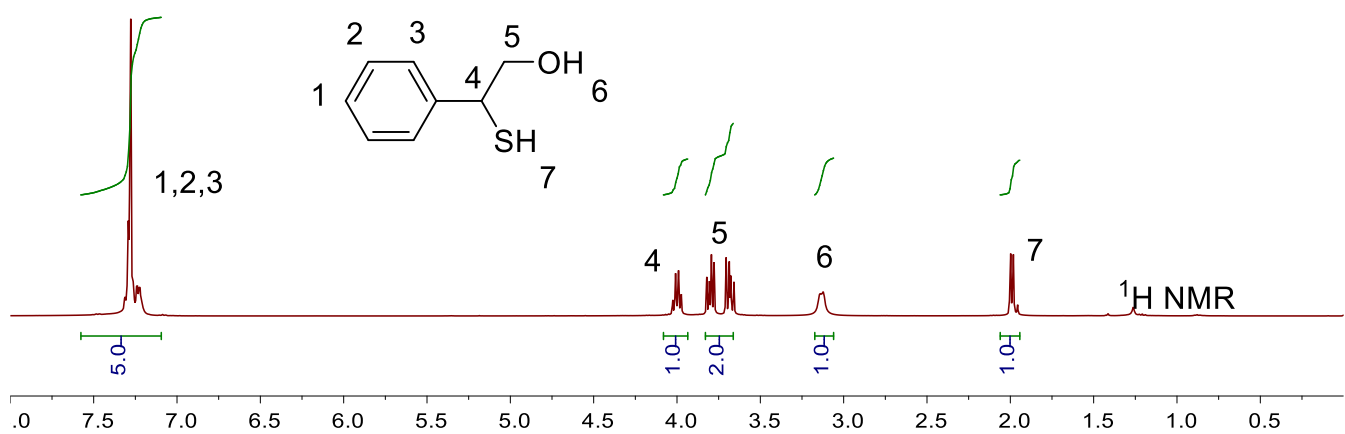


Figure S6. ^1H NMR of 2-mercaptopropanoic acid (1c).

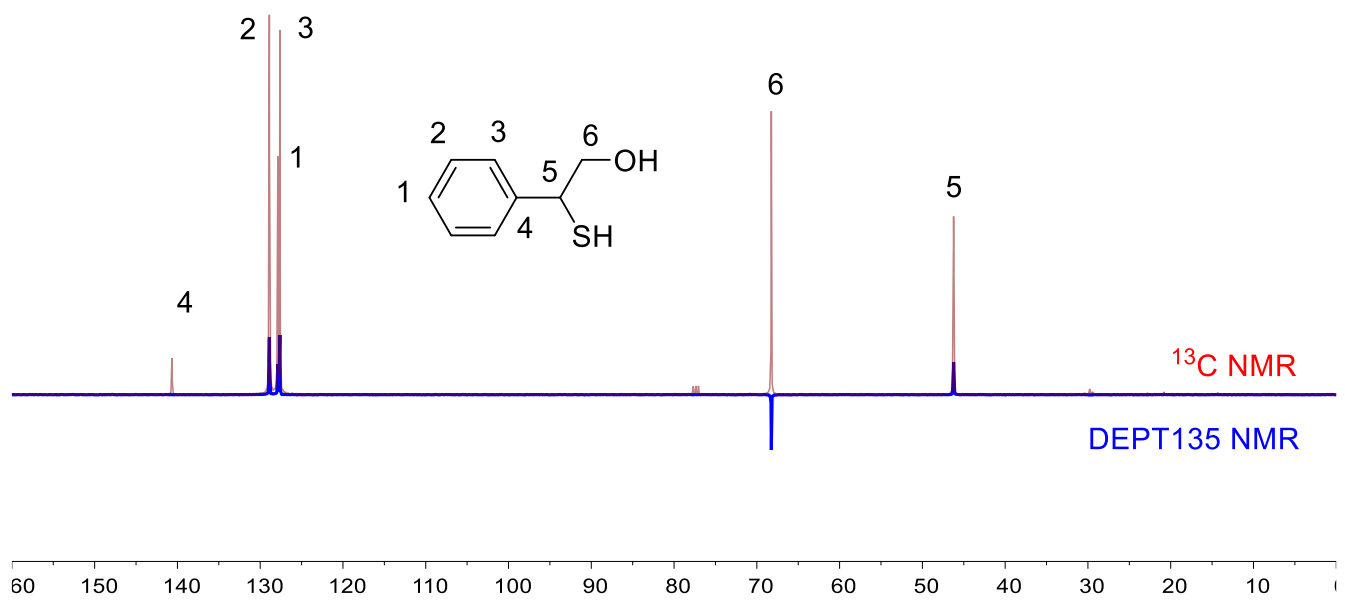


Figure S7. ^{13}C NMR of 2-mercaptopropanoic acid (1c).

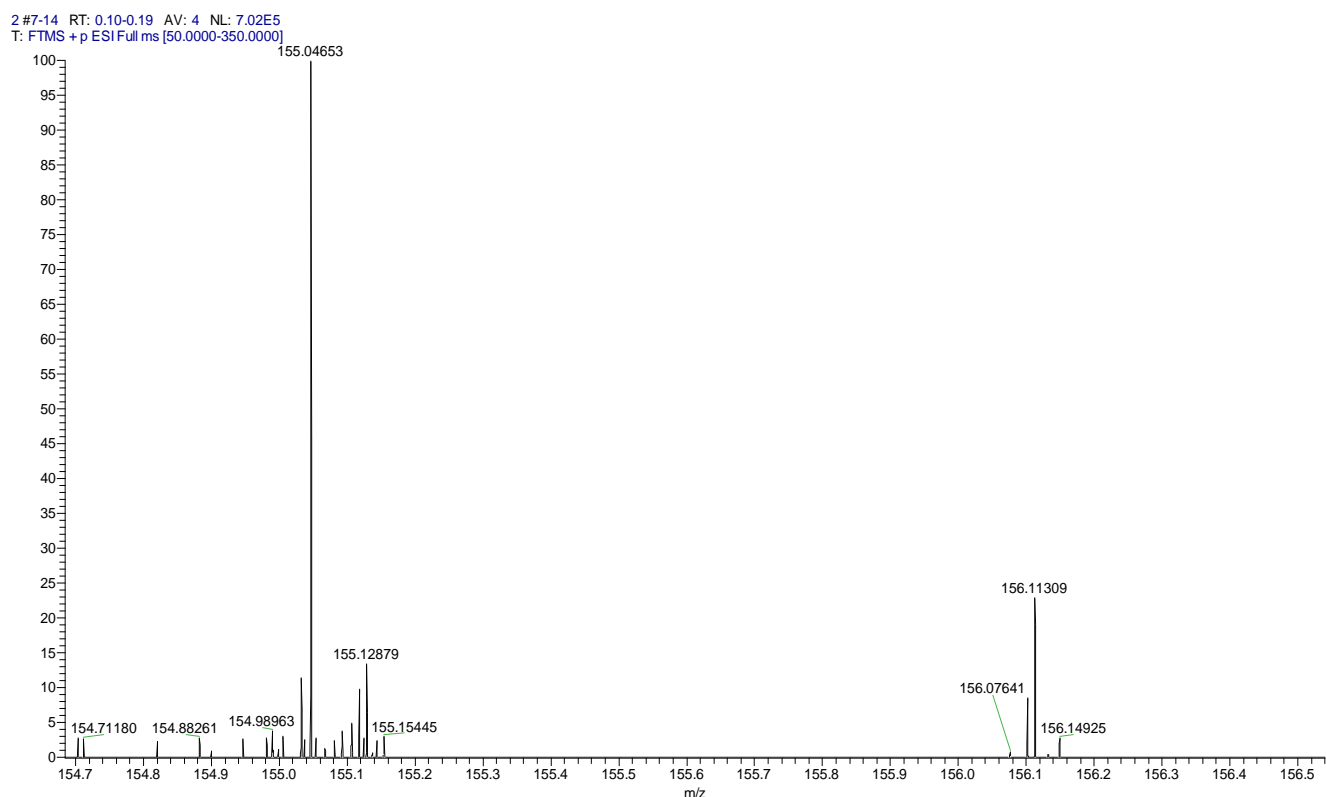


Figure S8. ESI-MS of 2-mercaptopropanoic acid (**1c**) at m/z $[M^++1]$.

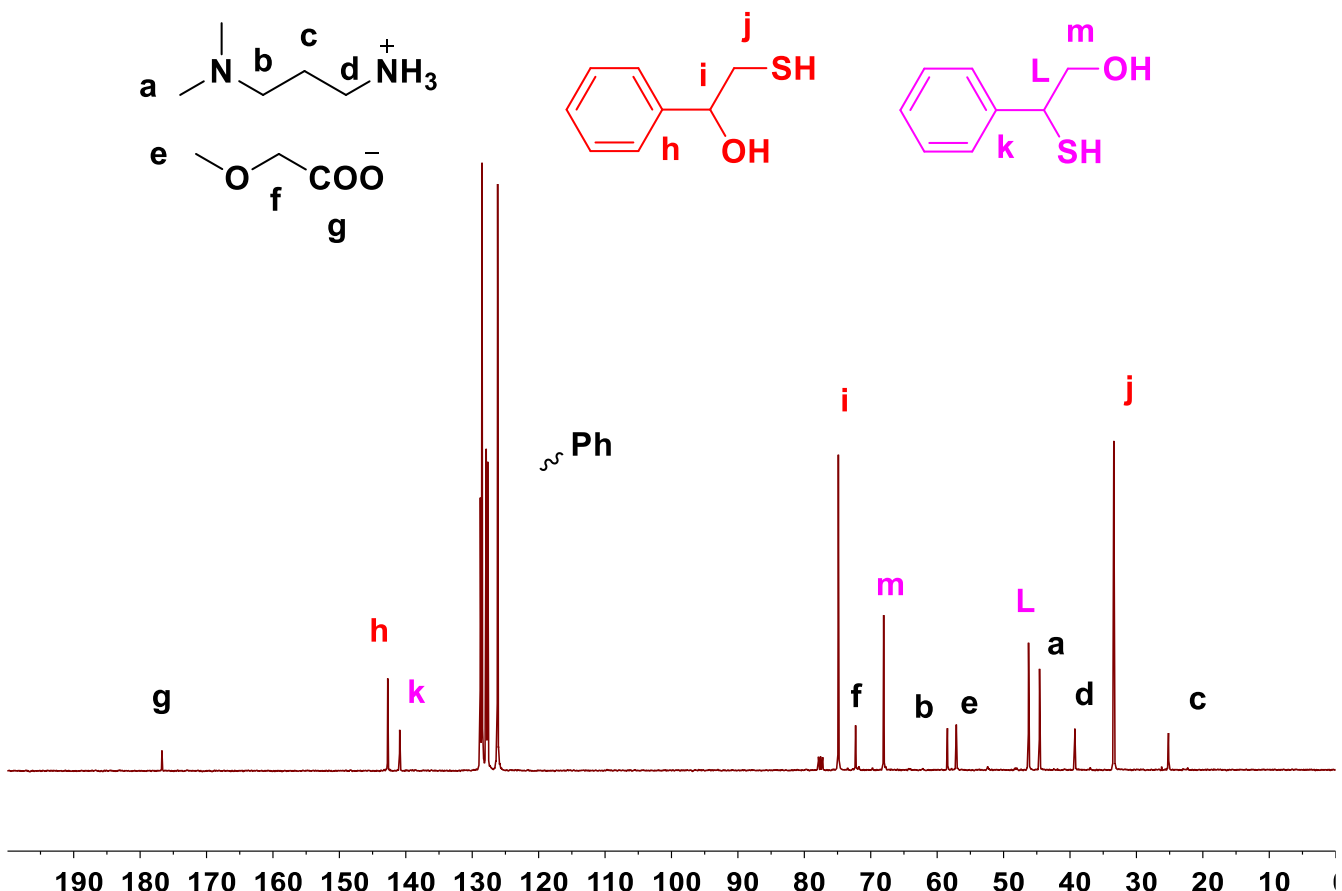


Figure S9. ^{13}C NMR of styrene oxide (**1a**) with [DMAPAH][MeOAc] after H_2S reaction.

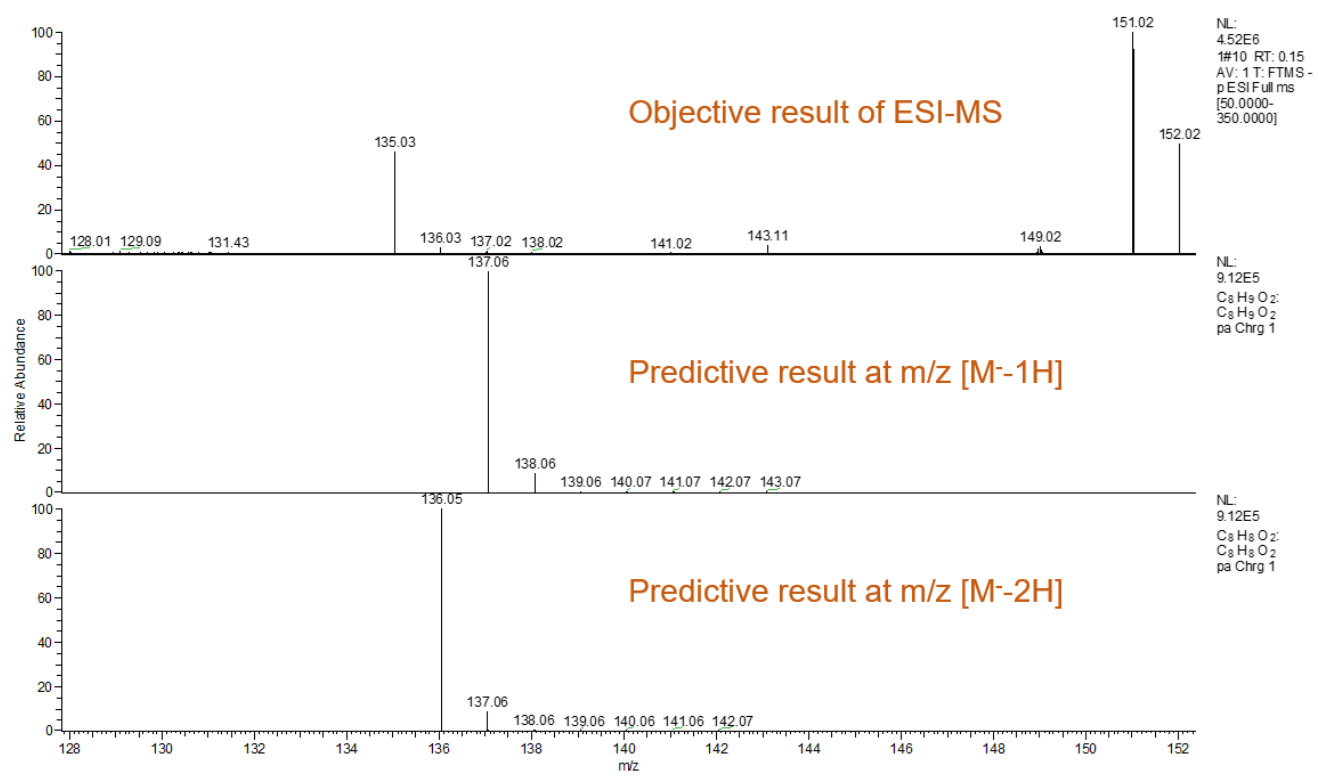


Figure S10. ESI-MS of styrene oxide (1a) with the catalyst [BDMAEEH][MeOAc] with 10 wt.% H₂O after H₂S reaction.

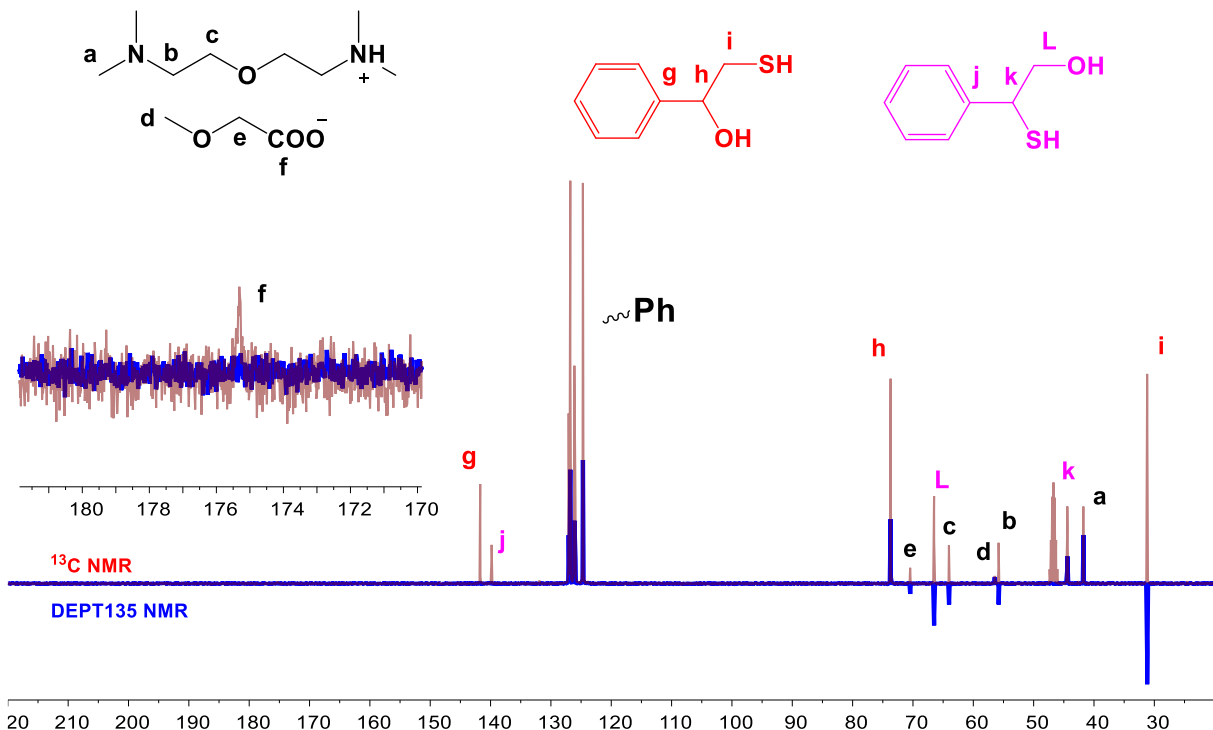


Figure S11. ^{13}C NMR of styrene oxide (**1a**) with the catalyst [BDMAEEH][MeOAc] with 10 wt.% H_2O after H_2S reaction.

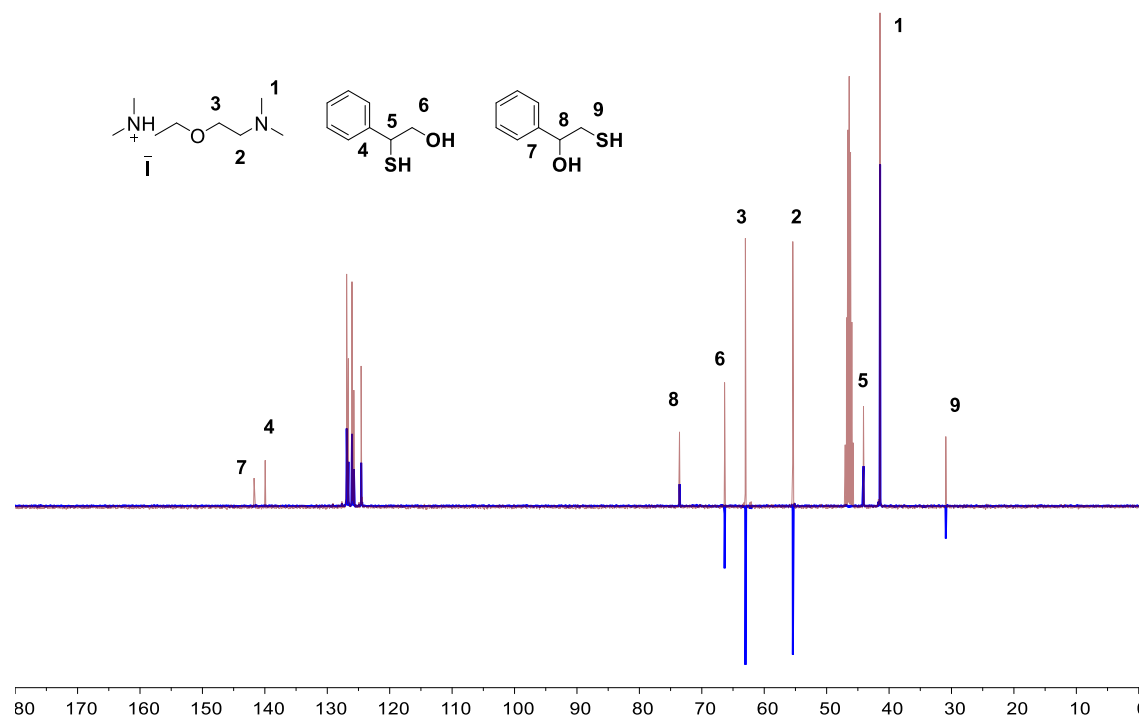


Figure S12. ^{13}C NMR and Dept135 of styrene oxide (**1a**) with [BDMAEEH][I] after H_2S reaction at 30 $^\circ\text{C}$, 2h, and 50 mol% catalyst loading.

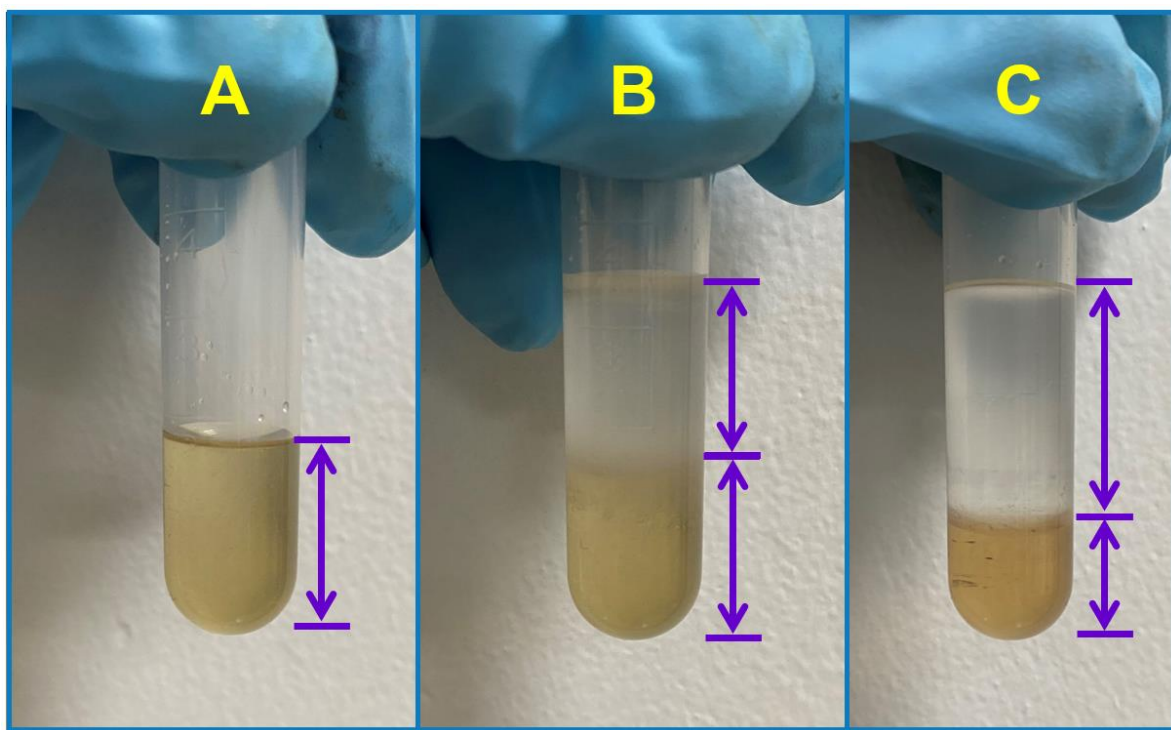


Figure S13. Water extraction for H_2S /epoxy reaction system.

A: Untreated system; B: Same volume of water addition; C: Centrifugation after water extraction.

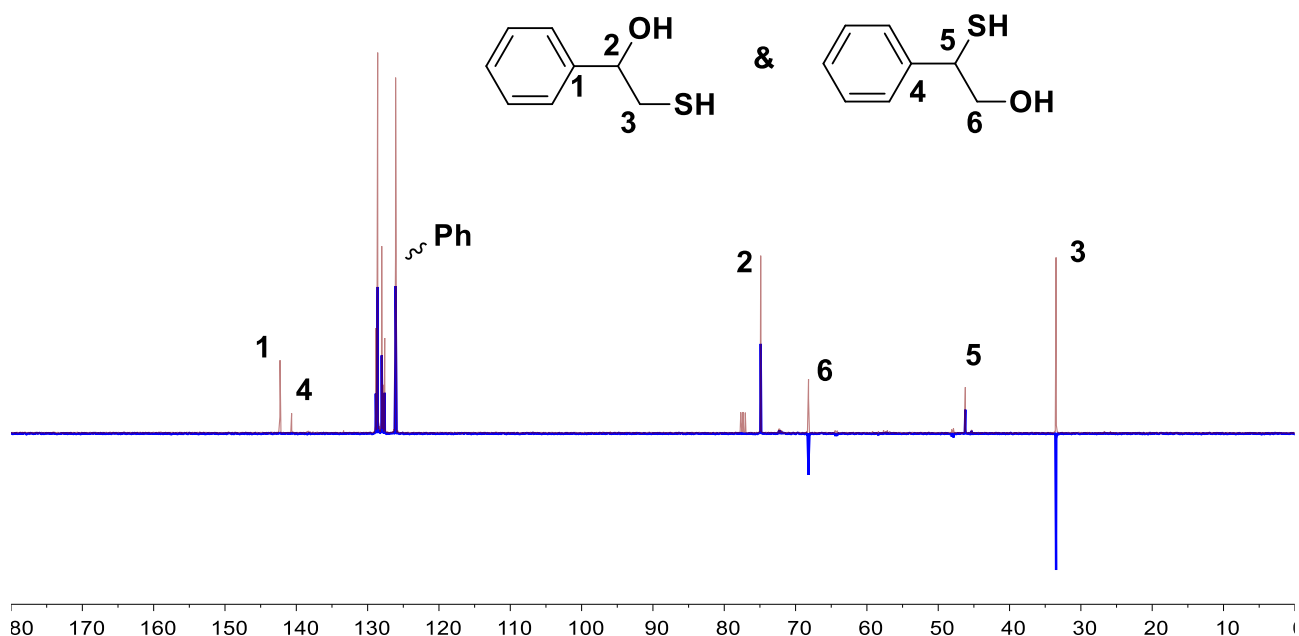


Figure S14. ^{13}C NMR and dept135 NMR of lower phase after water extraction.

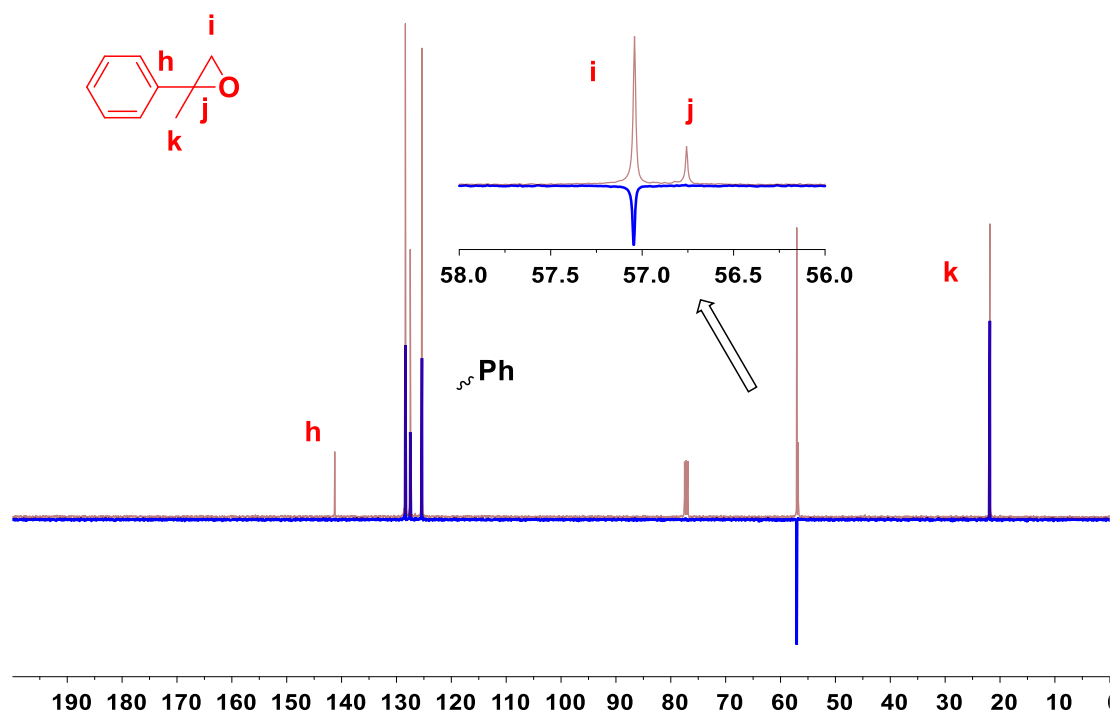


Figure S15. ^{13}C NMR and dept135 NMR of 2-phenylpropylene oxide (2a).

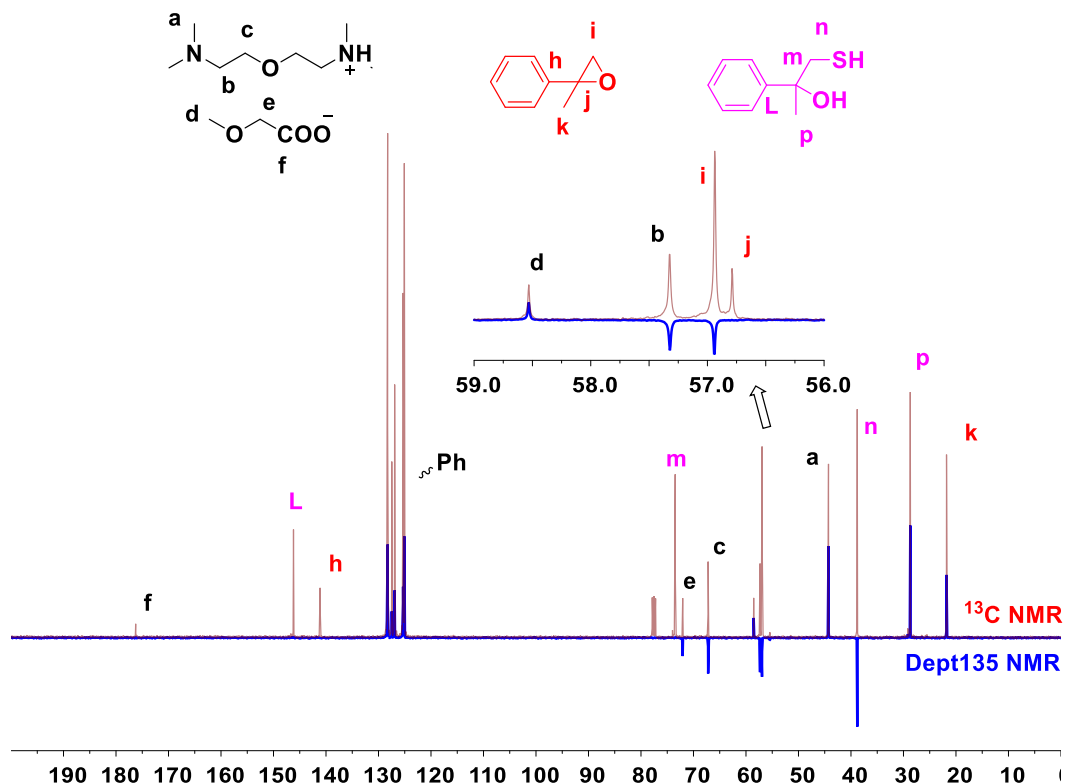


Figure S16. Dept135 and ^{13}C NMR and of 2-phenylpropylene oxide (2a) in [BDMAEEH][MeOAc] after the reaction with H_2S at 30 °C for 2.0 h.

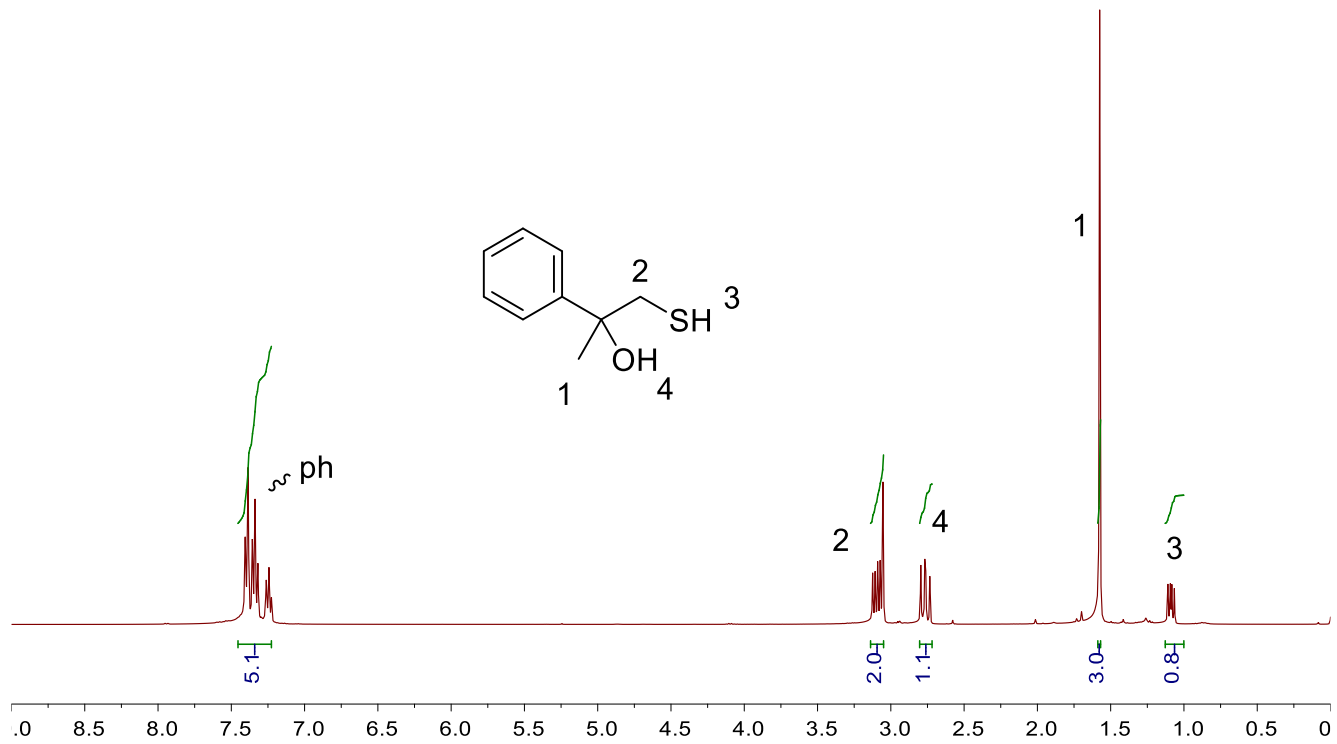


Figure S17. ^1H NMR of 2b.

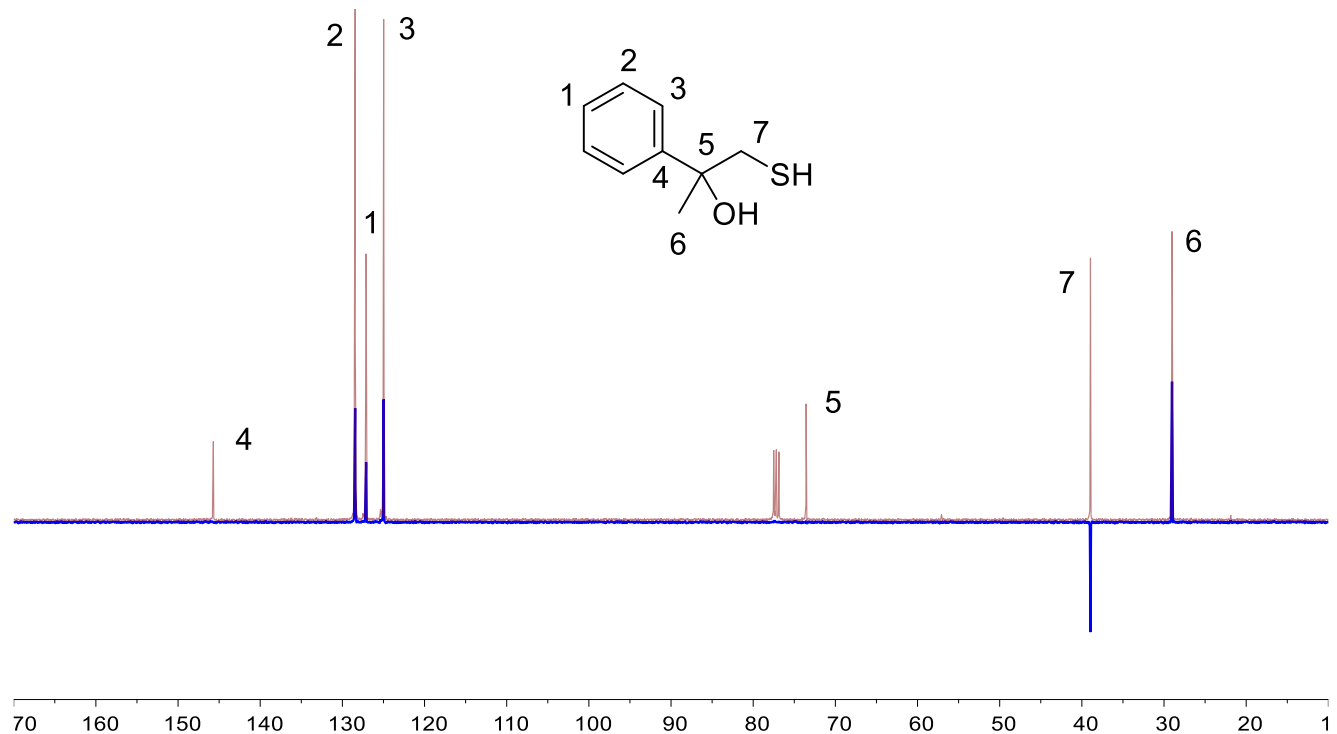


Figure S18. ^{13}C NMR and dept135 NMR of 2b.

25 #18 RT: 0.25 AV: 1 NL: 6.69E7
T: FTMS - p ESI Full ms [50.0000-500.0000]

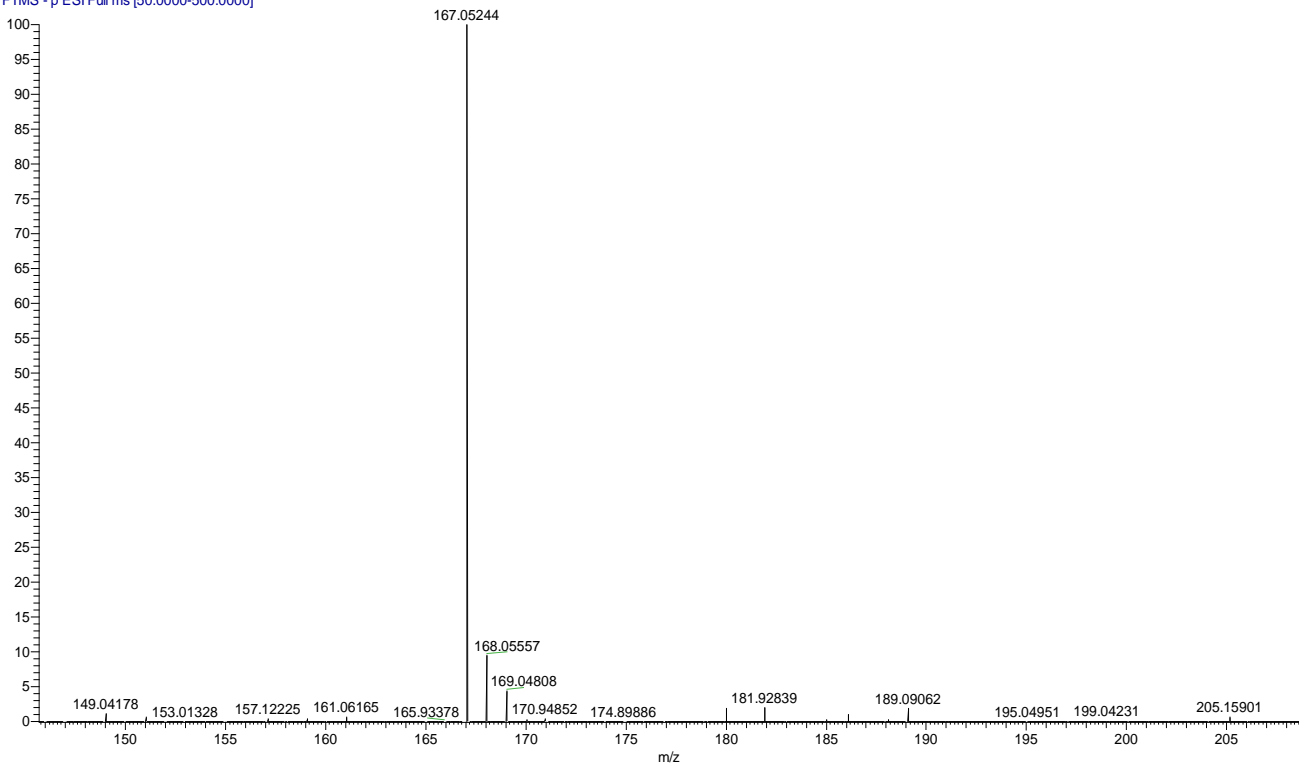


Figure S19. ESI-MS of (2b) at m/z $[M^-1]$.

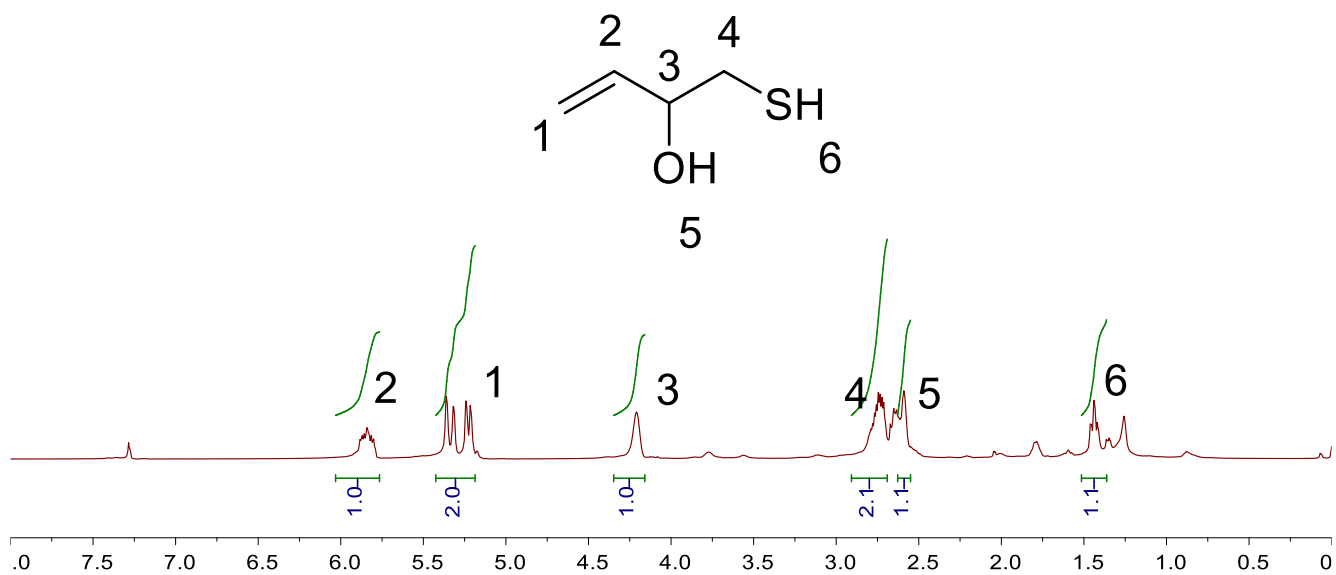


Figure S20. ^1H NMR of 3b.

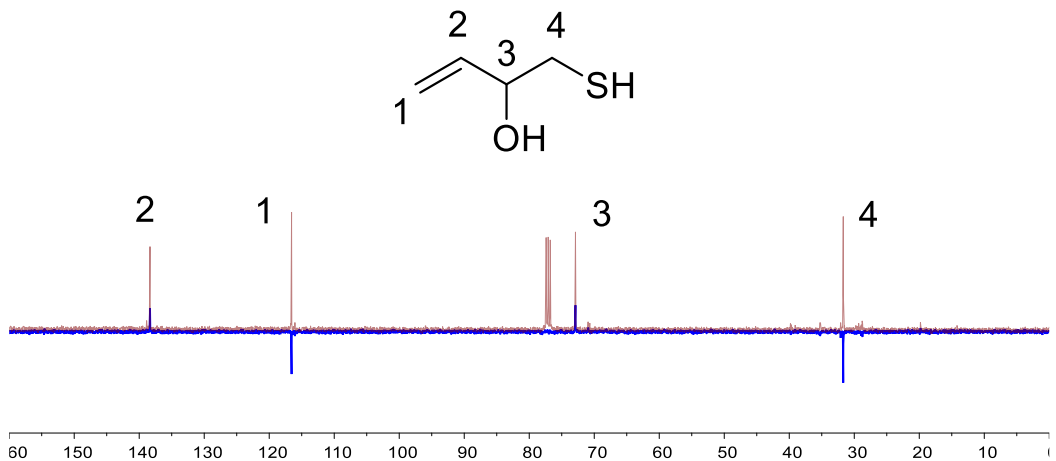


Figure S21. ^{13}C NMR of 3b.

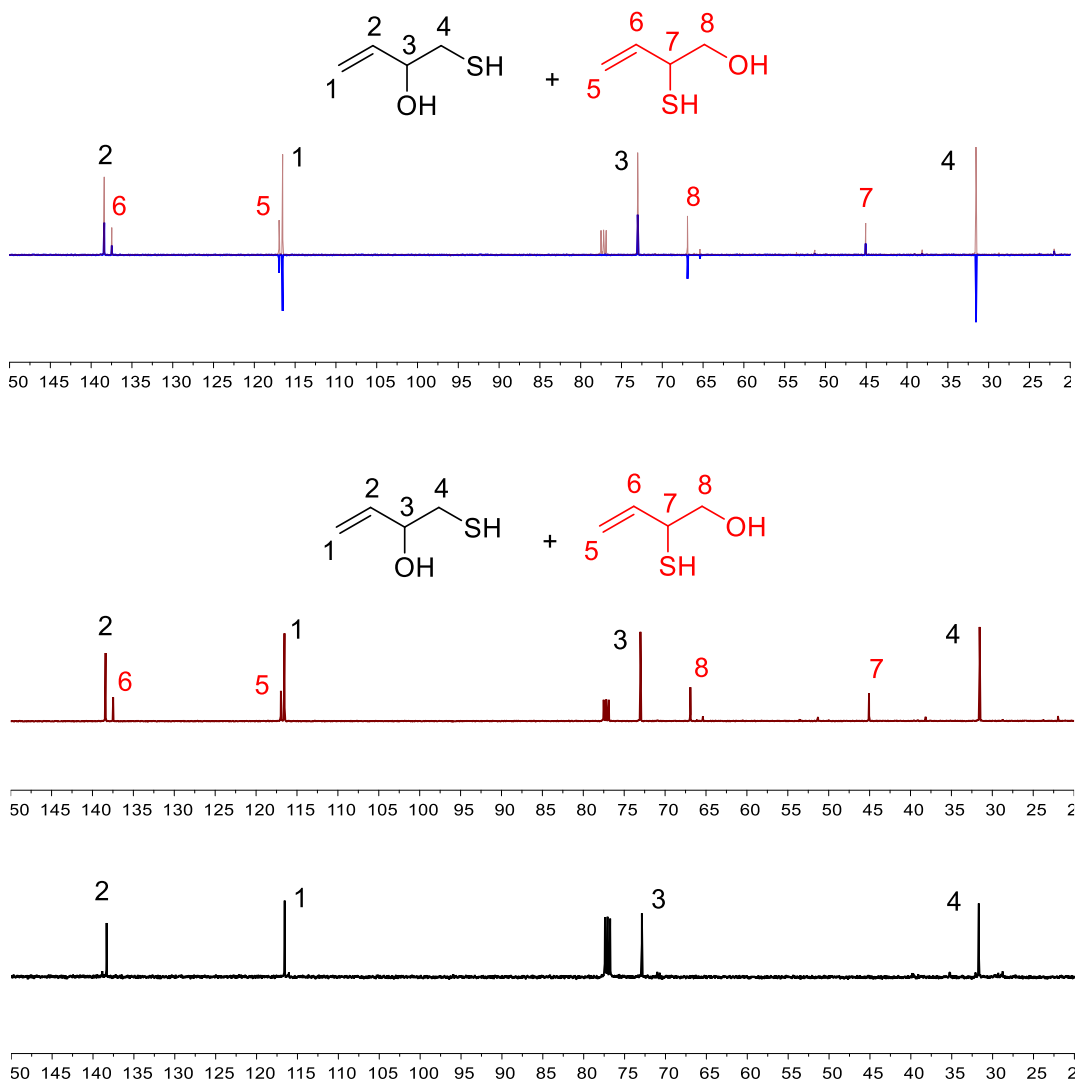


Figure S22. ^{13}C NMR of 3b+3c.

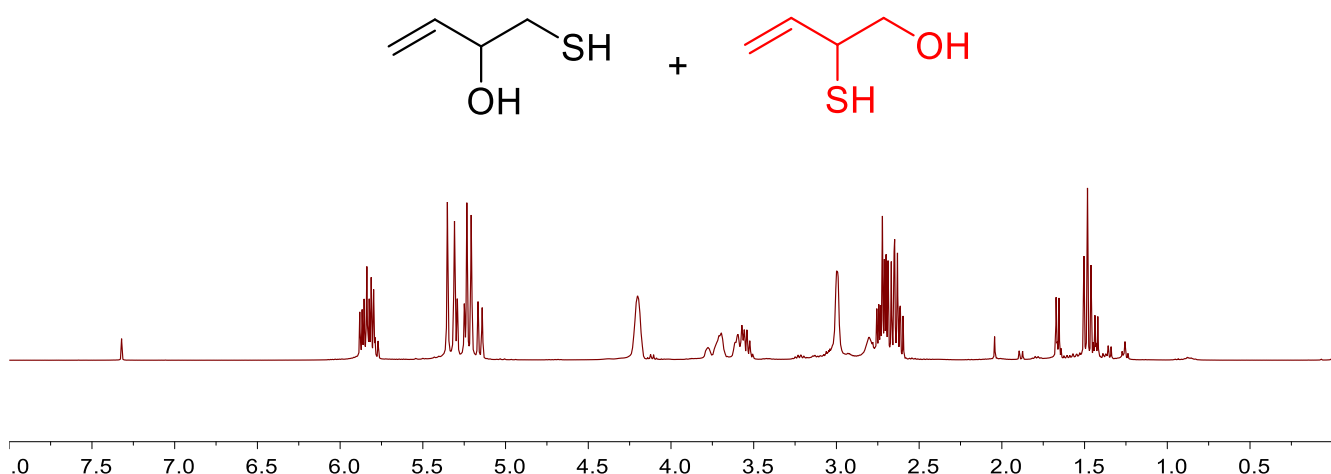


Figure S23. ^1H NMR of 3b+3c.

21 #10 RT: 0.14 AV: 1 NL: 1.07E7
T: FTMS - p ESI Full ms [50.0000-500.0000]

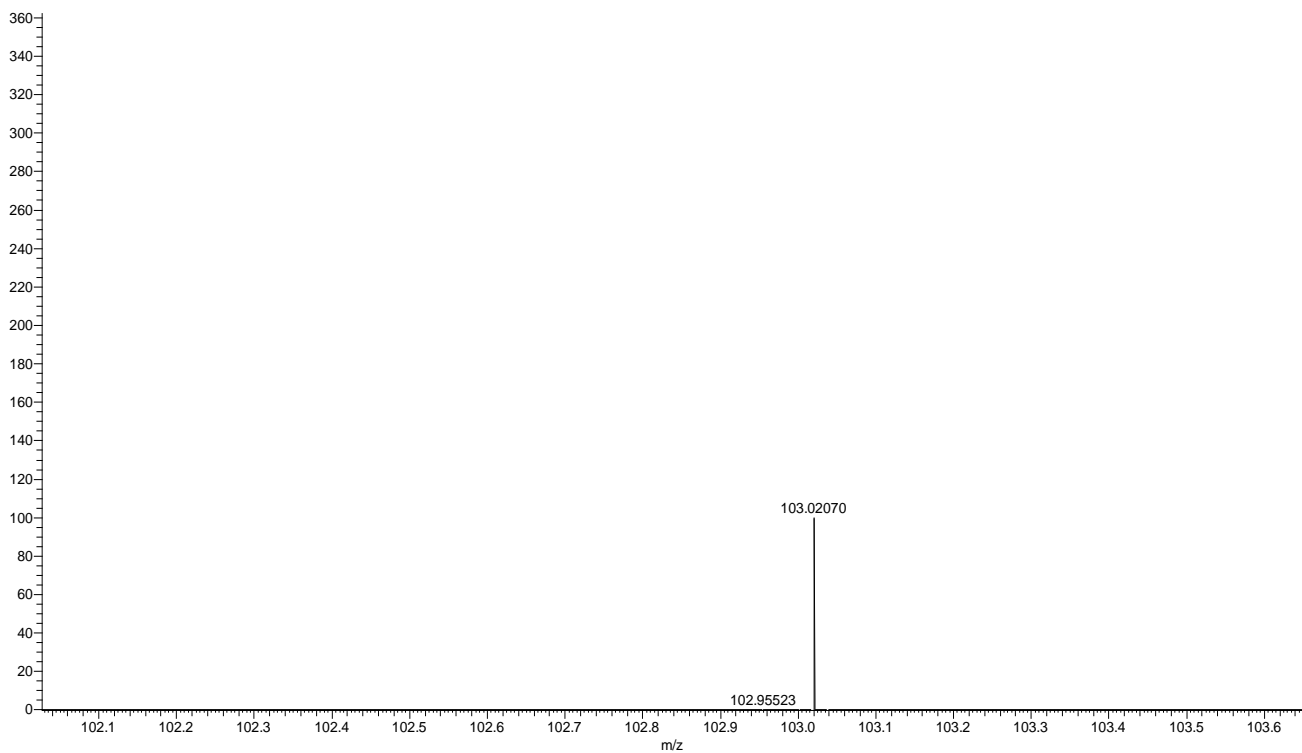


Figure S24. ESI-MS of 3b.

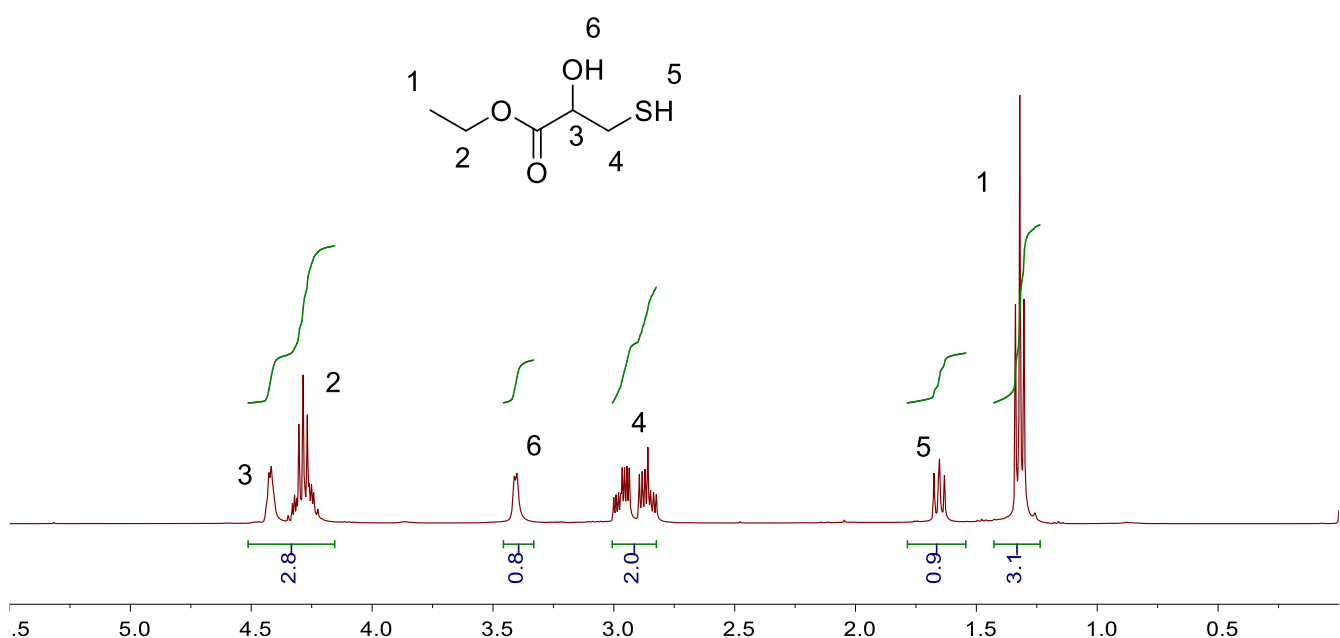


Figure S25. ^1H NMR of 4b.

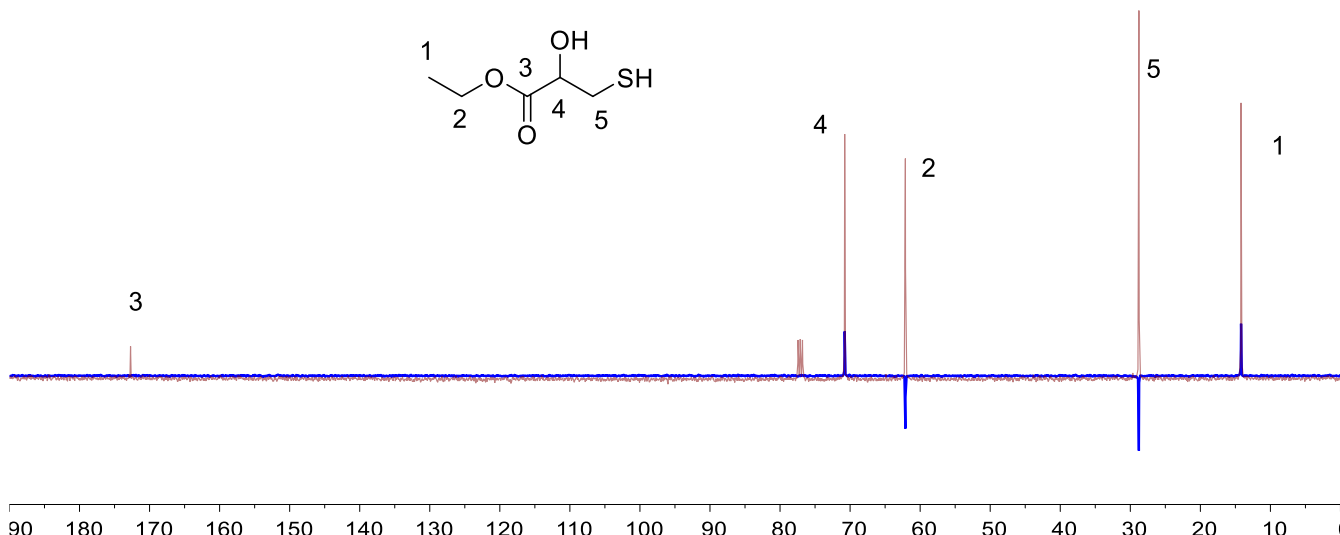


Figure S26. ^{13}C NMR of 4b.

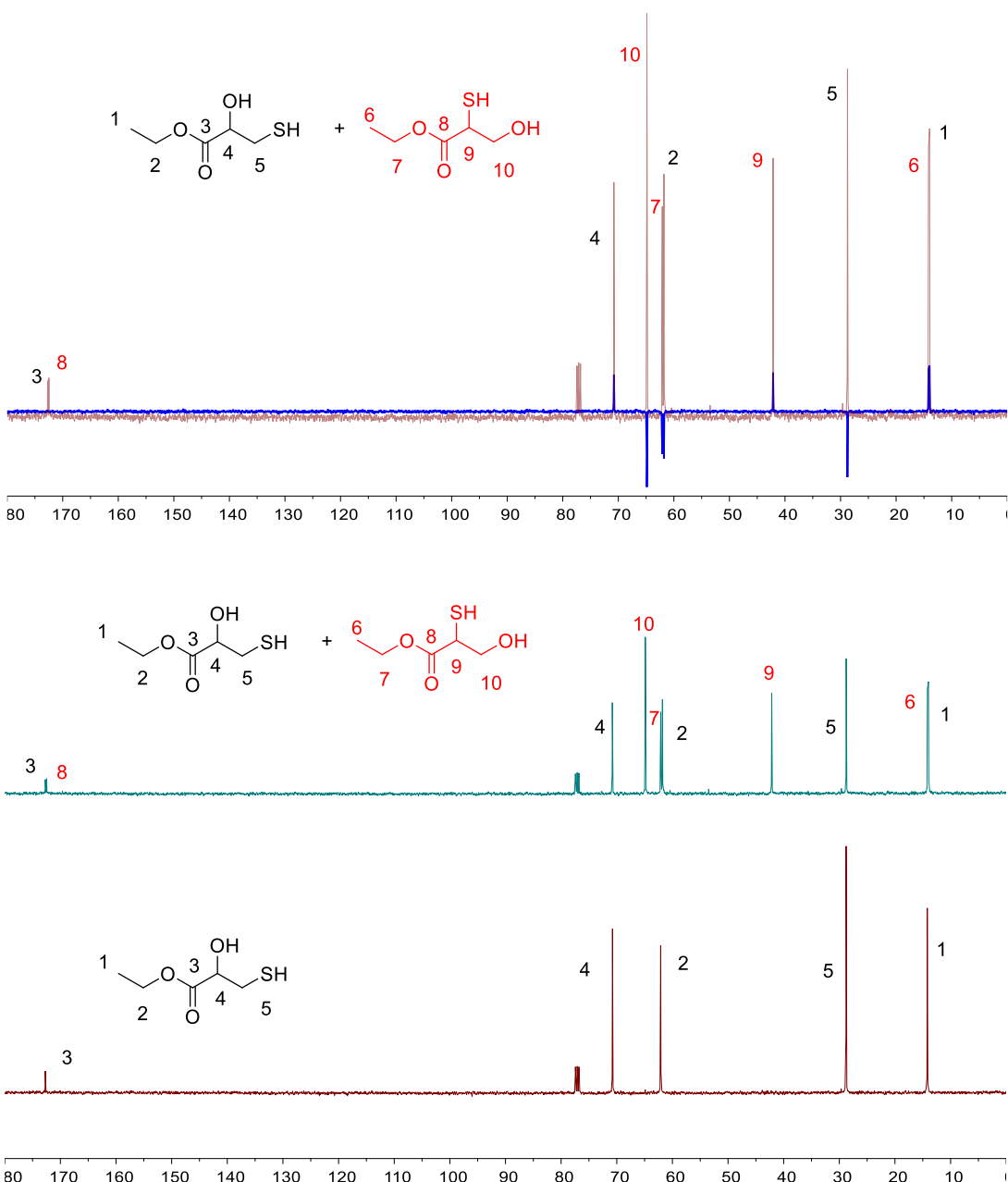


Figure S27. ^{13}C NMR of 4b+4c.

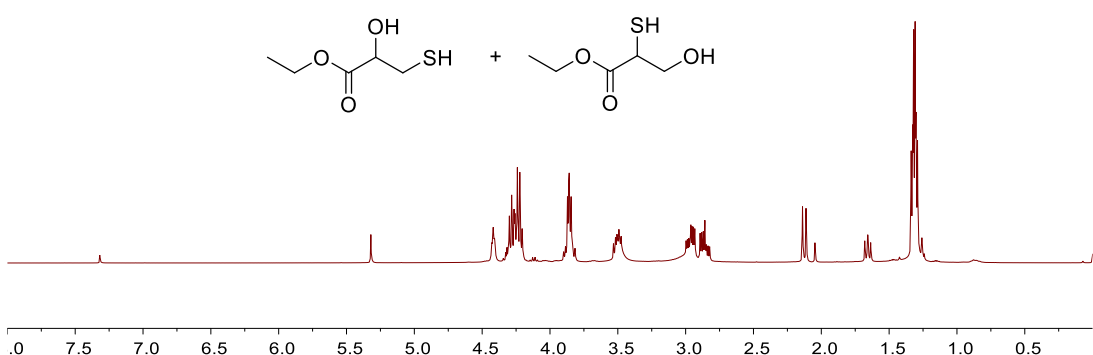


Figure S28. ^1H NMR of 4b+4c.

20_20201222154540 #13 RT: 0.18 AV: 1 NL: 2.33E8
T: FTMS + p ESI Full ms [50.0000-500.0000]

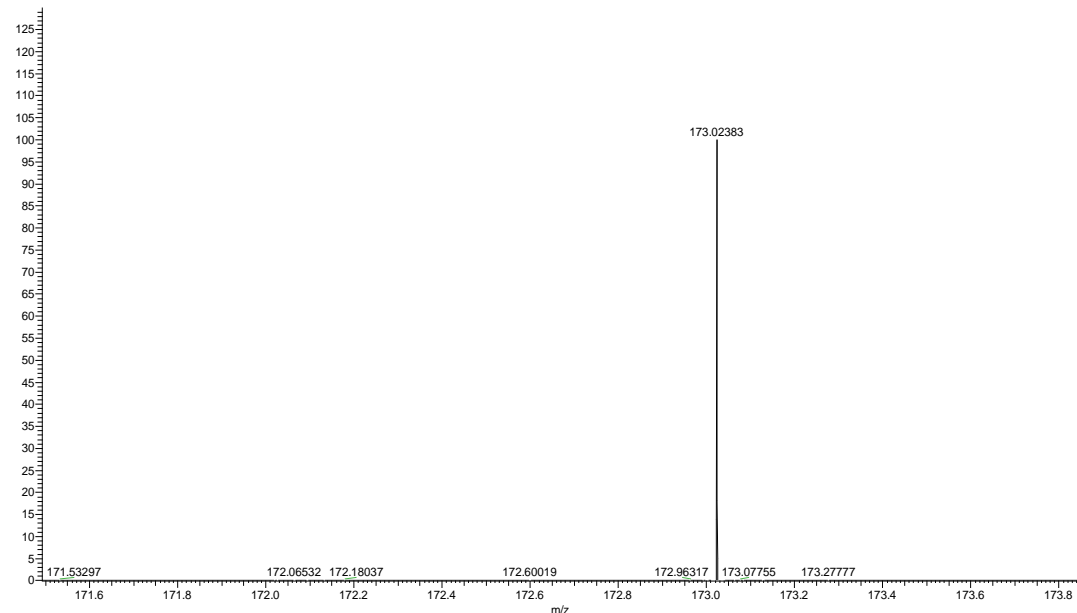


Figure S29. ESI-MS of 4b.

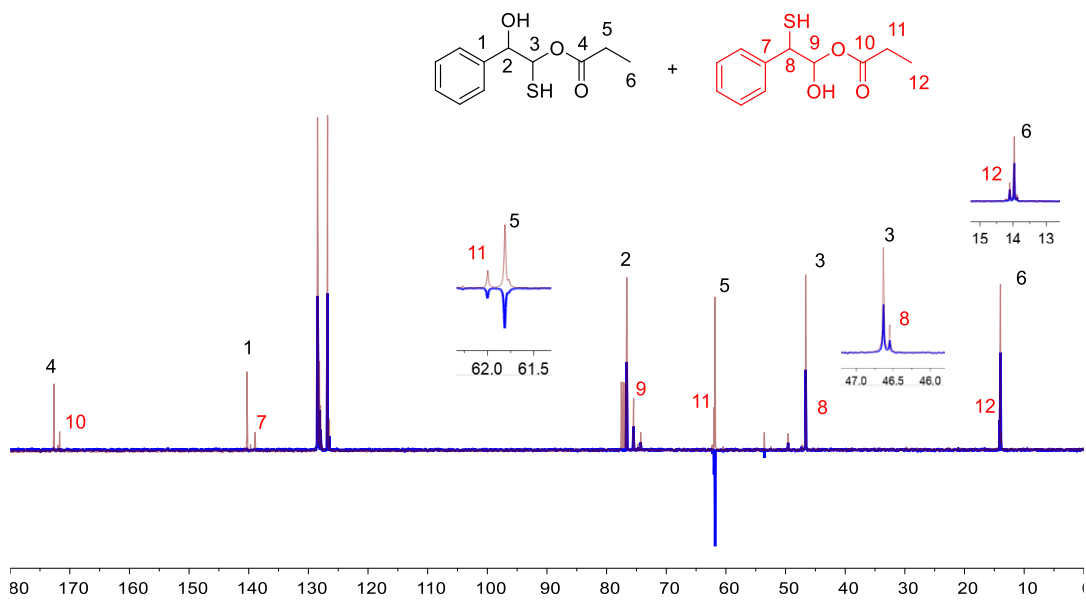


Figure S30. ¹³C NMR of 5b+5c.

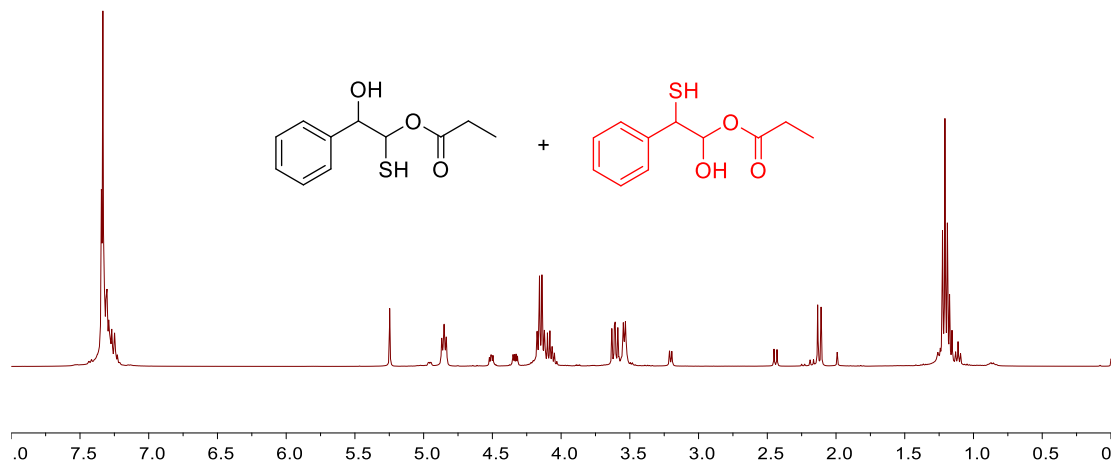


Figure S31. ^1H NMR of 5b+5c.

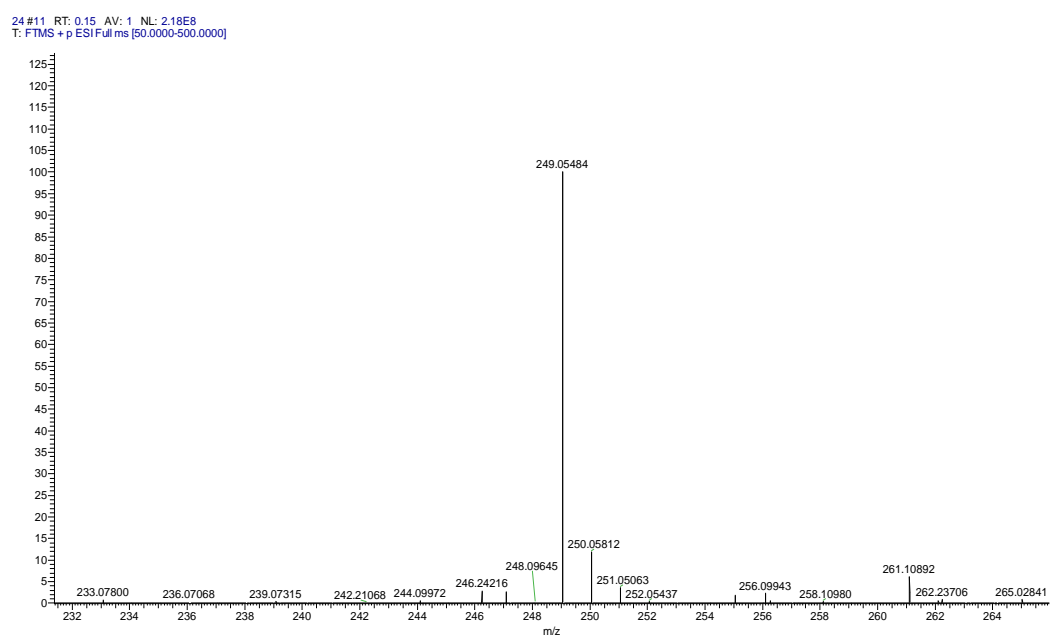


Figure S32. ESI-MS of 5b+5c.

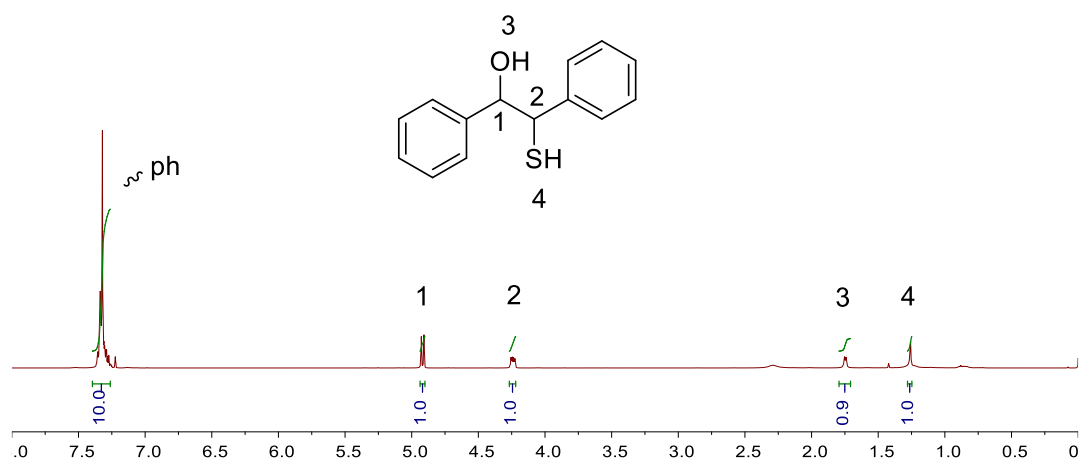


Figure S33. ^1H NMR of 6b.

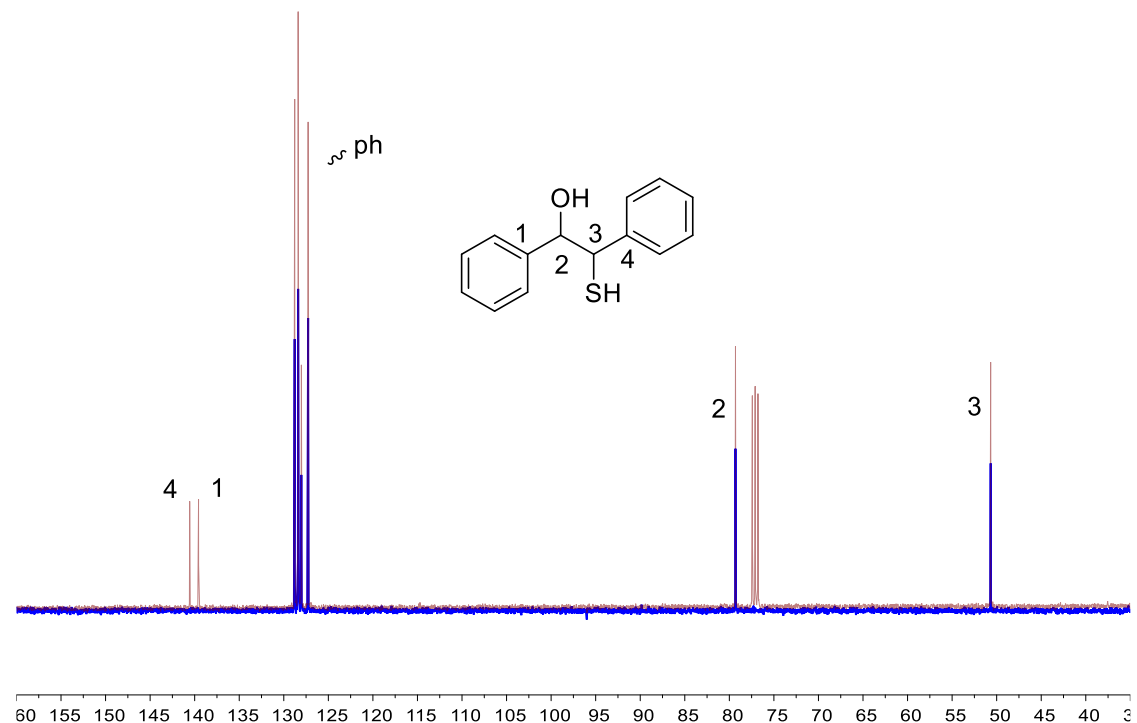


Figure S34. ^{13}C NMR of 6b.

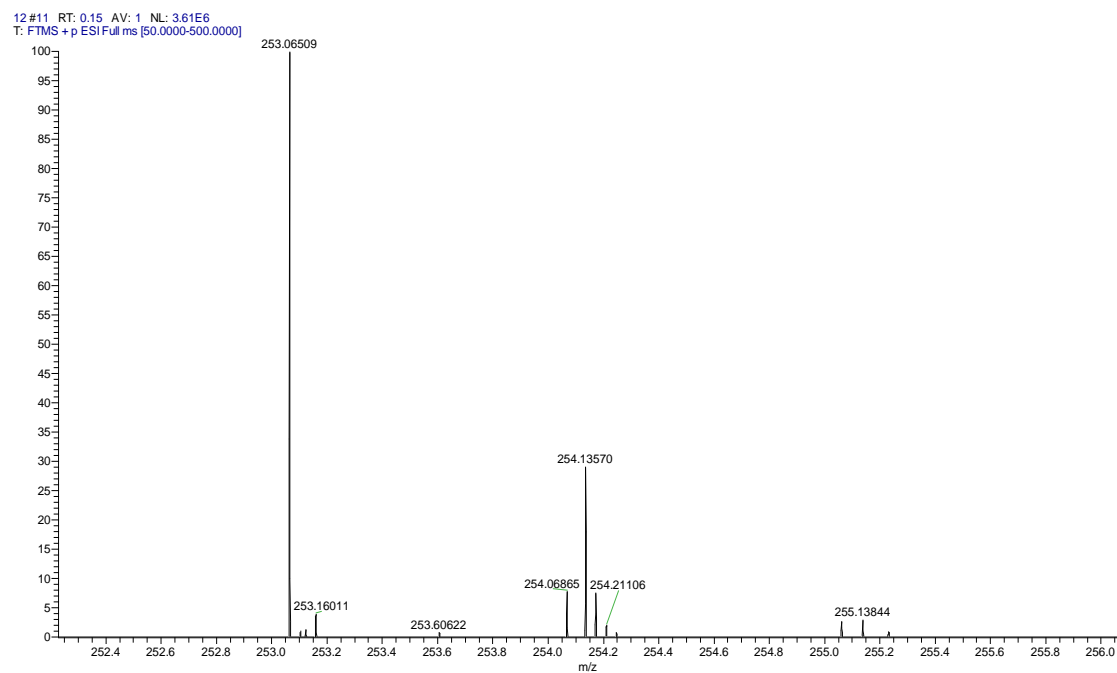


Figure S35. ESI-MS of 6b.

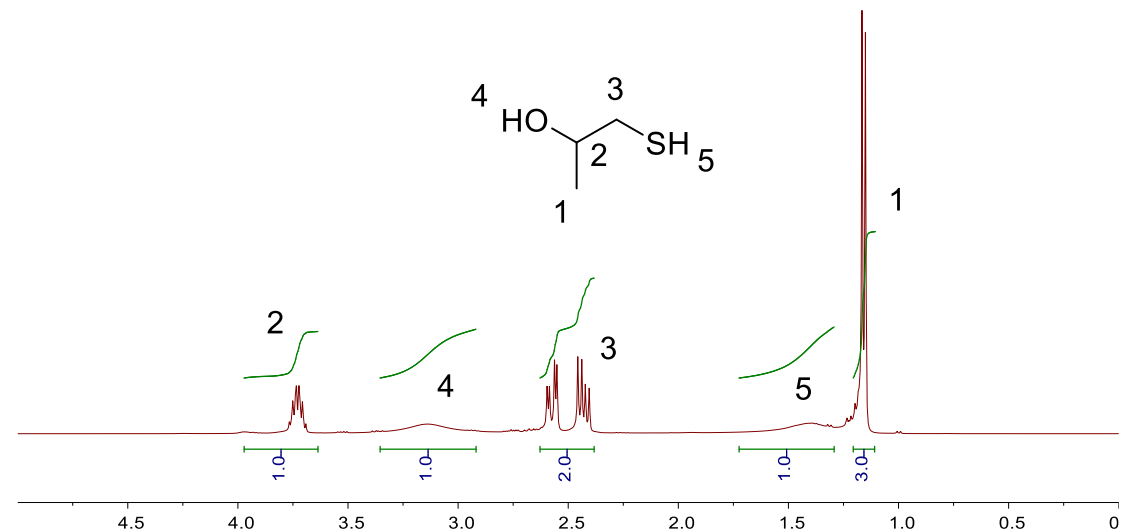


Figure S36. ¹H NMR of 7b.

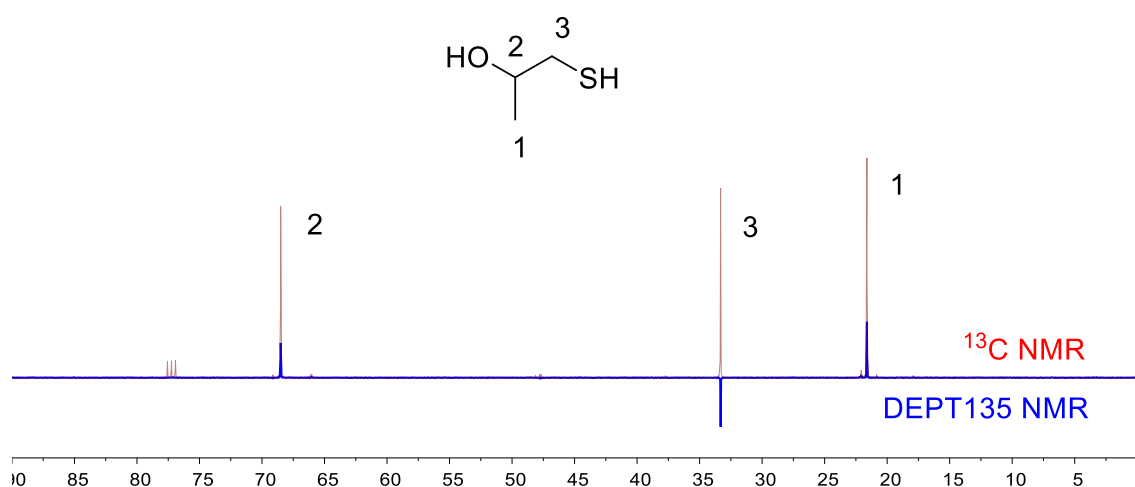


Figure S37. ${}^{13}\text{C}$ NMR of 7b.

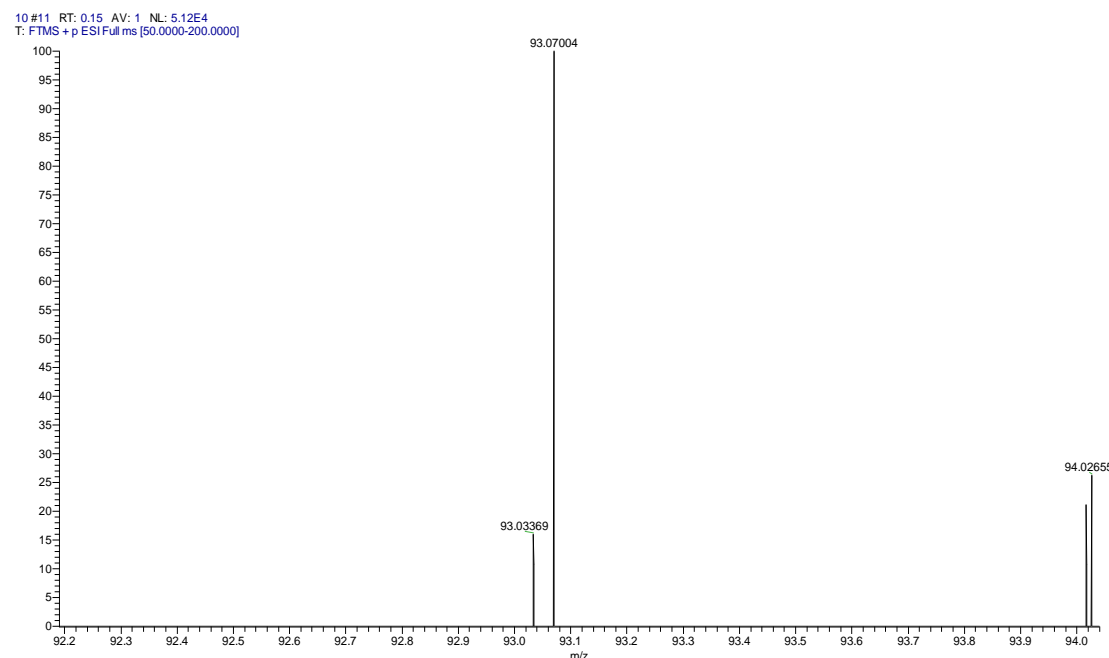


Figure S38. ESI-MS of 7b.

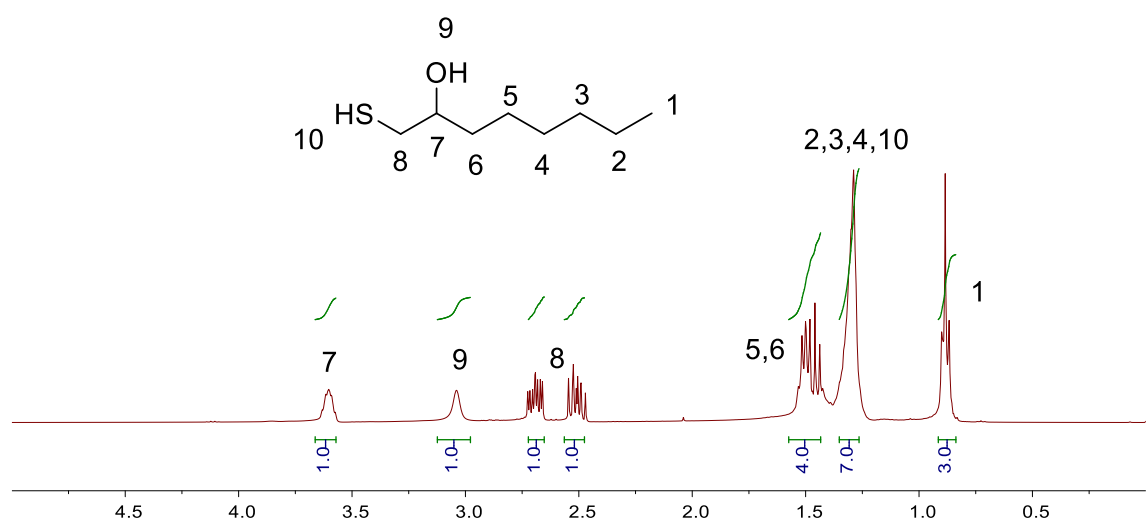


Figure S39. ^1H NMR of 8b.

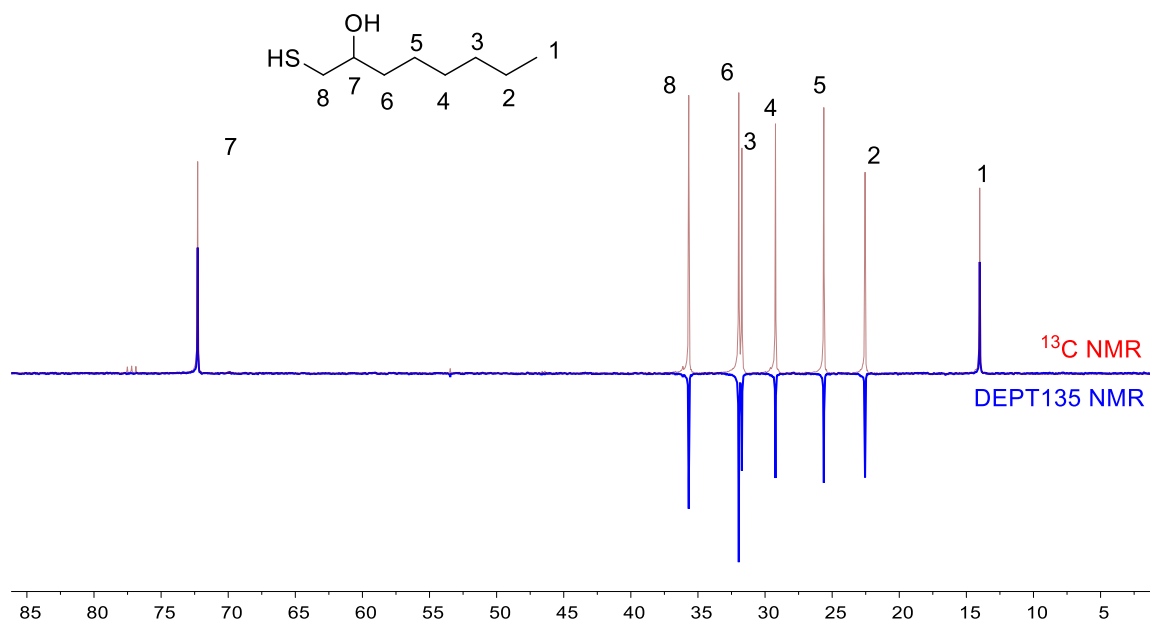


Figure S40. ^{13}C NMR of 8b.

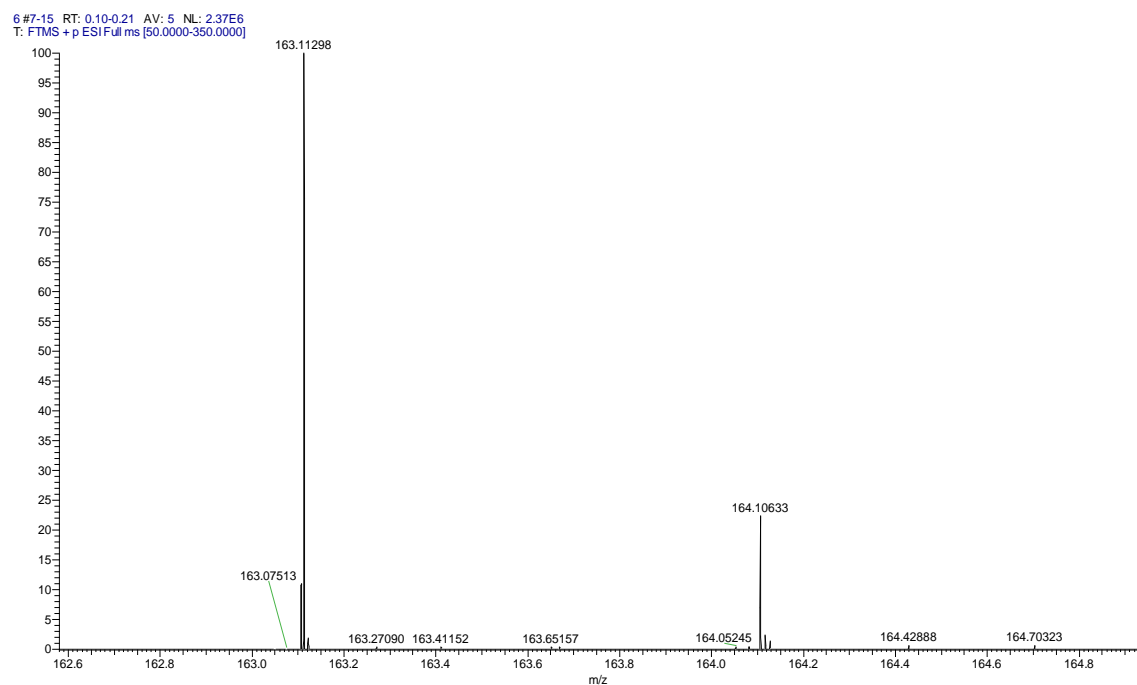


Figure S41. ^{13}C NMR of 8b.

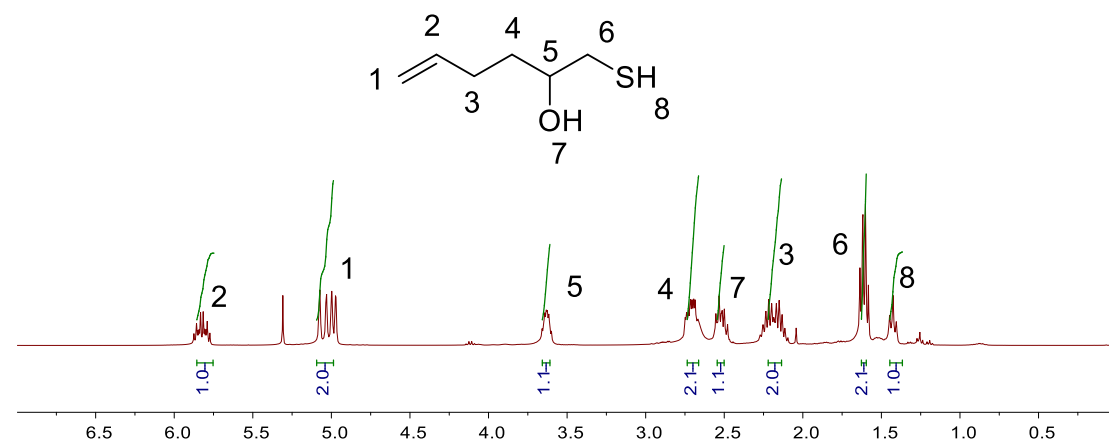


Figure S42. ^1H NMR of 9b.

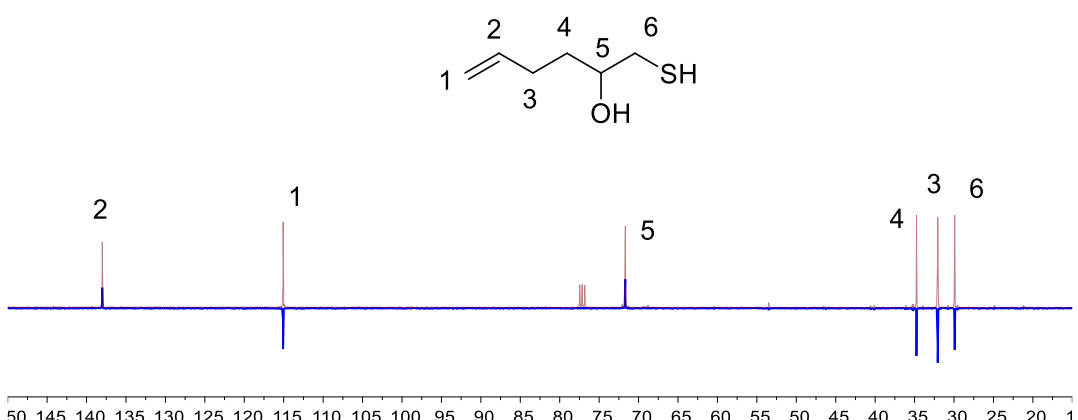


Figure S43. ^{13}C NMR of 9b.

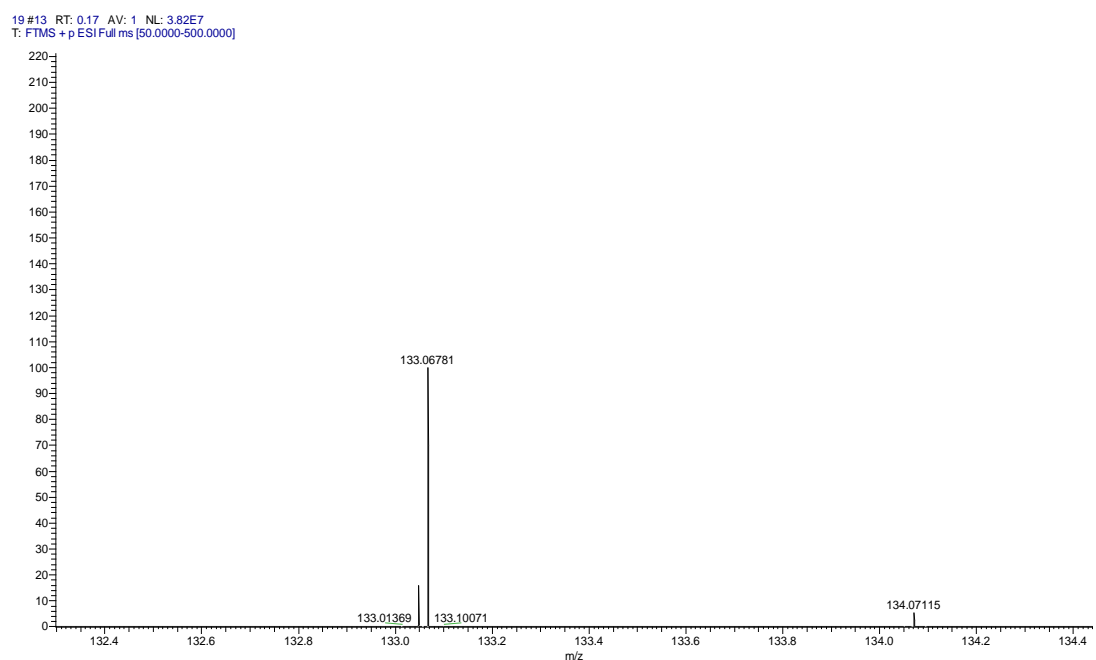


Figure S44. ESI-MS of 9b.

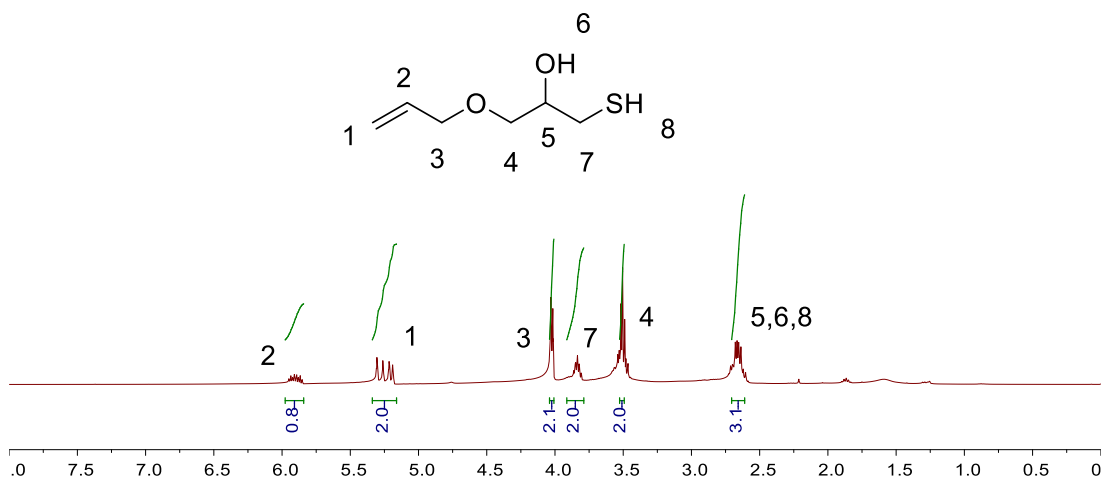


Figure S45. ^1H NMR of 10b.

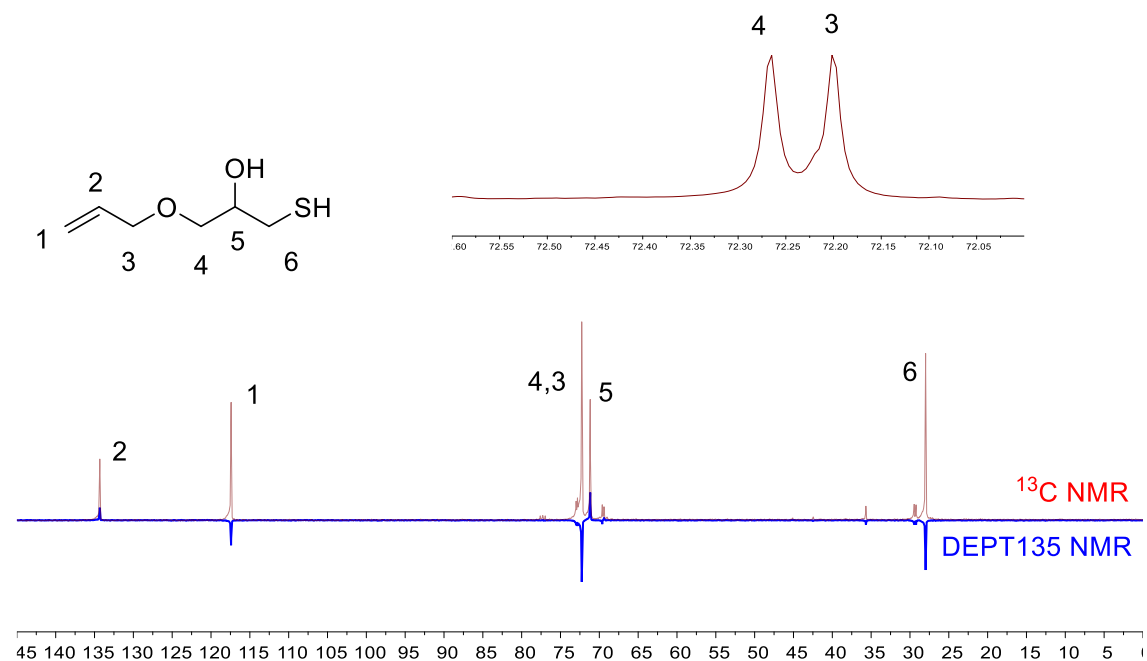


Figure S46. ^{13}C NMR of 10b.

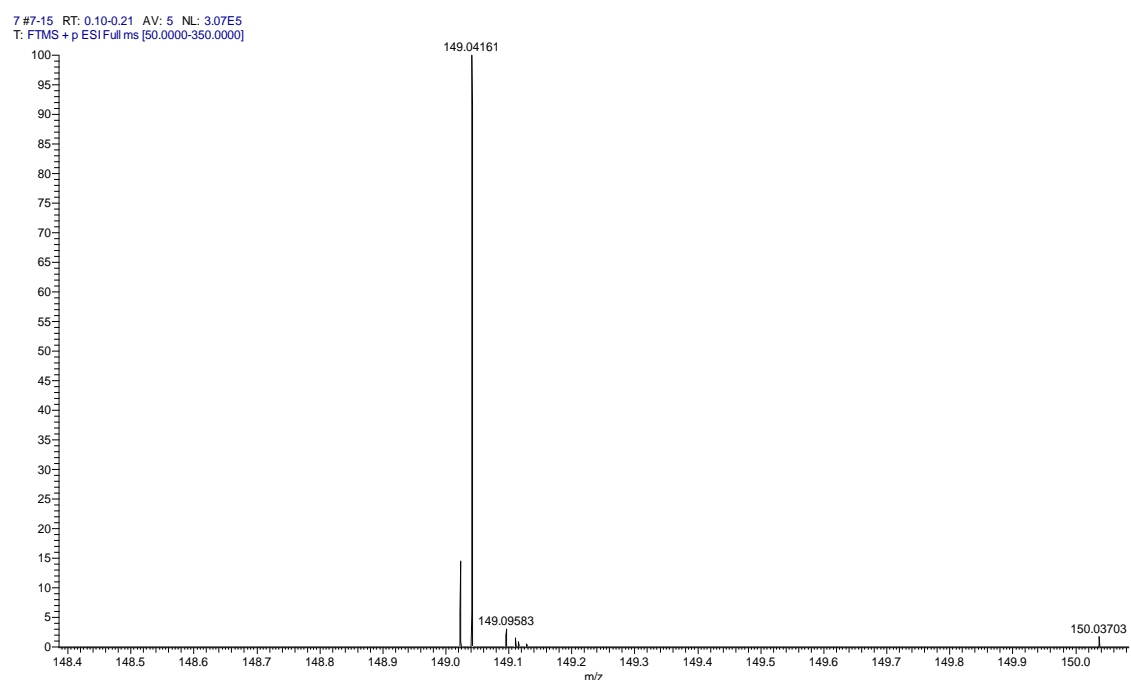


Figure S47. ESI-MS of 10b.

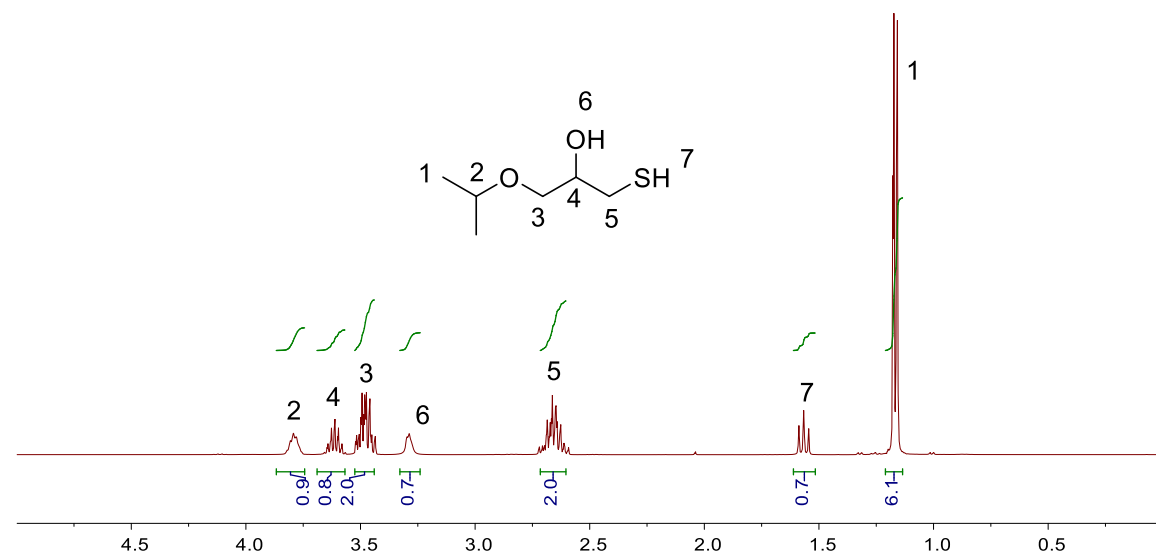


Figure S48. ¹H NMR of 11b.

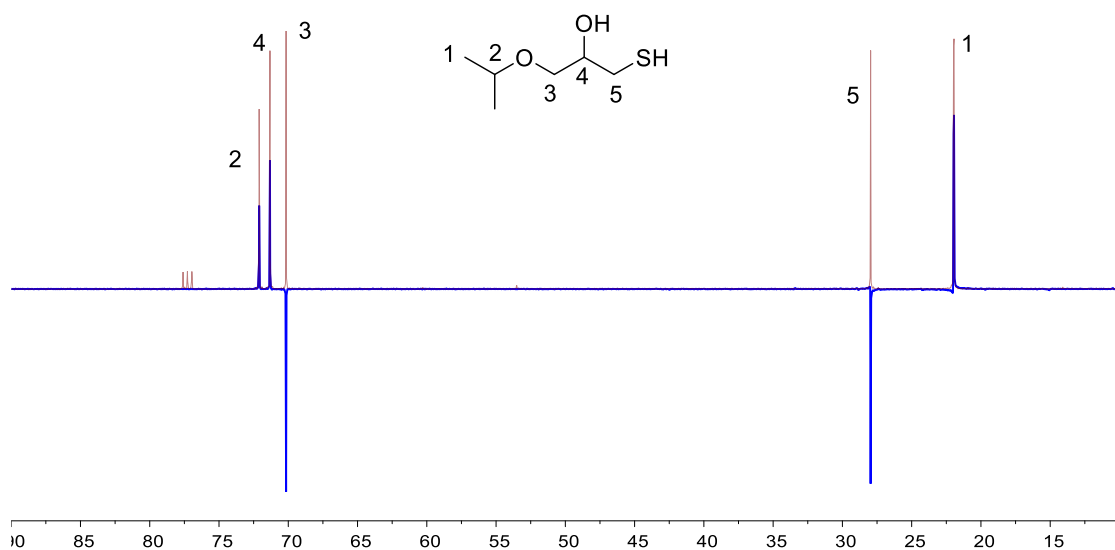


Figure S49. ^{13}C NMR of 11b.

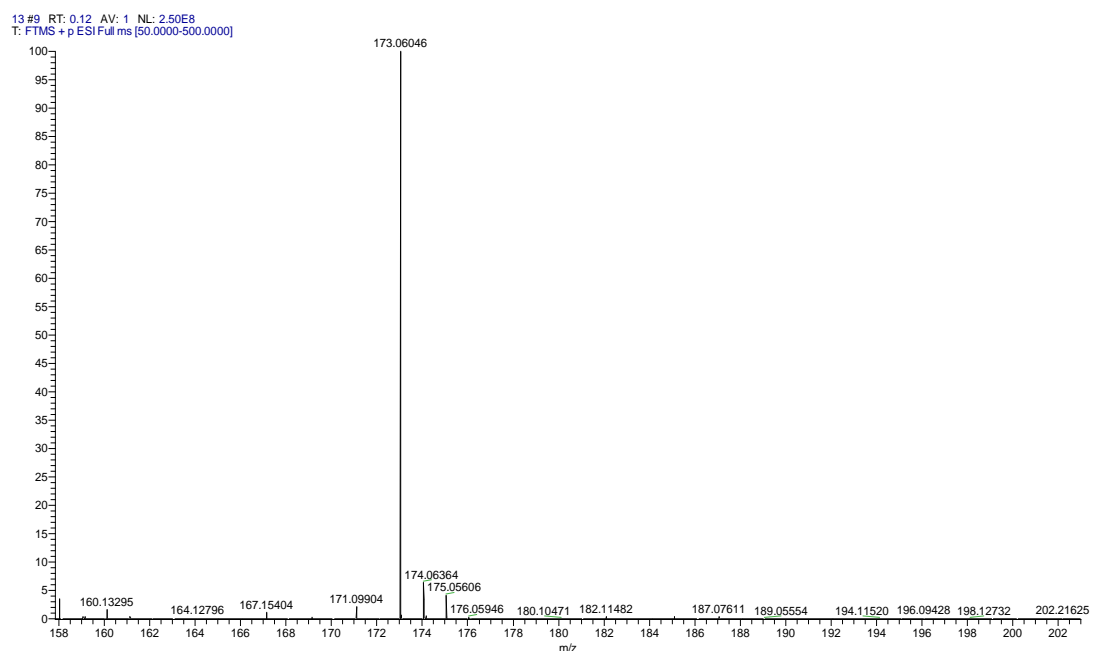


Figure S50. ESI-MS of 11b.

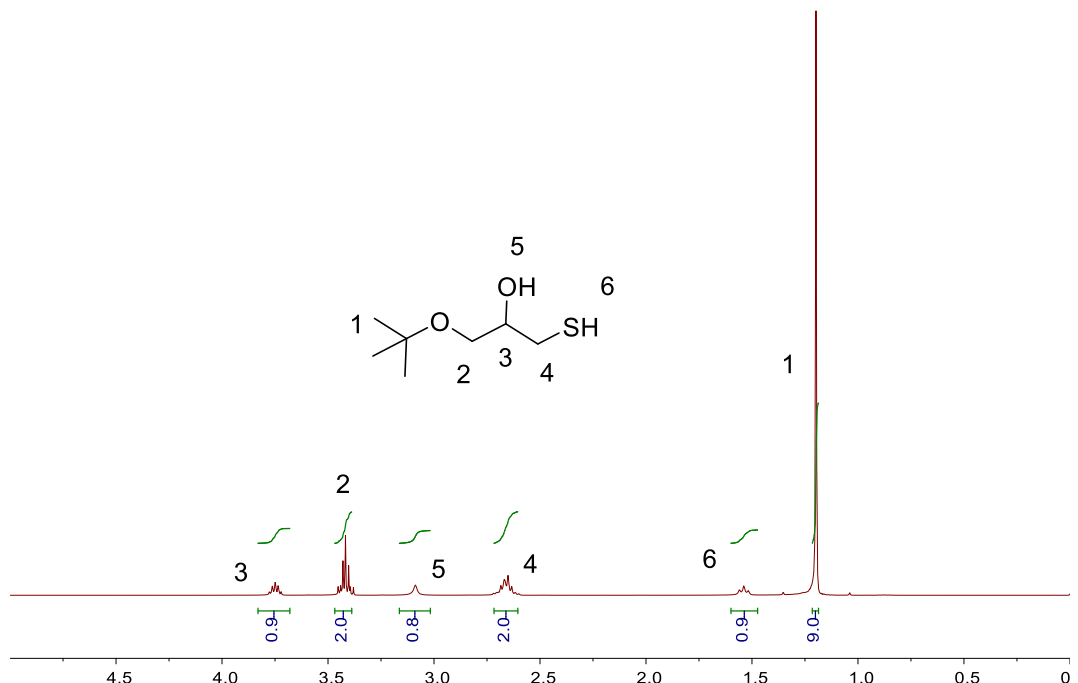


Figure S51. ^1H NMR of 12b.

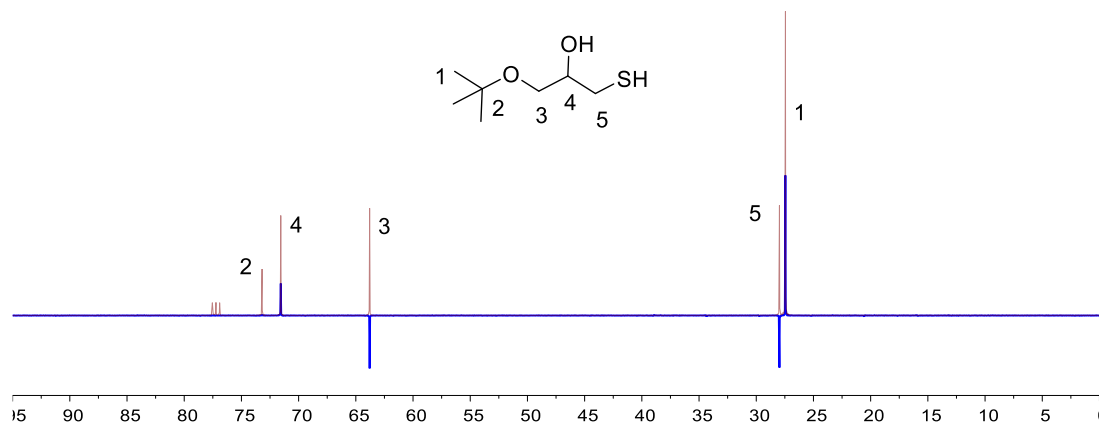


Figure S52. ^{13}C NMR of 12b.

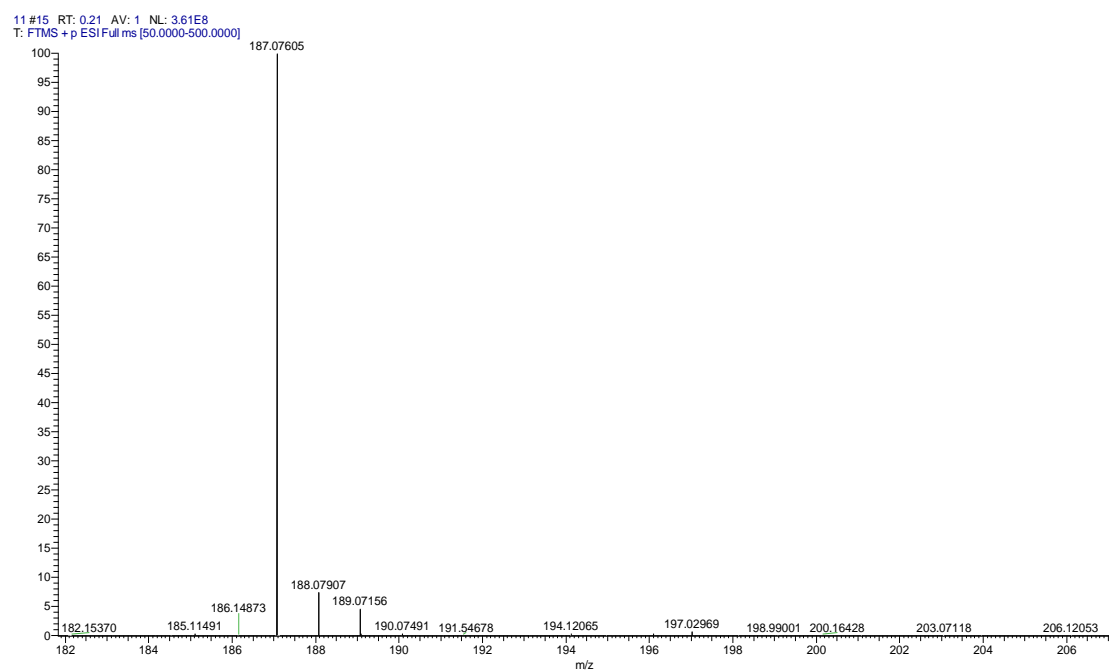


Figure S53. ESI-MS of 12b.

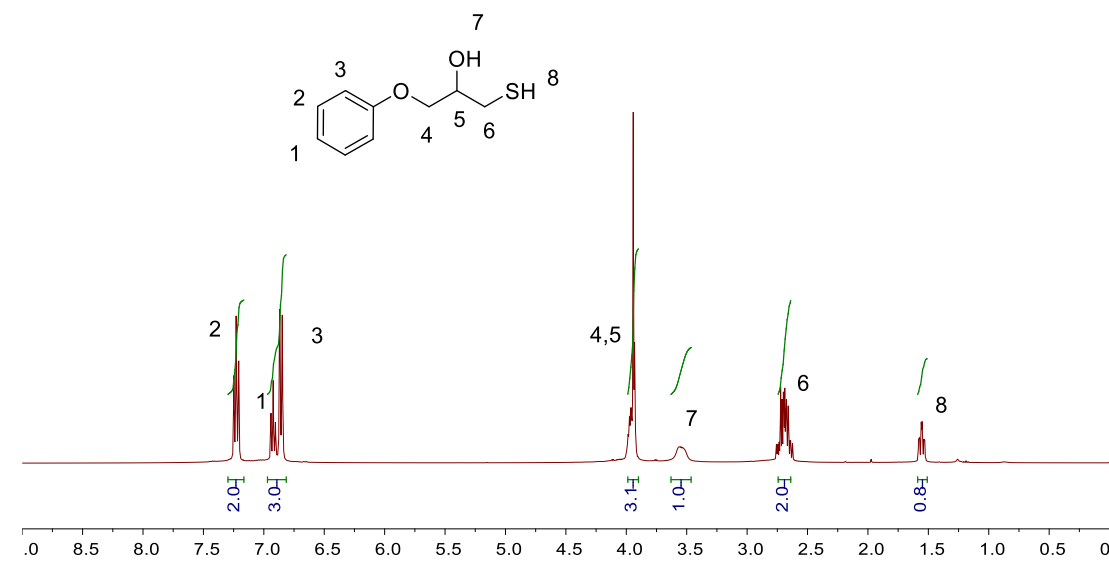


Figure S54. ^1H NMR of 13b.

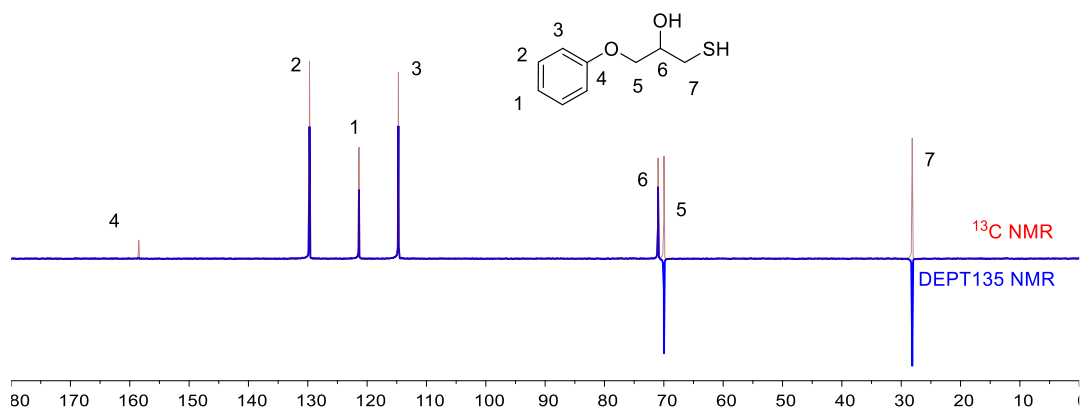


Figure S55. ^{13}C NMR of 13b.

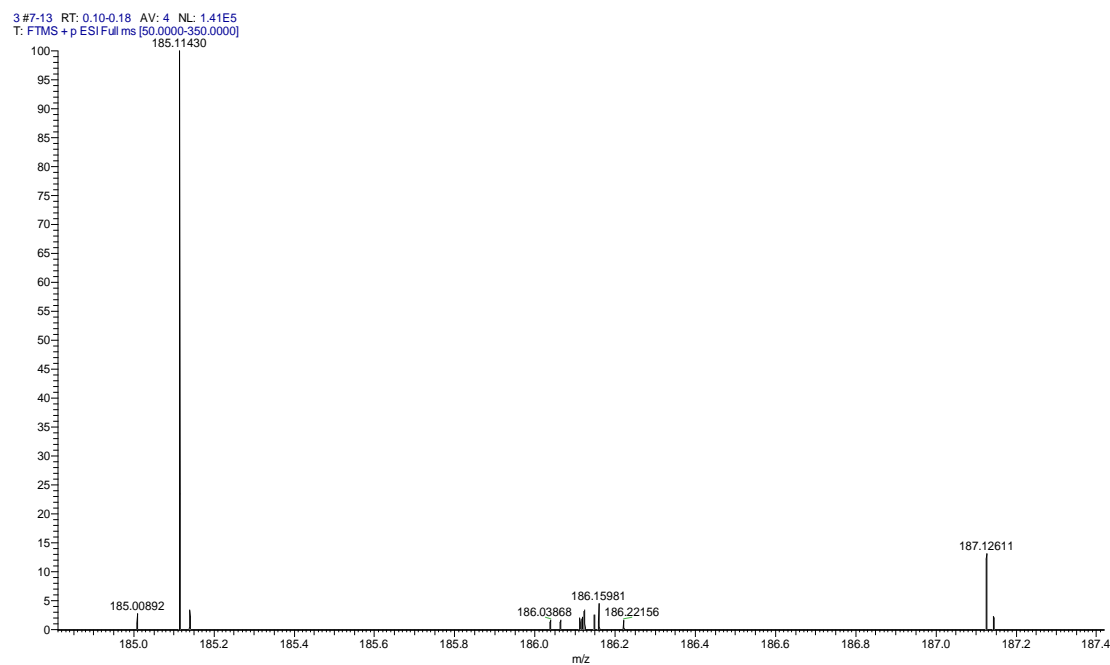


Figure S56. ESI-MS of 13b.

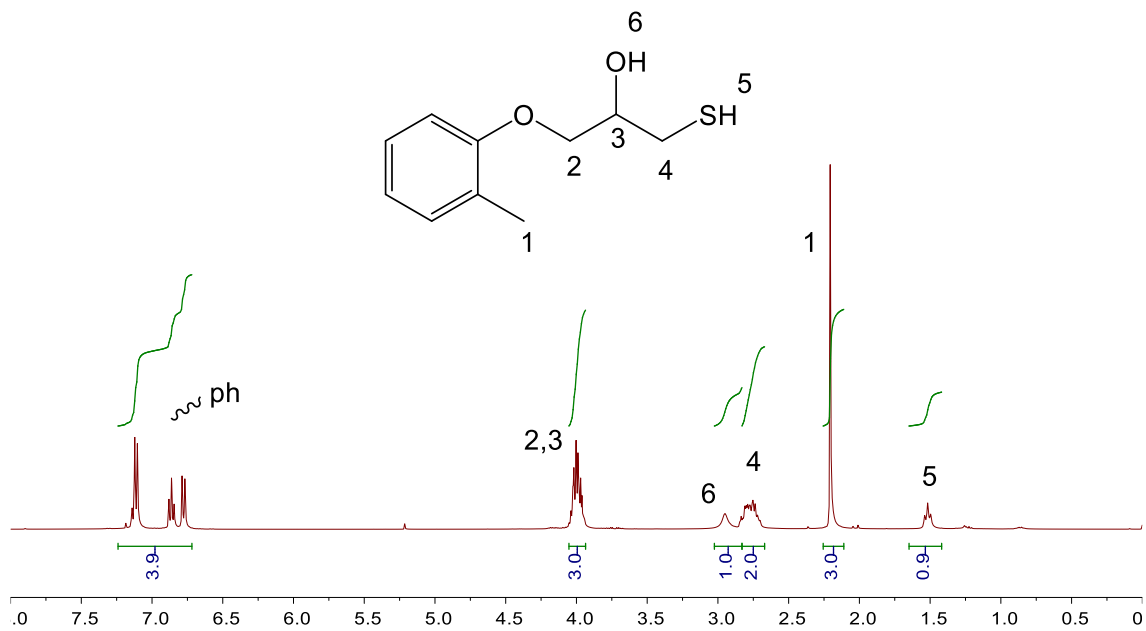


Figure S57. ^1H NMR of 14b.

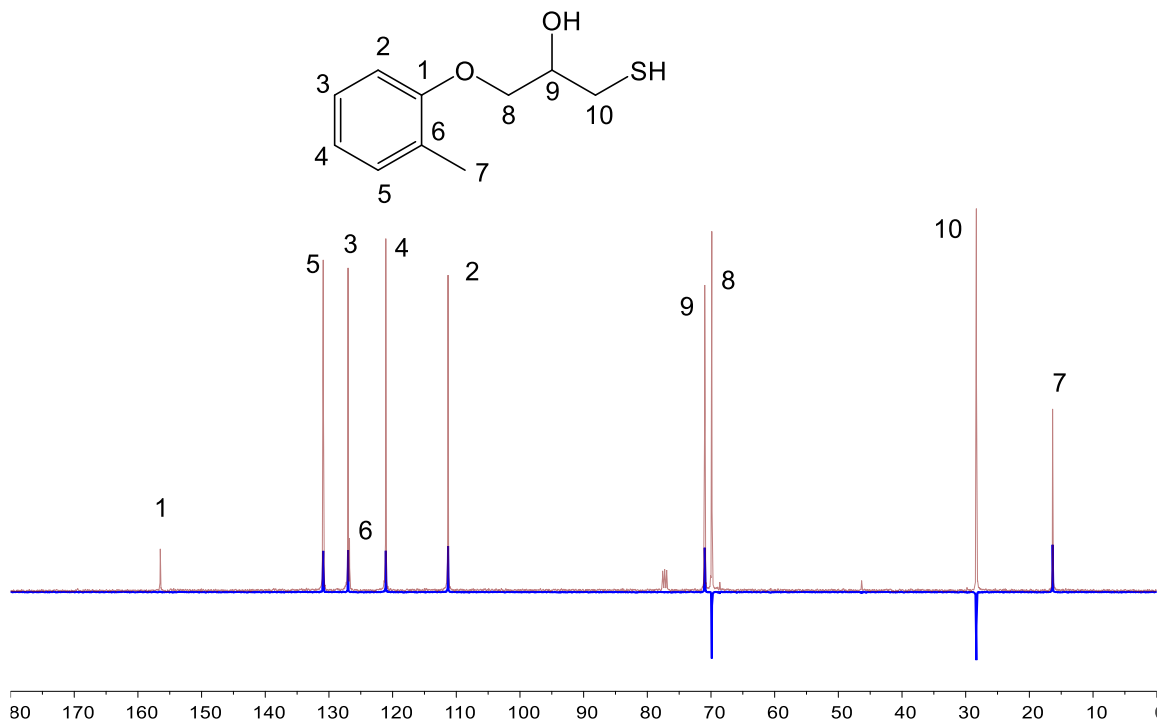


Figure S58. ^{13}C NMR of 14b.

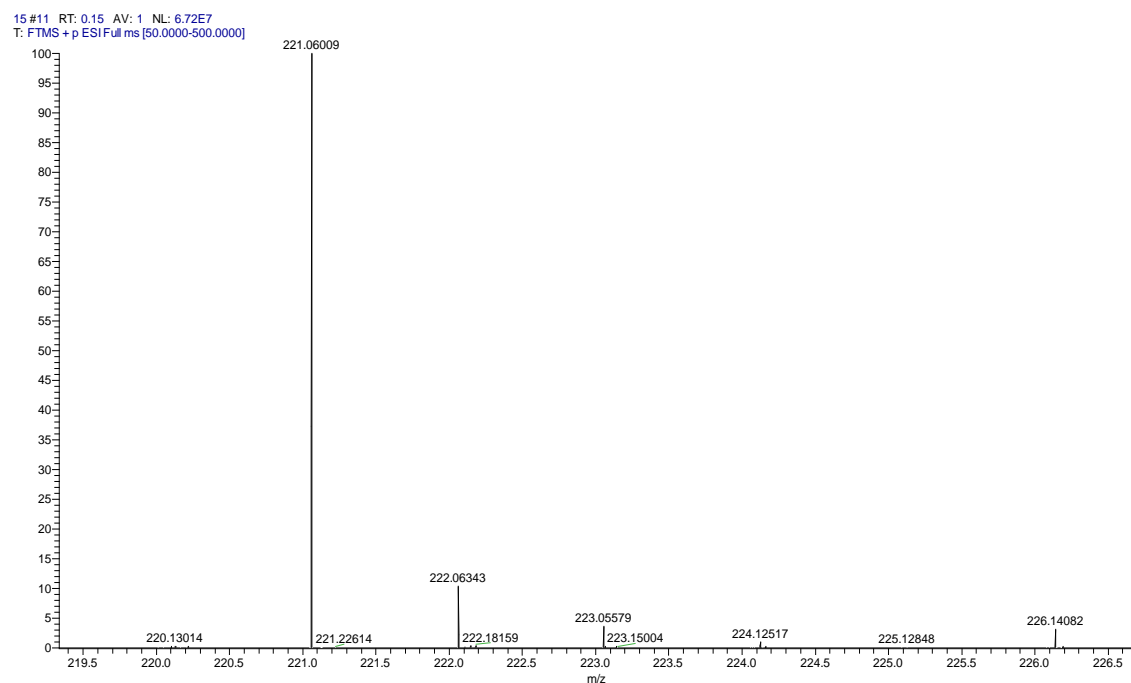


Figure S59. ^{13}C NMR of 14b.

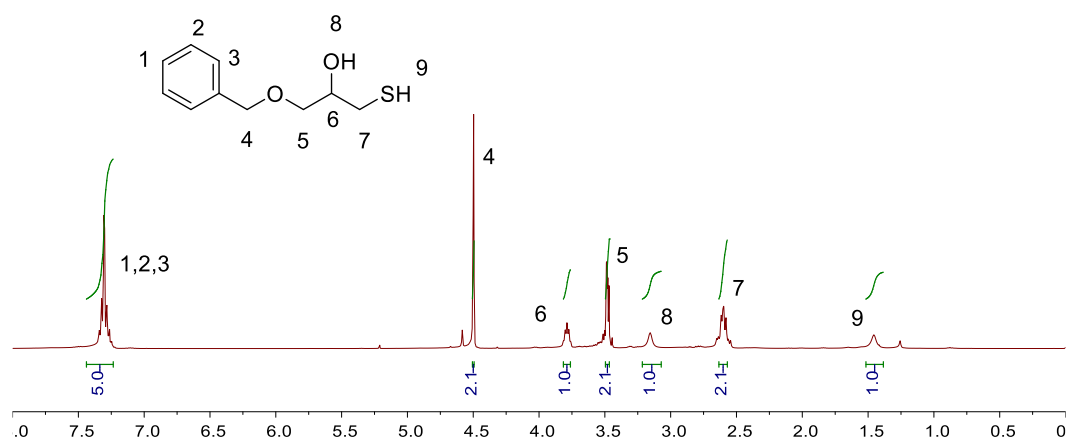


Figure S60. ^1H NMR of 15b.

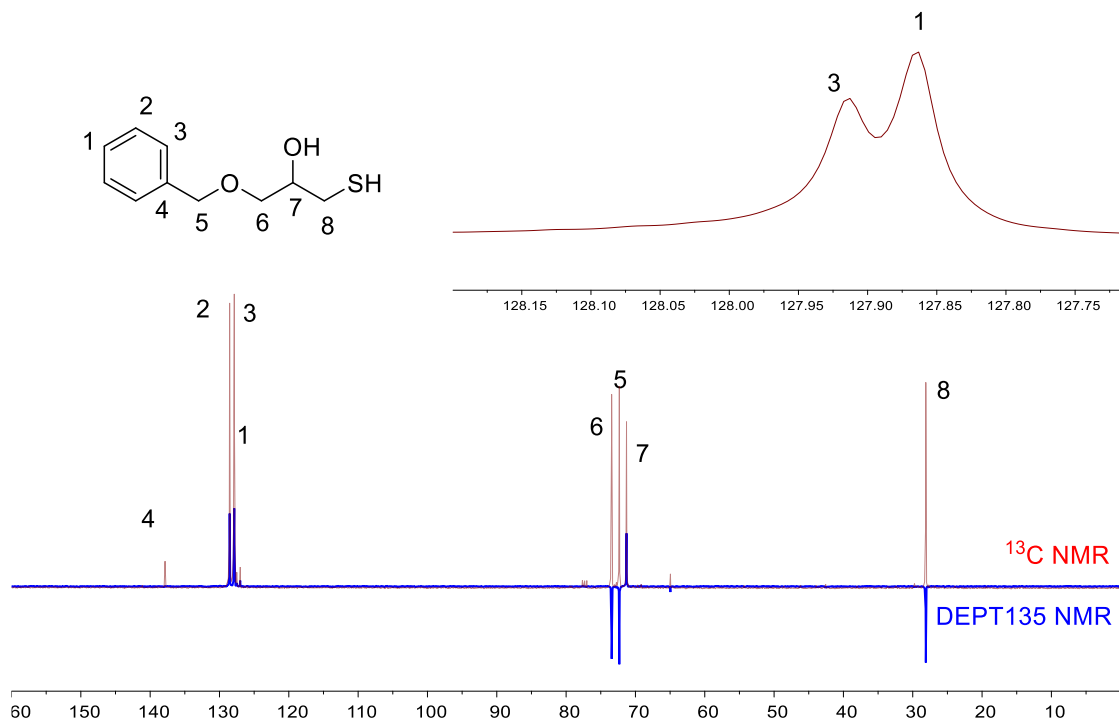


Figure S61. ^{13}C NMR of 15b.

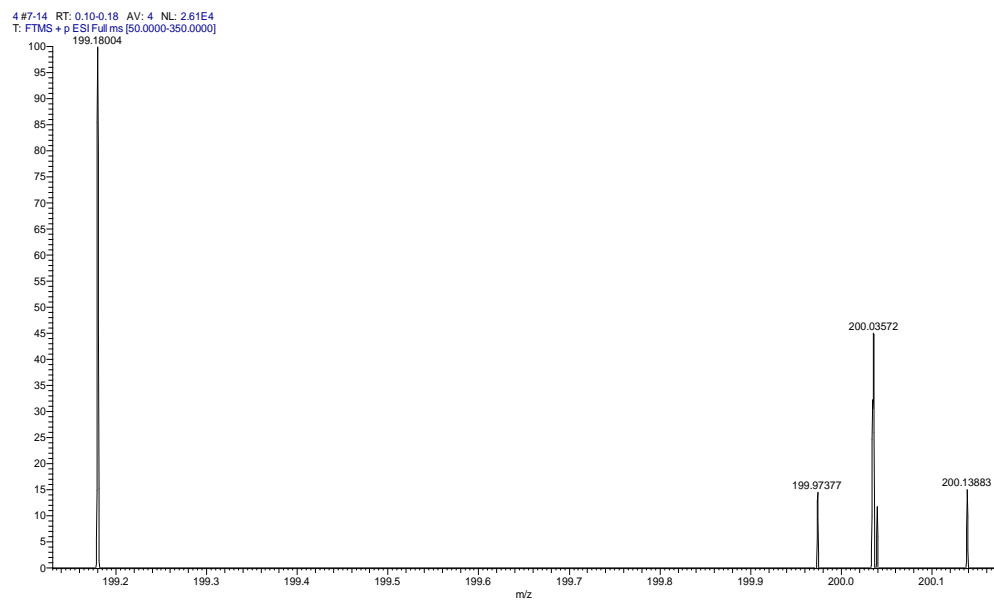


Figure S62. ESI-MS of 15b.

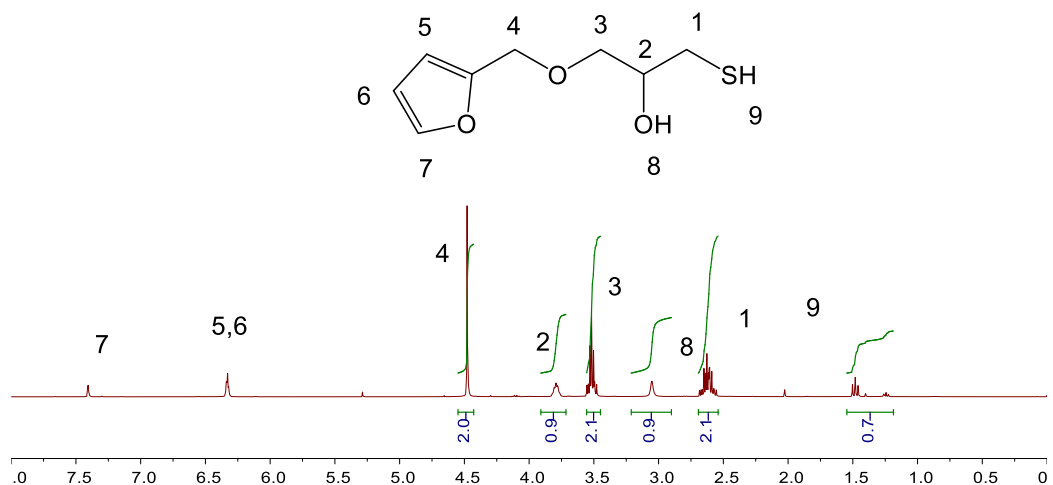


Figure S63. ^1H NMR of 16b.

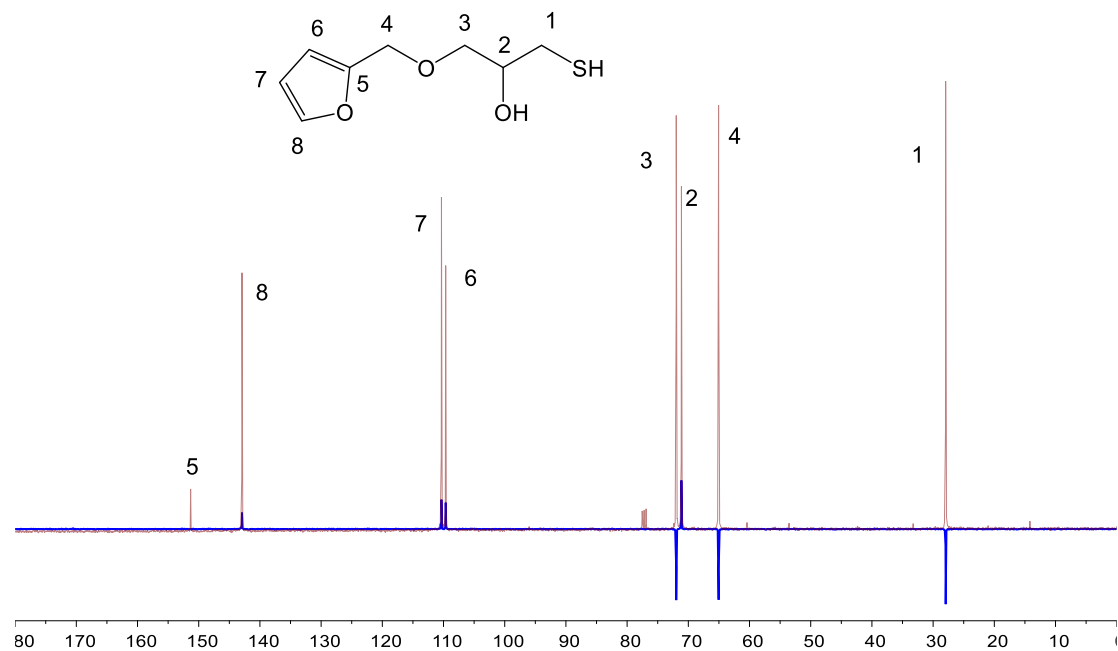


Figure S64. ^{13}C NMR of 16b.

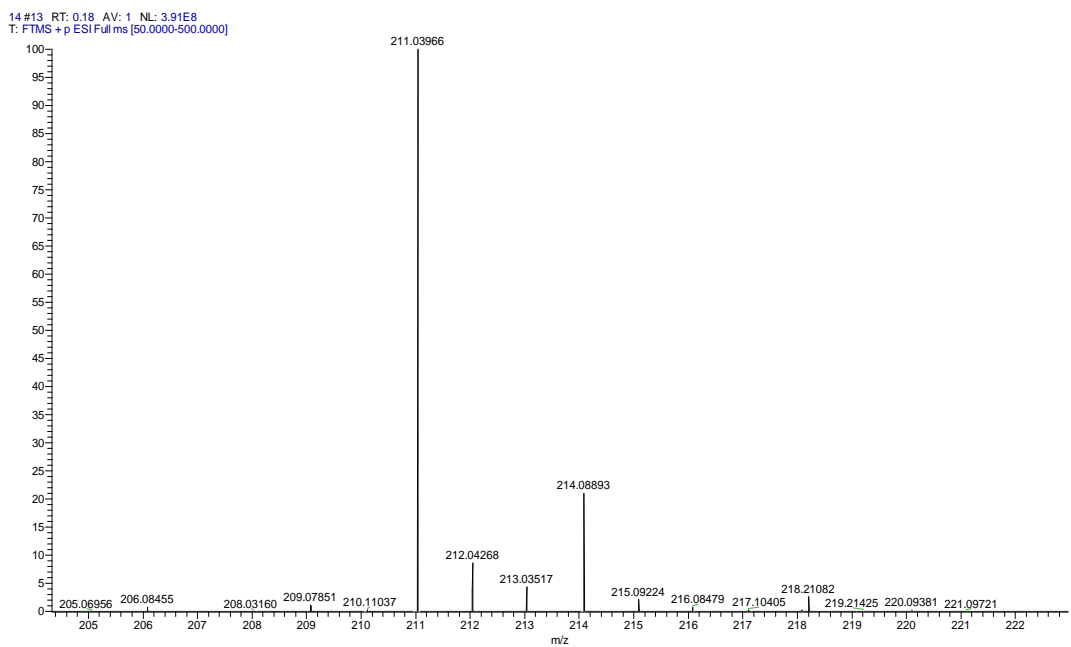


Figure S65. ESI-MS of 16b.

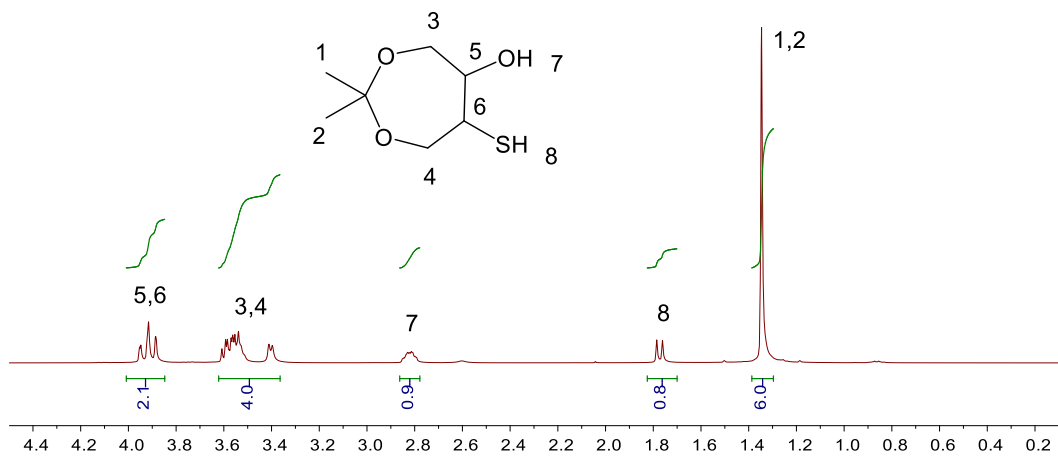


Figure S66. ^1H NMR of 17b.

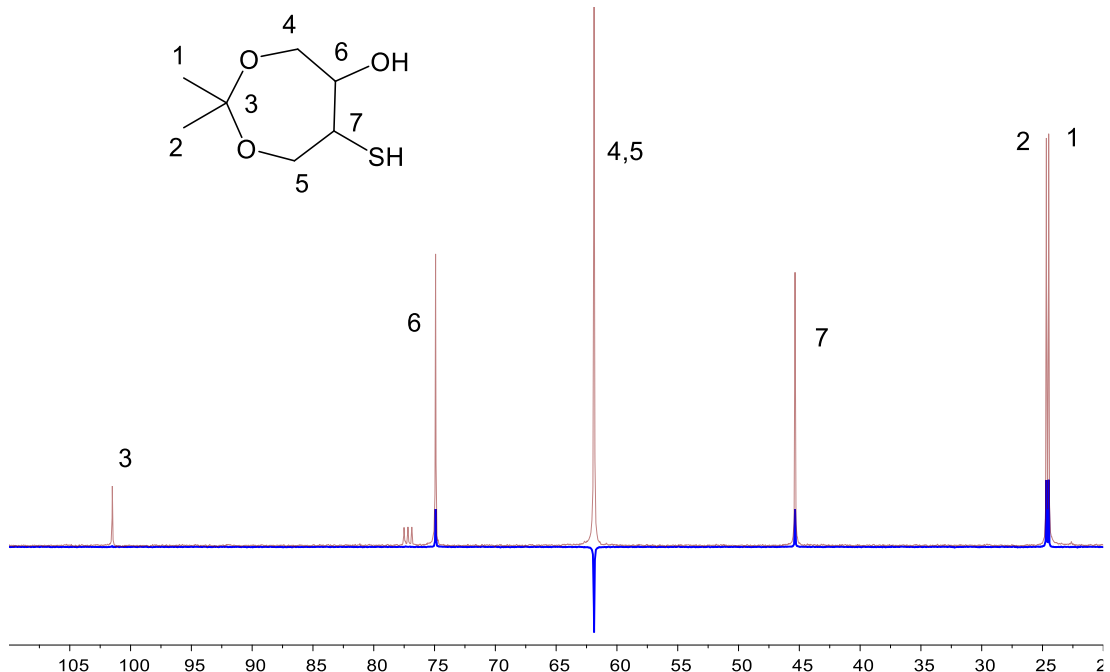


Figure S67. ^{13}C NMR of 17b.

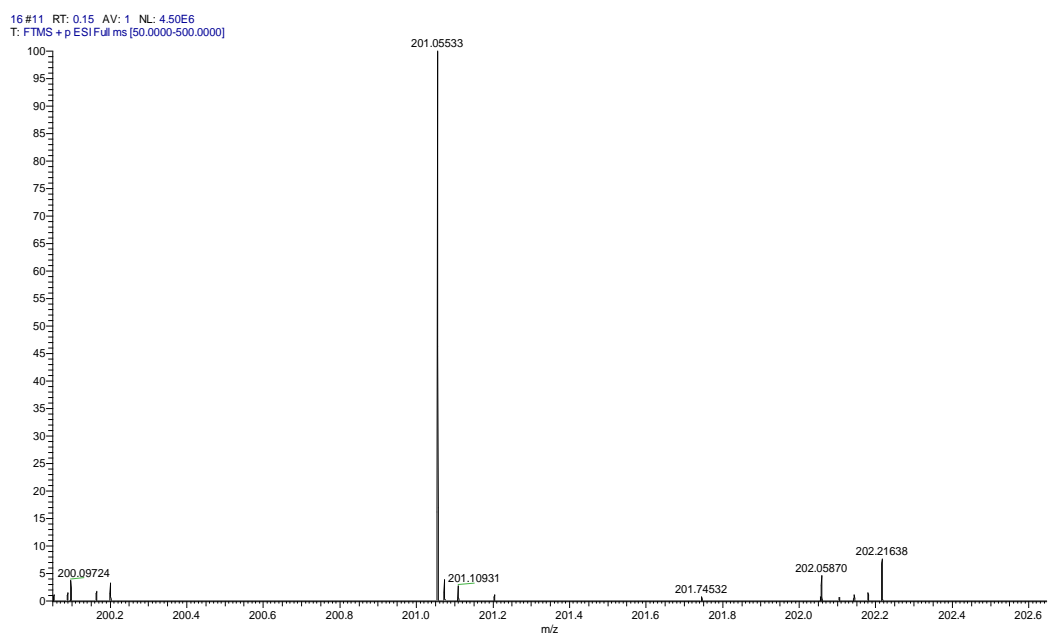


Figure S68. ESI-MS of 17b.

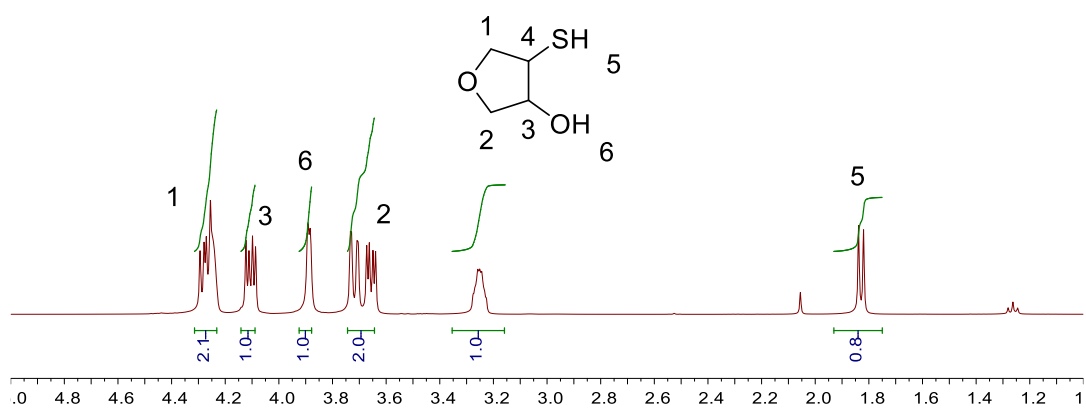


Figure S69. ^1H NMR of 18b.

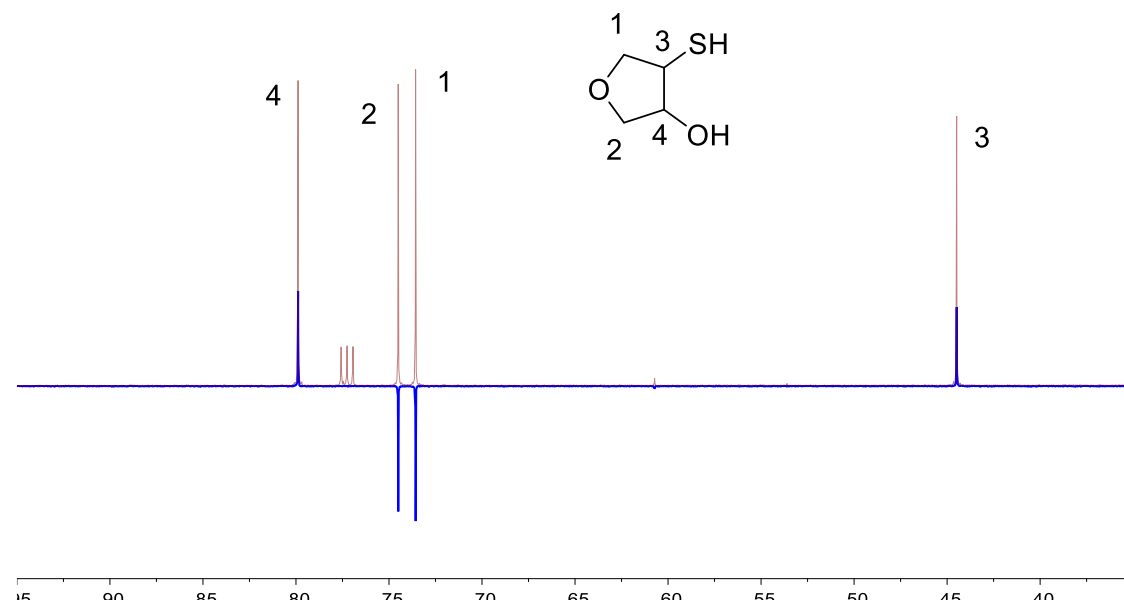


Figure S70. ^{13}C NMR of 18b.

23 #10 RT: 0.14 AV: 1 NL: 2.08E7
T: FTMS - p ESI Full ms [50.0000-500.0000]

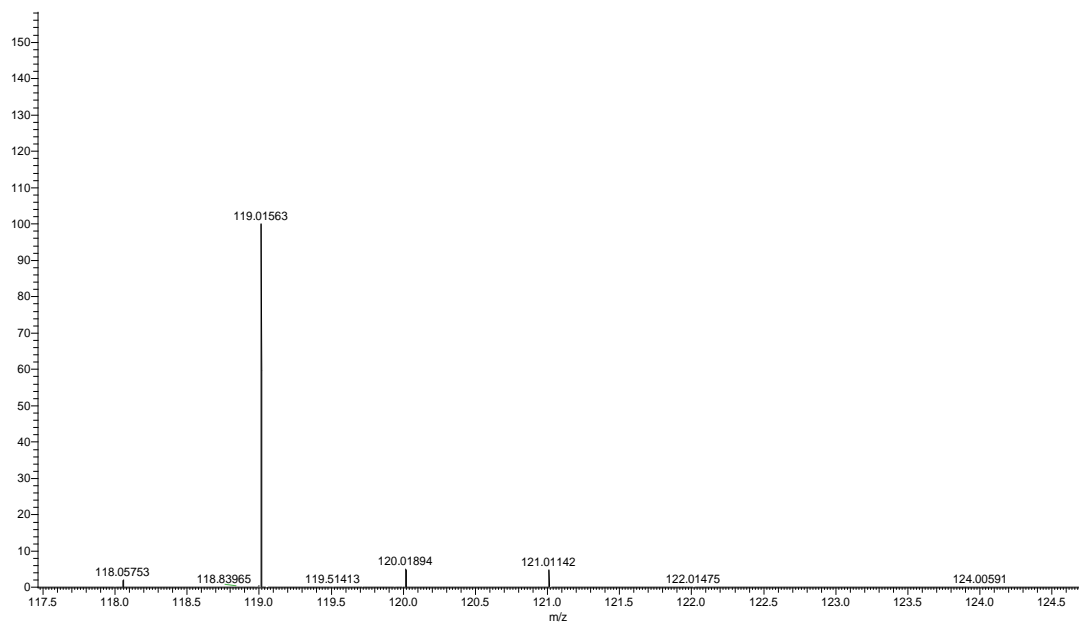


Figure S71. ESI-MS of 18b.

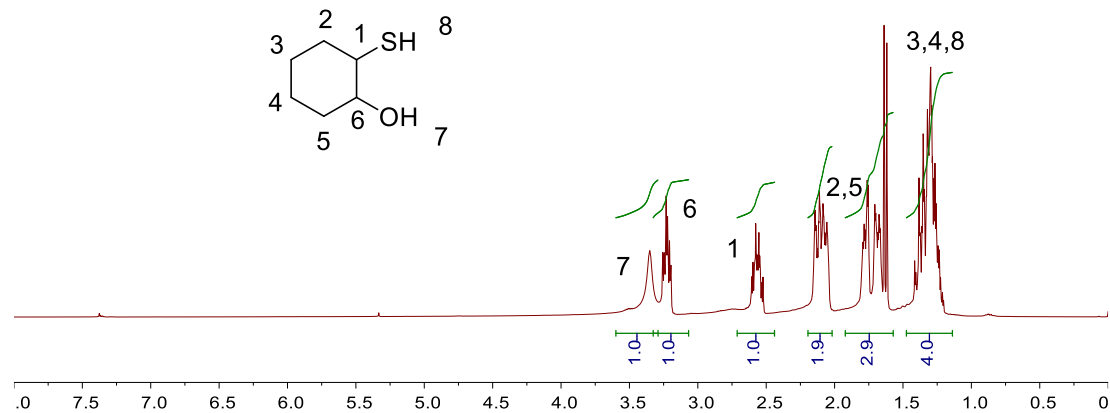


Figure S72. ¹H NMR of 19b.

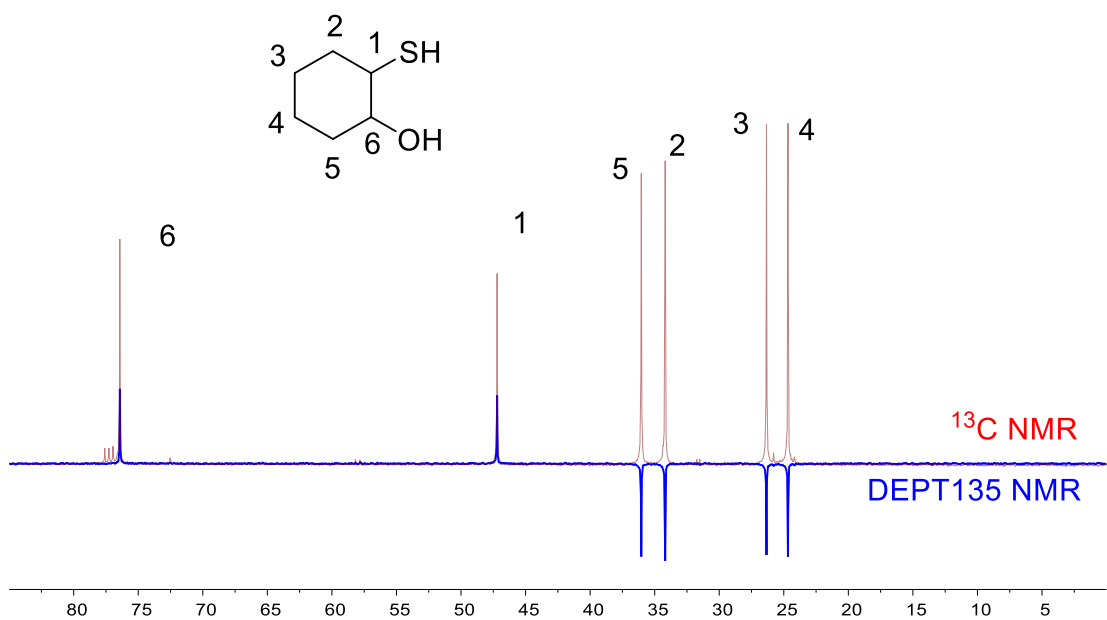


Figure S73. ^{13}C NMR of 19b.

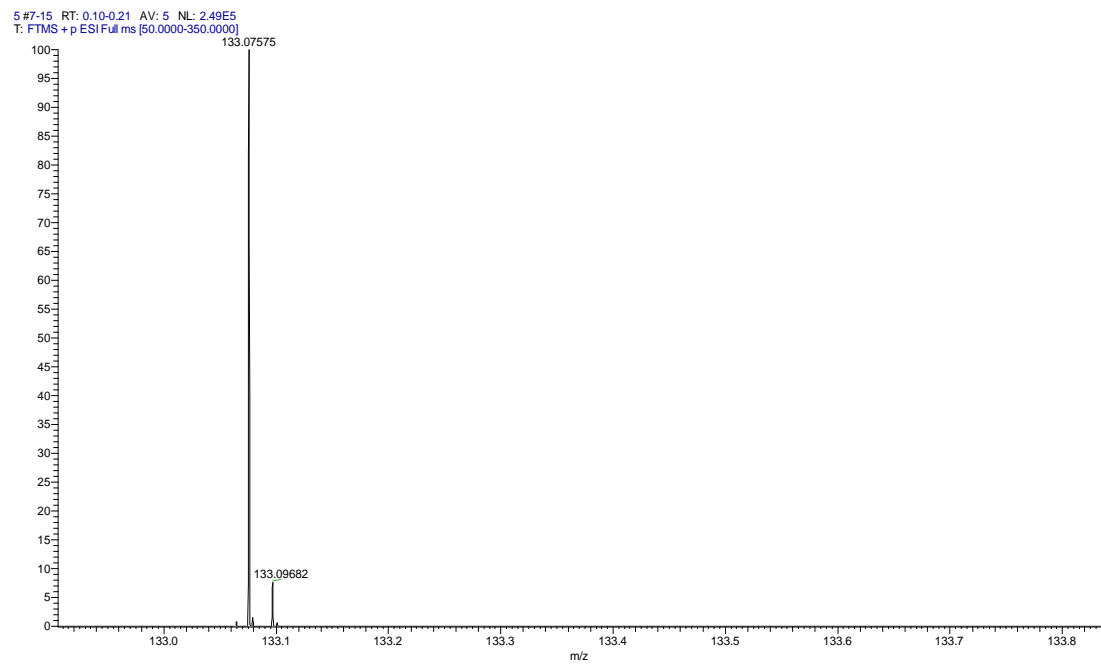


Figure S74. ESI-MS of 19b.

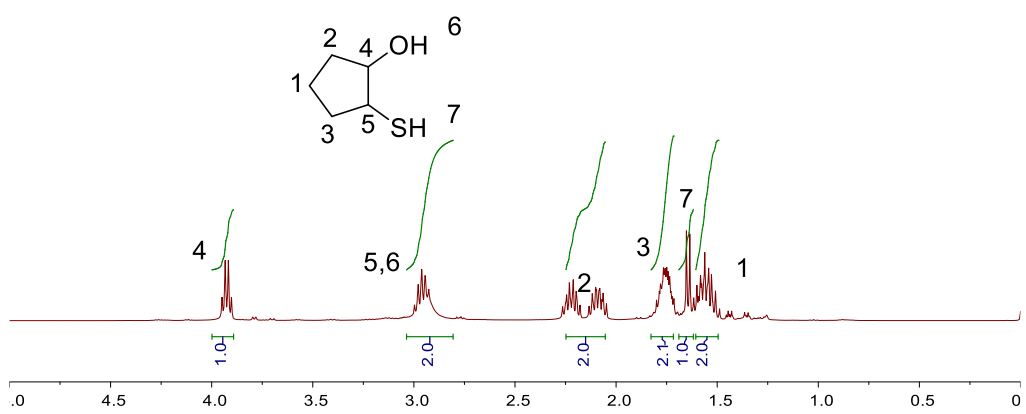


Figure S75. ^1H NMR of 20b.

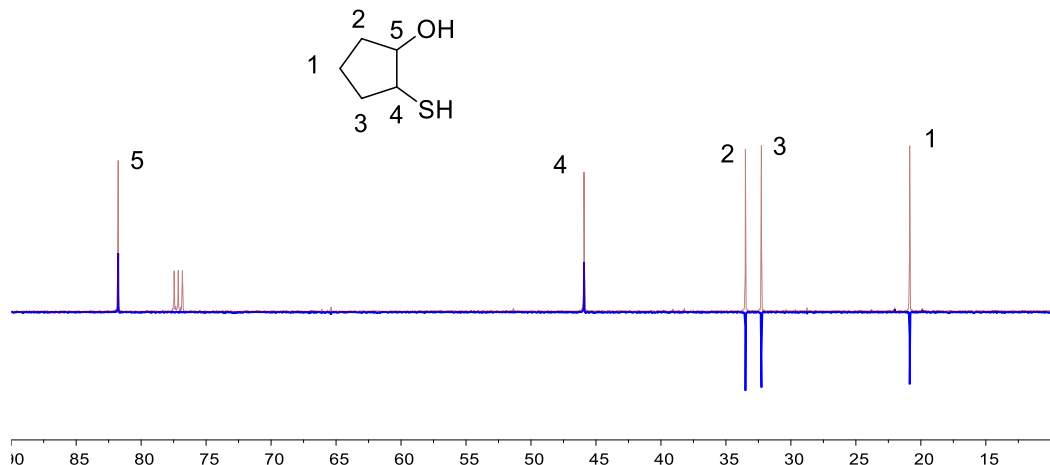


Figure S76. ^{13}C NMR of 20b.

22#10 RT: 0.14 AV: 1 NL: 2.57E6
T: FTMS - p ESI Full ms [50.0000-500.0000]

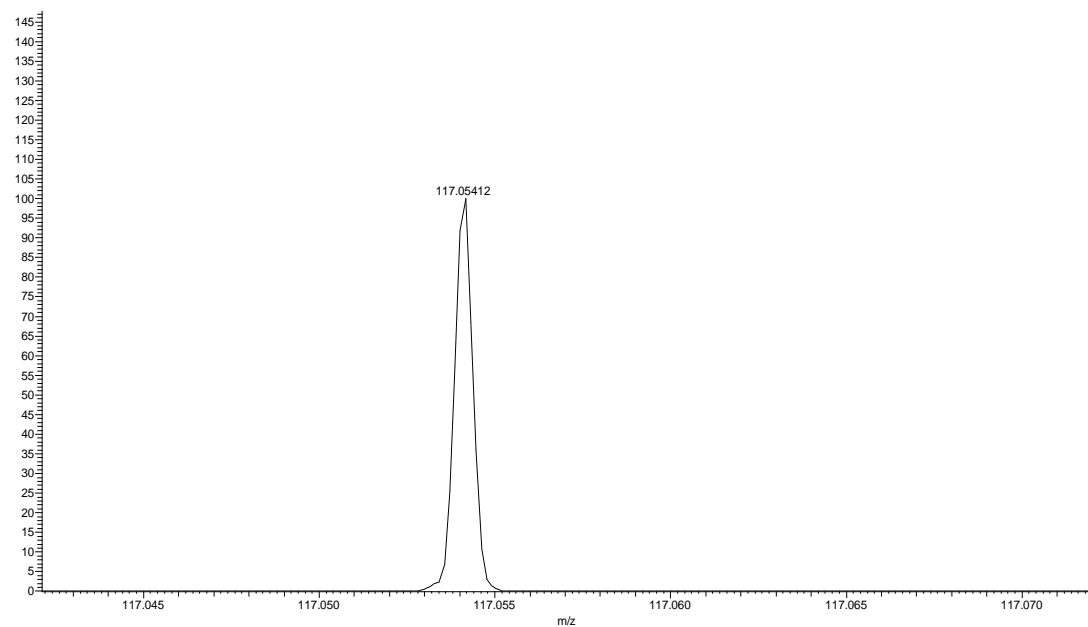


Figure S77. ESI-MS of 20b.

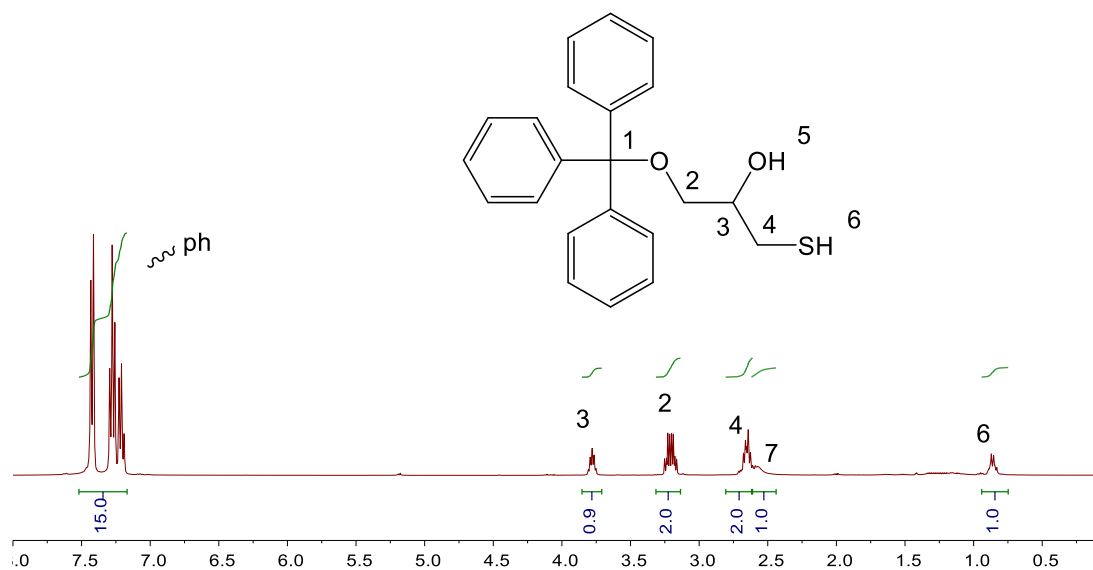


Figure S78. ^1H NMR of 21b.

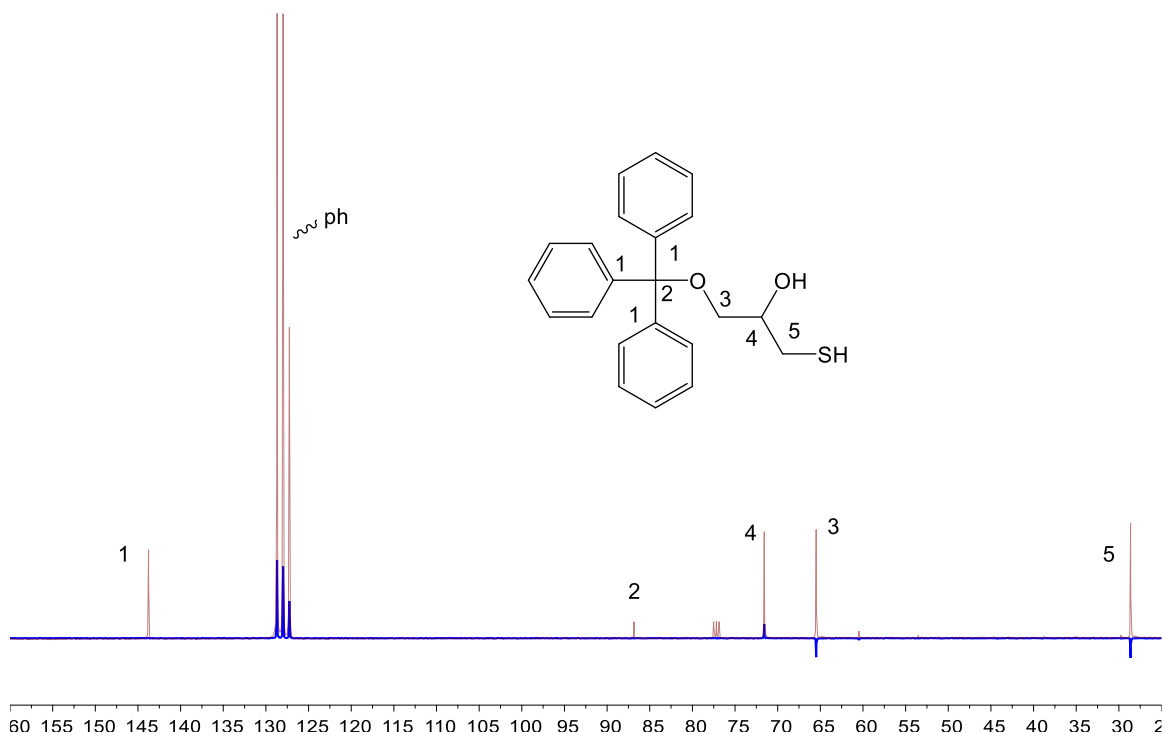


Figure S79. ^{13}C NMR of 21b.

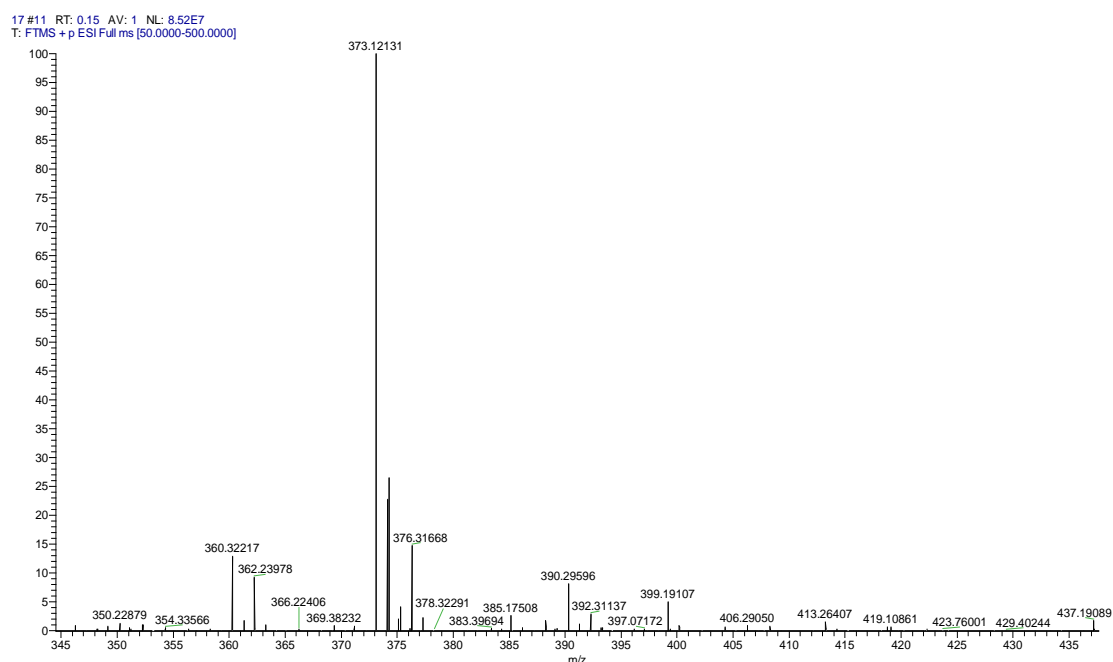


Figure S80. ^{13}C NMR of 21b.

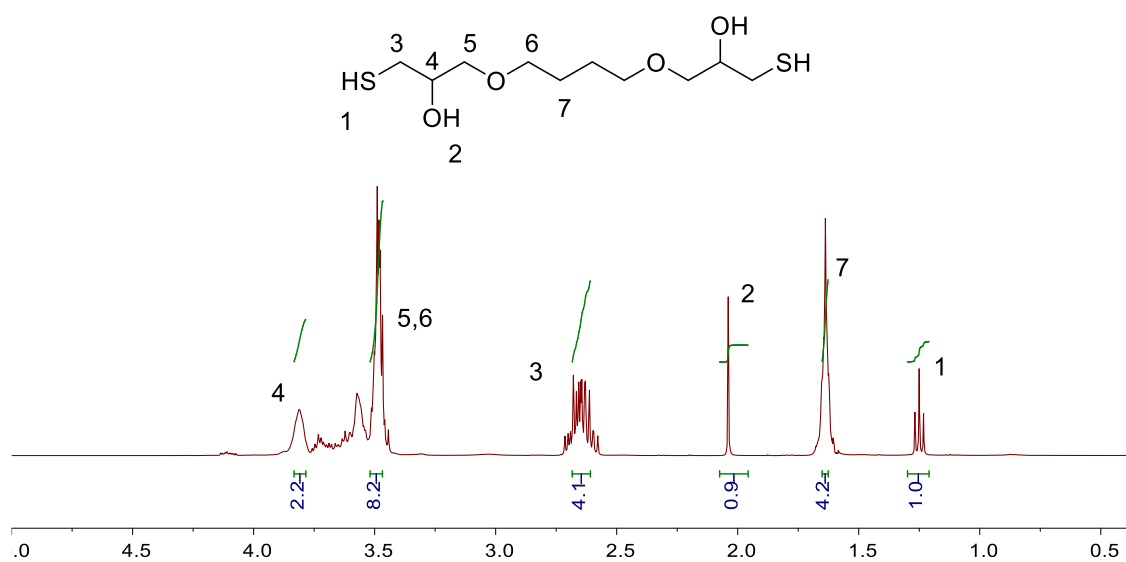


Figure S81. ^1H NMR of 22b.

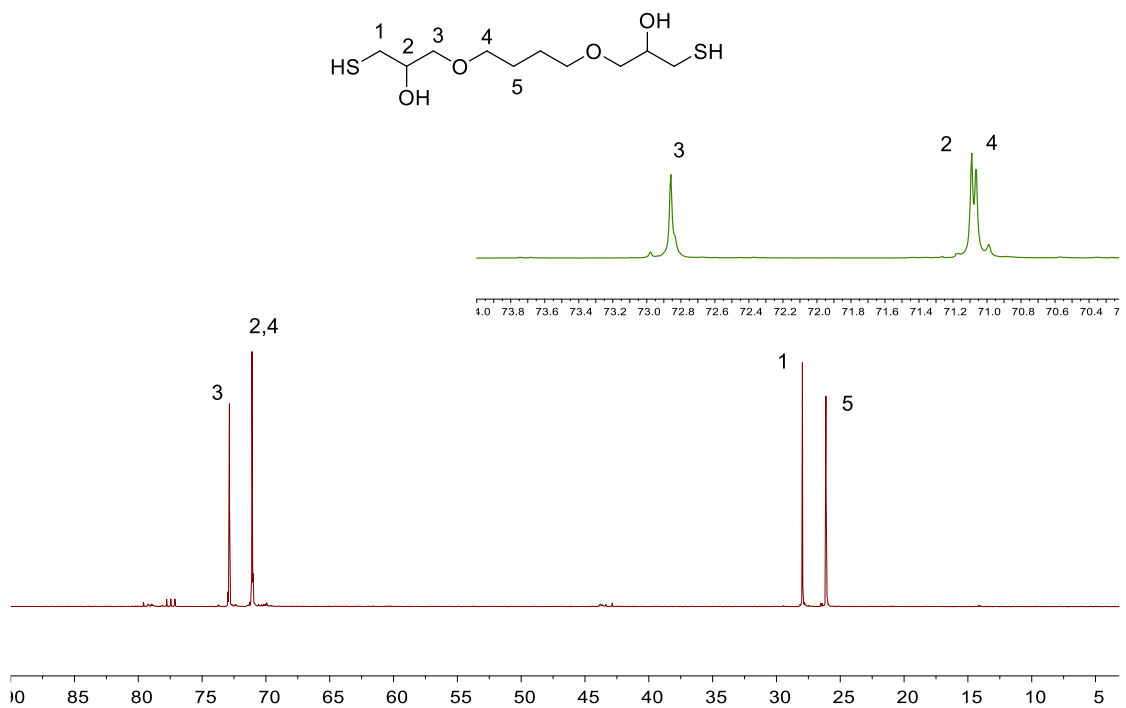


Figure S82. ^{13}C NMR of 22b.

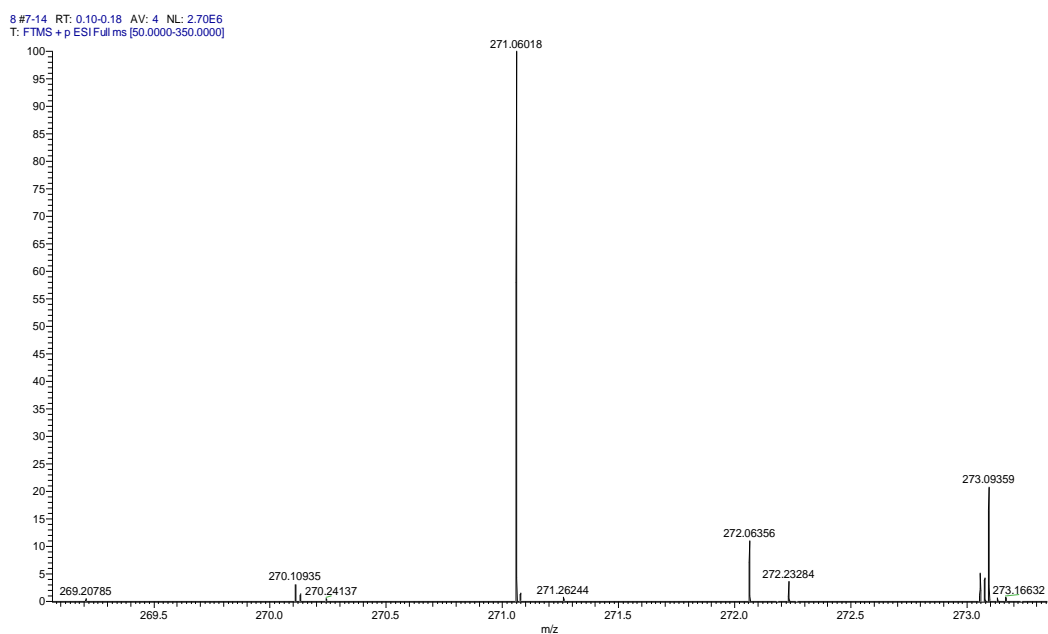


Figure S83. ESI-MS of 22b.

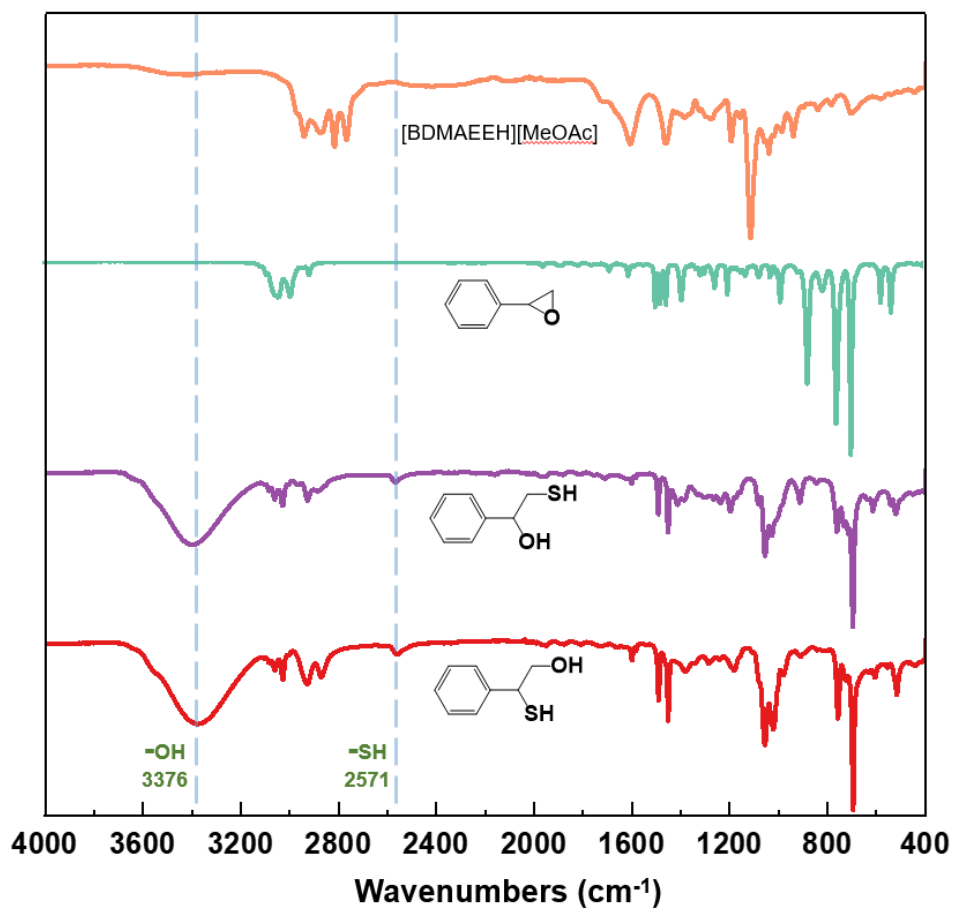


Figure S84. The FT-IR details of pure (**1a**), (**1b**), (**1c**), and [BDMAEEH][MeOAc].

Theoretical calculation method

All the structures were fully optimized with the DFT method including the dispersion corrections (B3LYP) method using the Empirical Dispersion = GD3BJ keyword.^[1] 6-311g(d,p) basis set was used for all atoms [abbreviation as B3LYP/6-311g(d,p)]. The influence of water solvent was investigated in condensed phase using the Polarizable Continuum Model (PCM) at B3LYP/6-311g(d,p) method. Energy calculations and Zero-point energy (ZPE) correction have been done by using the same level of theory. The computed stationary points have been characterized as minima or transition states by diagonalizing the Hessian matrix and analyzing the vibrational normal modes. In this way, if the imaginary frequency is not displayed, the stationary point can be classified as minima, and if only one imaginary frequency is obtained, the stationary point can be classified as a transition state. The particular nature of the transition states has been determined by analyzing the motion described by the eigenvector associated with the imaginary frequency. All calculations were performed with the Gaussian 09 suite of programs.^[2]

The coordinates of the optimized structures

Components		Rea		
1	7	-5.00465	-0.03353	0.133381
2	6	-5.62591	-0.93861	-0.83542
3	1	-6.71156	-0.87535	-0.73524
4	1	-5.35298	-0.62931	-1.84563

5	1	-5.32866	-1.98522	-0.69349
6	6	-5.34699	-0.37126	1.516257
7	1	-4.88234	0.350675	2.189725
8	1	-6.43049	-0.31157	1.63844
9	1	-5.02462	-1.38027	1.80243
10	6	-3.57552	0.20016	-0.09255
11	1	-3.45376	0.592617	-1.10595
12	1	-3.24761	0.979114	0.601226
13	6	-2.66286	-1.01298	0.073848
14	1	-2.74219	-1.43248	1.085237
15	1	-2.92253	-1.80391	-0.64178
16	8	-1.33945	-0.55625	-0.16101
17	6	-0.36499	-1.58315	-0.04766
18	1	-0.42208	-2.04557	0.94603
19	1	-0.55252	-2.36447	-0.79579
20	6	0.988092	-0.91304	-0.26703
21	1	1.132337	-0.13847	0.488465
22	1	0.980946	-0.42436	-1.2447
23	7	2.166313	-1.79612	-0.21612
24	6	2.221231	-2.76822	-1.31703
25	1	3.201839	-3.24745	-1.31899
26	1	1.456333	-3.5482	-1.22758

27	1	2.0847	-2.24726	-2.26578
28	6	2.35488	-2.43845	1.093775
29	1	1.581973	-3.18322	1.313061
30	1	3.325688	-2.93741	1.103948
31	1	2.351124	-1.66768	1.864147
32	1	3.350151	-0.83392	-0.33765
33	6	7.277266	2.420978	-0.55433
34	1	7.892523	2.208365	-1.42814
35	1	7.887896	2.311726	0.351743
36	1	6.916845	3.456678	-0.61069
37	8	6.199922	1.496888	-0.56579
38	6	5.335559	1.686554	0.528678
39	1	4.896871	2.694943	0.524768
40	1	5.867751	1.57347	1.484687
41	6	4.181525	0.698579	0.543982
42	8	4.180748	-0.17998	-0.42851
43	8	3.344891	0.768528	1.431996
44	16	-6.28377	2.741173	-0.38726
45	1	-7.54166	2.266751	-0.29206
46	1	-5.6878	1.453545	-0.14374

Components			1a	
1	6	-1.59921	0.600788	-0.15822
2	6	-2.58427	-0.03884	0.734327
3	8	-2.48722	-0.42466	-0.64412
4	6	-0.14728	0.273506	-0.09493
5	6	0.794817	1.307023	-0.04234
6	6	2.156892	1.017273	0.051487
7	6	2.589341	-0.30986	0.083952
8	6	1.652705	-1.34538	0.020005
9	6	0.291953	-1.05621	-0.06916
10	1	-1.83473	1.60012	-0.52518
11	1	-3.49419	0.494479	1.007379
12	1	-2.23647	-0.78312	1.449687
13	1	0.460134	2.340959	-0.0741
14	1	2.879007	1.827691	0.092966
15	1	3.649358	-0.5366	0.1525
16	1	1.983922	-2.37993	0.03548
17	1	-0.43896	-1.85609	-0.13652

Components			Rea-1a	
1	7	3.81012	-0.9577	-1.44753
2	6	4.208977	-2.33277	-1.01586
3	1	5.29087	-2.4146	-1.09796
4	1	3.89125	-2.46013	0.019213
5	1	3.733836	-3.06695	-1.66195
6	6	4.203506	-0.67123	-2.85898
7	1	3.885634	0.338354	-3.11051
8	1	5.285699	-0.75031	-2.93547
9	1	3.734741	-1.39179	-3.52469
10	6	2.36763	-0.65094	-1.15248
11	1	2.252298	-0.79932	-0.07938
12	1	2.213192	0.399878	-1.38848
13	6	1.356153	-1.49482	-1.92624
14	1	1.48569	-1.38162	-3.0032
15	1	1.441115	-2.55852	-1.67734
16	8	0.050835	-1.01935	-1.63662
17	6	-0.48068	-1.48688	-0.39565
18	1	-0.57281	-2.57923	-0.42741
19	1	0.17993	-1.22789	0.43775
20	6	-1.8439	-0.8185	-0.25289

21	1	-2.469	-1.08768	-1.1064
22	1	-1.7045	0.265169	-0.27481
23	7	-2.60139	-1.14887	0.966354
24	6	-1.98321	-0.6395	2.19845
25	1	-2.67044	-0.79828	3.031113
26	1	-1.03377	-1.13433	2.432992
27	1	-1.80702	0.432133	2.094431
28	6	-2.94527	-2.57506	1.0691
29	1	-2.06996	-3.20887	1.249325
30	1	-3.64329	-2.70923	1.897476
31	1	-3.43678	-2.8828	0.14637
32	1	-3.93582	-0.42519	0.753688
33	6	-8.30614	2.031909	-0.20044
34	1	-8.4684	2.811127	0.543763
35	1	-9.13952	1.317901	-0.16258
36	1	-8.28013	2.487195	-1.19933
37	8	-7.07261	1.403427	0.113458
38	6	-6.7659	0.370915	-0.79244
39	1	-6.69017	0.748556	-1.82228
40	1	-7.54476	-0.40611	-0.79346
41	6	-5.45022	-0.31847	-0.47308
42	8	-4.84467	0.10113	0.611391

43	8	-5.04006	-1.19977	-1.21325
44	8	5.399323	0.790746	-0.01418
45	6	5.381472	0.853811	1.435532
46	1	6.364155	0.956009	1.883146
47	1	4.71136	0.137481	1.901986
48	6	4.835749	1.967825	0.656637
49	1	5.468343	2.838288	0.511974
50	1	4.359432	-0.29536	-0.85402
51	16	2.662278	-1.70976	2.457652
52	1	2.805934	-3.01326	2.78529
53	6	3.375727	2.194689	0.468636
54	6	2.427414	1.688714	1.360111
55	6	2.944852	2.905483	-0.65852
56	6	1.067906	1.867863	1.115034
57	1	2.743904	1.140205	2.237347
58	6	1.586517	3.07733	-0.90687
59	1	3.677752	3.309283	-1.3482
60	6	0.644372	2.552578	-0.02111
61	1	0.342536	1.465411	1.810665
62	1	1.262418	3.616736	-1.78871
63	1	-0.41367	2.682601	-0.21463

Components		TS-1b		
1	7	-3.51582	-2.09202	0.027333
2	6	-4.29937	-2.84864	-0.9882
3	1	-5.32426	-2.93808	-0.63313
4	1	-4.28323	-2.29353	-1.92386
5	1	-3.87268	-3.83921	-1.13291
6	6	-3.52619	-2.76422	1.357279
7	1	-2.91702	-2.18085	2.044831
8	1	-4.55319	-2.79522	1.714652
9	1	-3.13479	-3.776	1.272841
10	6	-2.14292	-1.72299	-0.4304
11	1	-2.24872	-1.20257	-1.38169
12	1	-1.74719	-1.0192	0.2968
13	6	-1.15453	-2.87238	-0.57334
14	1	-0.99937	-3.37453	0.387283
15	1	-1.47976	-3.62056	-1.30529
16	8	0.03973	-2.23641	-0.99651
17	6	1.252258	-2.87831	-0.61778
18	1	1.171562	-3.24897	0.410237
19	1	1.459723	-3.73066	-1.27598
20	6	2.318356	-1.79029	-0.72094

21	1	2.026408	-0.96598	-0.06864
22	1	2.335696	-1.41128	-1.74581
23	7	3.694721	-2.16581	-0.35819
24	6	4.325336	-3.08759	-1.31258
25	1	5.386043	-3.17822	-1.07219
26	1	3.878499	-4.08841	-1.2864
27	1	4.228488	-2.68461	-2.32167
28	6	3.823823	-2.63565	1.029418
29	1	3.356431	-3.61405	1.188474
30	1	4.884088	-2.71837	1.275302
31	1	3.368241	-1.89981	1.69175
32	1	4.402507	-0.80304	-0.37406
33	6	6.44101	3.873201	-0.43198
34	1	7.275868	3.906307	-1.13138
35	1	6.795955	4.158585	0.567085
36	1	5.674846	4.592304	-0.75053
37	8	5.93904	2.54515	-0.44247
38	6	4.847273	2.3914	0.431593
39	1	4.019641	3.064547	0.162851
40	1	5.125067	2.625046	1.469516
41	6	4.288609	0.979706	0.42457
42	8	4.866237	0.149679	-0.40755

43	8	3.356748	0.698891	1.16583
44	8	-4.90671	0.056289	0.518989
45	6	-4.90527	1.462625	-0.61462
46	1	-5.95194	1.693688	-0.69665
47	1	-4.3794	1.090066	-1.47617
48	6	-4.30808	1.338389	0.705913
49	1	-4.80531	1.910576	1.493479
50	1	-4.03794	-1.15006	0.18007
51	16	-4.45986	3.89738	-1.4884
52	1	-5.72371	4.111223	-1.91494
53	6	-2.8138	1.334546	0.882039
54	6	-1.93411	1.723607	-0.12993
55	6	-2.2902	0.858343	2.089979
56	6	-0.55555	1.61837	0.055406
57	1	-2.32522	2.108862	-1.0631
58	6	-0.91435	0.74871	2.272671
59	1	-2.96741	0.559403	2.88314
60	6	-0.03891	1.125565	1.251952
61	1	0.117246	1.915943	-0.74061
62	1	-0.52373	0.368113	3.209345
63	1	1.033376	1.040036	1.384997

Components		TS-1c		
1	7	-2.56517	2.88307	-0.49111
2	6	-2.94268	3.160562	0.923503
3	1	-3.99533	3.434857	0.947011
4	1	-2.78836	2.256308	1.508959
5	1	-2.34306	3.974761	1.325091
6	6	-2.78544	4.065099	-1.37061
7	1	-2.48532	3.807862	-2.38464
8	1	-3.84595	4.30893	-1.3542
9	1	-2.20877	4.916368	-1.01365
10	6	-1.20006	2.285303	-0.63143
11	1	-1.18584	1.395447	-0.00246
12	1	-1.09327	1.969485	-1.6691
13	6	-0.03836	3.208255	-0.25849
14	1	0.030073	4.046755	-0.95224
15	1	-0.14982	3.609984	0.753962
16	8	1.175206	2.482105	-0.37926
17	6	1.544207	1.764311	0.797985
18	1	1.801788	2.472212	1.594021
19	1	0.714686	1.142079	1.151073
20	6	2.74063	0.902212	0.408606

21	1	3.536847	1.541293	0.022372
22	1	2.437092	0.229225	-0.39741
23	7	3.320201	0.081923	1.485549
24	6	2.411444	-0.95875	1.986128
25	1	2.971995	-1.64155	2.626996
26	1	1.578449	-0.54667	2.567961
27	1	2.007852	-1.52203	1.143504
28	6	3.900781	0.878834	2.577123
29	1	3.142766	1.413045	3.160992
30	1	4.443499	0.211118	3.248809
31	1	4.605661	1.593032	2.151862
32	1	4.537044	-0.59363	0.81383
33	6	8.622202	-2.65082	-1.43729
34	1	8.546044	-3.73775	-1.42897
35	1	9.530788	-2.34883	-0.89969
36	1	8.697488	-2.30249	-2.47588
37	8	7.455742	-2.14475	-0.80586
38	6	7.450634	-0.73801	-0.76565
39	1	7.49294	-0.30661	-1.77635
40	1	8.319827	-0.3486	-0.21534
41	6	6.21033	-0.1749	-0.09287
42	8	5.363976	-1.06812	0.361391

43	8	6.068913	1.03553	-0.00949
44	8	-4.27753	1.077261	-1.19431
45	6	-3.73728	-0.62825	-0.74837
46	1	-2.78867	-0.47105	-0.26188
47	6	-3.91452	0.003379	-2.04703
48	1	-4.72699	-0.35725	-2.67901
49	1	-3.25645	2.107543	-0.83219
50	16	-2.456	-3.02188	-1.48825
51	1	-3.33147	-3.72462	-0.74042
52	6	-4.7966	-1.2511	0.040506
53	6	-6.04078	-1.59015	-0.50963
54	6	-4.55936	-1.51429	1.397147
55	6	-7.01922	-2.18105	0.280024
56	1	-6.24184	-1.39644	-1.55525
57	6	-5.53794	-2.10808	2.185561
58	1	-3.59763	-1.25651	1.825678
59	6	-6.77122	-2.44416	1.628254
60	1	-7.97676	-2.44126	-0.15517
61	1	-5.34094	-2.30842	3.231958
62	1	-7.53578	-2.90803	2.240081
63	1	-3.00293	0.150007	-2.6301

Components		Pro-1b		
1	7	3.514108	2.104664	0.086858
2	6	3.99819	2.924415	-1.02448
3	1	5.060223	3.134577	-0.87957
4	1	3.881324	2.371699	-1.9587
5	1	3.470532	3.884271	-1.11693
6	6	3.668598	2.775665	1.378913
7	1	3.307792	2.116422	2.170455
8	1	4.727641	2.977184	1.554199
9	1	3.125292	3.728922	1.438967
10	6	2.17317	1.554895	-0.12535
11	1	2.1883	0.96502	-1.04523
12	1	1.958335	0.866076	0.691879
13	6	1.019249	2.552203	-0.21113
14	1	0.947079	3.155323	0.703383
15	1	1.131653	3.237519	-1.06152
16	8	-0.15447	1.765733	-0.36762
17	6	-1.35343	2.524014	-0.38599
18	1	-1.44168	3.109359	0.538386
19	1	-1.34748	3.224526	-1.2313
20	6	-2.48616	1.508772	-0.50847

21	1	-2.42528	0.804774	0.323395
22	1	-2.34519	0.940037	-1.43136
23	7	-3.85519	2.051245	-0.52129
24	6	-4.14935	2.877575	-1.70001
25	1	-5.22101	3.082015	-1.73274
26	1	-3.61576	3.835193	-1.68651
27	1	-3.86993	2.331725	-2.60248
28	6	-4.22681	2.725188	0.731531
29	1	-3.68317	3.664287	0.884276
30	1	-5.29541	2.947083	0.707643
31	1	-4.0299	2.049127	1.563459
32	1	-4.73629	0.789228	-0.55049
33	6	-7.57212	-3.45095	-0.48705
34	1	-8.23719	-3.46889	-1.34999
35	1	-8.17253	-3.48641	0.431633
36	1	-6.92171	-4.33523	-0.51472
37	8	-6.81732	-2.25123	-0.5652
38	6	-5.92176	-2.12492	0.513238
39	1	-5.20922	-2.96217	0.543955
40	1	-6.45147	-2.12081	1.477075
41	6	-5.10272	-0.84683	0.450195
42	8	-5.34707	-0.07386	-0.58049

43	8	-4.28775	-0.61268	1.329719
44	8	5.397663	0.093245	0.3968
45	6	4.950375	-1.40791	-1.4296
46	1	5.877199	-0.97043	-1.79464
47	1	4.123284	-0.9003	-1.92904
48	6	4.896878	-1.20398	0.089267
49	1	5.60674	-1.90454	0.543346
50	1	4.678716	0.760707	0.234193
51	16	4.876662	-3.16244	-1.99014
52	1	6.081471	-3.52942	-1.50943
53	6	3.533224	-1.42042	0.736039
54	6	2.402931	-1.8604	0.045957
55	6	3.399561	-1.09416	2.091783
56	6	1.167157	-1.95769	0.686675
57	1	2.463823	-2.11899	-1.00214
58	6	2.170389	-1.19028	2.73469
59	1	4.266968	-0.7347	2.632167
60	6	1.044253	-1.61972	2.030599
61	1	0.299277	-2.28725	0.127393
62	1	2.087803	-0.92392	3.782196
63	1	0.08248	-1.68691	2.525504

Components		Pro-1c		
1	7	-2.65136	2.938574	-0.16105
2	6	-3.03628	2.950158	1.252057
3	1	-4.09141	3.219444	1.33356
4	1	-2.90404	1.952606	1.675202
5	1	-2.45415	3.661812	1.853357
6	6	-2.79919	4.256793	-0.78152
7	1	-2.53011	4.191624	-1.83722
8	1	-3.84307	4.569653	-0.71074
9	1	-2.17975	5.030676	-0.3073
10	6	-1.3454	2.315576	-0.41078
11	1	-1.40755	1.280585	-0.0688
12	1	-1.18375	2.288661	-1.49169
13	6	-0.12111	2.976206	0.237027
14	1	-0.01146	4.007205	-0.10212
15	1	-0.20778	2.9819	1.330625
16	8	1.079835	2.313384	-0.15089
17	6	1.268689	1.041058	0.460271
18	1	1.161172	1.132725	1.548449
19	1	0.524197	0.319973	0.10627
20	6	2.674947	0.590018	0.07818

21	1	3.411215	1.261026	0.524646
22	1	2.775552	0.662648	-1.00769
23	7	3.035879	-0.78403	0.470161
24	6	2.289139	-1.81961	-0.25869
25	1	2.740228	-2.79203	-0.05296
26	1	1.231975	-1.86208	0.027765
27	1	2.354399	-1.62409	-1.33003
28	6	2.997825	-0.9988	1.924562
29	1	1.979555	-0.96286	2.328266
30	1	3.421998	-1.97957	2.147177
31	1	3.610032	-0.23668	2.406558
32	1	4.52056	-0.89682	0.096983
33	6	9.490228	-1.20151	-1.01571
34	1	9.668413	-2.01989	-1.71272
35	1	10.07843	-1.36999	-0.10391
36	1	9.817772	-0.2592	-1.47459
37	8	8.098314	-1.18401	-0.73746
38	6	7.757384	-0.15633	0.161809
39	1	8.036568	0.831549	-0.23333
40	1	8.277658	-0.27415	1.123451
41	6	6.268835	-0.10969	0.462797
42	8	5.540072	-0.99623	-0.17094

43	8	5.840945	0.72241	1.248446
44	8	-4.45663	1.26088	-1.45144
45	6	-3.43392	-0.75551	-0.54098
46	1	-2.95887	-0.13338	0.216972
47	6	-3.69809	0.117708	-1.78292
48	1	-4.26338	-0.46046	-2.51785
49	1	-3.84961	1.883585	-0.9758
50	16	-2.17187	-2.03425	-1.0287
51	1	-2.18856	-2.71138	0.135774
52	6	-4.69144	-1.34746	0.041627
53	6	-5.46871	-2.26528	-0.67352
54	6	-5.12326	-0.94127	1.305644
55	6	-6.65083	-2.76249	-0.13545
56	1	-5.14008	-2.59851	-1.6511
57	6	-6.30783	-1.43832	1.848474
58	1	-4.52936	-0.22882	1.867158
59	6	-7.07504	-2.35047	1.129066
60	1	-7.24225	-3.47346	-0.70079
61	1	-6.62824	-1.11265	2.83136
62	1	-7.99538	-2.73985	1.548322
63	1	-2.73863	0.390295	-2.24121

References:

- [1] a) S. Grimme, S. Ehrlich, L. Goerigk, *J. Comput. Chem.* **2011**, 32, 1456-1465; b) R. Sure, J. Antony, S. Grimme, *J. Phys. Chem. B* **2014**, 118, 3431-3440; c) M. J. Turner, S. Grabowsky, D. Jaytilaka, M. A. Spackman, M. J. Turner, S. Grabowsky, D. Jaytilaka, M. A. Spackman, *J. Phys. Chem. Lett.* **2014**, 55, 4249-4255; d) Z. Li, K. Su, J. Ren, D. Yang, B. Cheng, C. K. Kim, X. Yao, Z. Li, K. Su, J. Ren, D. Yang, B. Cheng, C. K. Kim, X. Yao, *Green Chem.*, **2018**, 20, 863-872.
- [2] M. J. Frisch, G. W. Trucks, H. B. Schlegel, G. E. Scuseria, M. A. Robb, J. R. Cheeseman, J. A. Montgomery, Jr., T. Vreven, K. N. Kudin, J. C. Burant, J. M. Millam, S. S. Iyengar, J. Tomasi, V. Barone, B. Mennucci, M. Cossi, G. Scalmani, N. Rega, G. A. Petersson, H. Nakatsuji, M. Hada, M. Ehara, K. Toyota, R. Fukuda, J. Hasegawa, M. Ishida, T. Nakajima, Y. Honda, O. Kitao, H. Nakai, M. Klene, X. Li, J. E. Knox, H. P. Hratchian, J. B. Cross, V. Bakken, C. Adamo, J. Jaramillo, R. Gomperts, R. E. Stratmann, O. Yazyev, A. J. Austin, R. Cammi, C. Pomelli, J. Ochterski, P. Y. Ayala, K. Morokuma, G. A. Voth, P. Salvador, J. J. Dannenberg, V. G. Zakrzewski, S. Dapprich, A. D. Daniels, M. C. Strain, O. Farkas, D. K. Malick, A. D. Rabuck, K. Raghavachari, J. B. Foresman, J. V. Ortiz, Q. Cui, A. G. Baboul, S. Clifford, J. Cioslowski, B. B. Stefanov, G. Liu, A. Liashenko, P. Piskorz, I. Komaromi, R. L. Martin, D. J. Fox, T. Keith, M. A. Al-Laham, C. Y. Peng, A. Nanayakkara, M. Challacombe, P. M. W. Gill, B. G. Johnson, W. Chen, M. W. Wong, C. Gonzalez, J. A. Pople, GAUSSIAN 03, Gaussian, Inc., Pittsburgh, PA, 2009.